Enhancing Anaerobic Digestion Efficiency of High Strength Wastes with Different Solid Contents

by

Najiaowa Yu

A thesis submitted in partial fulfillment of the requirements for the degree of

Doctor of Philosophy

in

Environmental Engineering

Department of Civil and Environmental Engineering
University of Alberta

ABSTRACT

Anaerobic digestion (AD) has been considered as a sustainable technology to treat a wide range of organic wastes and to recovery value-added products such as methane and fatty acids. However, several factors such as low temperature and high solids content of substrates would lead to the imbalance of AD steps (*i.e.*, hydrolysis, acidogenesis, acetogenesis and methanogenesis) and result in process failure. This thesis aims to develop novel strategies to facilitate the economic treatment of high strength wastes, including two pre-treatment strategies treating substrates with medium and high solid contents (*i.e.*, blackwater and waste activated sludge) to improve solid hydrolysis, and conductive materials amendment strategies treating low solid content wastewater to improve syntrophic and methanogenic activities. All three strategies were assessed and optimized in continuous operating reactors, with a focus on their specific roles on improving anaerobic digestion efficiency. The performances and microbial communities of the experimental bioreactors were compared to conventional anaerobic treatment systems.

The thesis first employs calcium hypochlorite to the treatment of waste activated sludge (WAS) generated from central wastewater treatment plants in traditional urban wastewater collection systems. Different doses of $Ca(ClO)_2$ was applied to WAS (COD ~ 6 g/L) and thickened WAS (TWAS, COD ~ 50 g/L) to improve AD treatment efficiency using laboratory reactors. Adding 5 – 20% $Ca(ClO)_2$ (total suspended solids basis) significantly enhanced WAS anaerobic digestibility at room temperature (22 ^oC), and led to significantly enhanced methane production rate and biomethane yield comparing to the AD of raw WAS ($P < 0.05$), while severe inhibition was observed for 0.5 g/g TSS $Ca(ClO)_2$ pretreated WAS. Low $Ca(ClO)_2$ (1%) also increased the methane yield in the batch reactors treating TWAS at 35^oC, by 4.8% and 8.3%, respectively, at F/I = 1 and F/I = 0.33. Then, two semi-continuous anaerobic sequencing batch reactors (ASBRs), one

fed with $Ca(ClO)_2$ pretreated TWAS (1%) and one with raw TWAS, were operated at mesophilic conditions (35 °C) for 145 days. The performance stability and resilience of TWAS digestion were improved with $Ca(ClO)_2$ pretreatment by transforming the biomass to more easily digested substrates.

Efforts were also made to develop an effective and cost-efficient strategy to treat blackwater with medium solids content generated in decentralized wastewater collection systems. Micro-aeration was applied to the treatment of blackwater collected from conventional toilet (9 L water/flush) in ASBRs at room temperature (22°C). The optimum micro-aeration intensity was 5 mg O_2/L-reactor/cycle, which accelerated COD solubilization and enhanced methane production by 40.3% and 28.1%, respectively, when compared to no aeration. However, excessive oxygen (150 mg O_2/L-reactor/cycle) had a negative effect on the AD process. VFAs accumulated in the 50 mg O_2/L-reactor/cycle reactor due to the lack of downstream VFA conversion, so medium-dose micro-aeration offers an operational strategy for a two-stage anaerobic digestion system.

The third aspect of this thesis is to develop a novel semi-two-phase AD reactor that separates hydrolytic/acidogenic from methanogenic in an up-flow anaerobic sludge blanket (UASB) reactor. Granular activated carbon (GAC) was packed in plastic carriers and added to the UASB reactor (GAC self-fluidized) to promote the syntrophic methanogenic reactions in the reactor column. Enhanced performance was achieved with respect to methane production and COD removal at an organic loading rate of 1500 g COD/m^3/d under the temperature of 20 °C using the self-fluidized GAC configuration; with the methanation rate increased from 0.33 ± 0.08 g CH_4-COD/g influent COD in the non-GAC reactor, to 0.66 ± 0.02 g CH_4-COD/g influent COD in the GAC-only reactor, and further increased to 0.77 ± 0.02 g CH_4-COD/g influent COD in the self-fluidized GAC reactor. The results indicate that the floated-GAC reactor combined the advantages of both reactors,

performing a semi-two-phase AD process — a fermentation zone existed at the wastewater inlet, and methanogenesis was promoted throughout the reactor column with the dispersed floated-GAC.

The microbial community analysis revealed that low oxidative stresses contribute to the development of fermentative and syntrophic bacteria, while high levels of oxygen reduced the activities of obligate anaerobes and leading to VFAs accumulation due to the lack of downstream conversion. Microbial community segregation was observed between the bottom and mid-top zones in the floated-GAC UASB. The non-GAC reactor and the floated-GAC reactor shared *Enterobacteriaceae* as the dominant bacteria at the bottom layers, while two GAC-amended reactors were more alike in the middle and top layers, with the dominant bacteria being *Clostridium*, *Bacteroidales* and *Treponema*. *Methanosarcina* were enriched throughout the settled-GAC reactor and mid-top of the SF-GAC reactor.

PREFACE

This thesis is an original work by Najiaowa Yu. I designed and conducted the research involved in this thesis at the University of Alberta under the supervision of Dr. Yang Liu. I was responsible for performing all the experiments, data collection and analysis, and manuscript composition. Dr. Yang Liu was the supervisory author and was involved with conceptualization, review and editing of the manuscript. Other contributions made by my collages are listed below.

A version of **Chapter 3** has been published as Yu, N., Sun, H., Mou, A. and Liu, Y. 2021b. Calcium hypochlorite enhances the digestibility of and the phosphorus recovery from waste activated sludge. Bioresource Technology 340, 125658. Dr. Huijuan Sun and Anqi Mou contributed to methodology.

A version of **Chapter 4** has been published as Yu, N., Mou, A., Sun, H. and Liu, Y. 2022. Anaerobic digestion of thickened waste activated sludge under calcium hypochlorite stress: Performance stability and microbial communities. Environmental Research 212, 113441. Anqi contributed to methodology. Dr. Huijuan Sun is responsible for the model development and analysis.

A version of **Chapter 5** has been published as Yu, N., Guo, B., Zhang, Y., Zhang, L., Zhou, Y. and Liu, Y. 2020a. Different micro-aeration rates facilitate production of different end-products from source-diverted blackwater. Water Research, 115783. Dr. Bing Guo contributed to the analysis of raw Miseq data, review and editing of the manuscript. Yingdi Zhang, Dr. Lei Zhang and Dr. Yun Zhou contributed to methodology.

A version of **Chapter 6** has been published as Yu, N., Guo, B., Zhang, Y., Zhang, L., Zhou, Y. and Liu, Y. 2020b. Self-fluidized GAC-amended UASB reactor for enhanced methane production. Chemical Engineering Journal, 127652. Dr. Bing Guo contributed to the review of the manuscript. Yingdi Zhang, Dr. Lei Zhang and Dr. Yun Zhou contributed to methodology.

A version of **Chapter 7** has been published as Yu, N., Guo, B. and Liu, Y. 2021a. Shaping biofilm microbiomes by changing GAC location during wastewater anaerobic digestion. Science of The Total Environment 780, 146488. Dr. Bing Guo contributed to the review of the manuscript.

DEDICATION

To my dear parents and my beloved husband

ACKNOWLEDGMENTS

Everything goes by so quickly. A minute ago, I was this little girl who had never left her parents for more than a week, and now, I am about to graduate from a prestigious university in Canada. It has been a beautiful and rewarding journey, in which I gained so much help and support from so many amazing people.

The deepest and sincerest gratitude goes to my supervisor, Professor Yang Liu, who is the best supervisor I could ever ask for. As a terrific scientist, she is always passionate, professional, and courageous. As a powerful woman, she treats her students with love, care, and patience. At the beginning of the program, I was at sea. Dr. Liu approached me with promising research ideas, leading me into the world of anaerobic treatment, and has always been there over the course of my research to keep me in track. Her critical insights and open attitude have inspired me and prompted me in every respect. Thank you Dr. Liu for offering the opportunity, guidance, encouragement, and support to me. I have also had the fortune of being prompted by another knowledgeable and exemplary woman researcher, Dr. Bing Guo. Thank you Bing for delivering workshops in molecular biology, fixing problems in my code, providing help in revising the papers, and giving me career advice. I have enjoyed working with you. I am also extremely grateful to the technologists in the civil and environmental engineering department as well as the chemistry department, for their technical support. Special thanks to Abdul, for enlightening the path to convert the laboratory results to industrial applications. I would also extend my gratitude to the supervisory committee members, for their contributed time, efforts, and suggestions.

It has been a great privilege for me to work with so many experienced researchers: Yun, Lei, Qianyi, Mengjiao and Yingdi. You set great examples for me, and I have learned so much from

you all. My gratitude goes as well to friends and families. Thank you Huixin, Xin, and Mozhu for your presence and deeply understanding in the most challenging moments of my life. Thank you my dear friends Anqi and Huijuan, for so many nice moments we shared during the bittersweet path of being PhD students, building life last friendships with me, and being witnesses at my wedding, the happiest moment of my life. Thank you, my dear husband Hongyu and my lovely dog Nina, for your unconditional love and companionship.

Finally, I would like to express my gratitude to the financial support of China Scholarship Council, Natural Sciences and Engineering Research Council of Canada, Canada Research Chair Program, Alberta Innovates, WaterWerx and City of Edmonton.

TABLE OF CONTENTS

LIST OF FIGURES

LIST OF TABLES

CHAPTER 1 INTRODUCTION AND RESEARCH OBJECTIVES

1.1 Background and motivations

Wastewaters are waterborne solids and liquids discharged into sewers that contains the wastes of community life, including dissolved and suspended organic solids. As a result of the worldwide population increasing, new strategies for wastewater treatment have been developed to achieve sufficient treatment and to protect the receiving waters (Sonune and Ghate, 2004). Activated sludge process has been applied worldwide in municipal sewage treatment practice (Spellman, 2008). However, large amounts of excess sludge were generated which has become a real challenge in the field of environmental engineering technology. Further, sanitation coverage is commonly lower in rural areas than in urban areas, especially in the developing countries (Fry et al., 2008). In this context, decentralized systems are adopted to serve low-density communities in a more cost-effective manner than centralized systems (Capodaglio et al., 2017; Singh et al., 2015). The source-diverted blackwater collected from toiles contains half the load of the organic wastes in household wastewater stream and is considered as a feasible substrate for energy recovery. However, the blackwater anaerobic treatment processes were limited due to high organic solids and ammonium contents (Gao et al., 2020a).

Anaerobic digestion is a promising technology that produces renewable energy from various wastes with low operational cost and low sludge production. AD has been widely applied for treating agriculture-wastes, food-wastes, and high-strength wastewater under mesophilic (30 – 40 ℃) and thermophilic (50 – 60 ℃) temperatures (Nag et al., 2019; Zhang et al., 2019b), while at ambient temperatures, challenges remain in terms of chemical oxygen demand (COD) removal and methane production. Hydrolysis is considered as the rate-limiting step in biomass

decomposition, especially when operating temperature is below 25 °C, which can result in longer hydraulic retention time (HRT) and a larger footprint (Tian et al., 2018).

Various pretreatment methods have been previously evaluated to improve the hydrolysis of refractory wastes such as sludge in the wastewater treatment plants and organic solid wastes, which can effectively improve the biodegradability and the solubilization of complex wastes. However, most pretreatments (*e.g.*, chemicals addition such as NaOH, H_2O_2, ozonation; mechanical methods such as milling and ultrasounds; thermal pretreatment) require high operational costs and intensive energy input. Energy and cost-efficient technologies are still in demand to facilitate AD performance when treating medium and high solid-content wastes such as blackwater and waste activated sludge. Recent studies demonstrated that oxidative pretreatment such as micro-aeration and chemical oxidation techniques could facilitate the hydrolysis efficiency in AD by promoting hydrolysis rates and enhancing solubility and biodegradability of recalcitrant wastes (Charles et al., 2009; Duarte et al., 2018; Gautam et al., 2019).

A two-stage AD system that separates the acidogenic stage from the methanogenic stage presents higher yields and better process stability than a single-stage system (Cremonez et al., 2021). The operational conditions favoring distinct microorganisms in stages with different functions (*i.e.*, fermentation and methanogenesis) can be optimized separately (Ding et al., 2021). However, the industrial acceptance of a two-stage AD system remains low due to economic issues of building and maintaining a second digester (Rajendran et al., 2020). The development of efficient and economical novel anaerobic digester configurations is required to expand the practical applications of anaerobic treatment over the conventional energy intensive aerobic wastewater treatment.

1.2 Research objective and approach

The objective of this research is to develop efficient and cost-effective anaerobic treatment strategies and elucidate the underlying microbial driving force to facilitate the bioenergy production from high strength wastewaters with different solids content. In order to accomplish this task, the specific objectives and approaches are provided as follows:

1) *Investigate the feasibility of using calcium hypochlorite pretreatment to enhance the solubility and biodegradability of WAS.*

The feasibility of applying calcium hypochlorite to the AD of WAS in terms of biodegradability promotion and P fixation were investigated. Values of the sludge solubilization degree and variations in calcium and phosphate concentrations in WAS after adding different amounts of $Ca(ClO)_2$ under aerobic pretreatment conditions were compared to values obtained in WAS with no $Ca(ClO)_2$ addition. The methane recovery from untreated WAS and WAS pretreated with hypochlorite were determined in batch reactors. Then, two semi-continuous anaerobic sequencing batch reactors (ASBRs), one fed with $Ca(ClO)_2$ pretreated thickened WAS (TWAS) and one with raw TWAS, were operated at mesophilic conditions (35 °C) for 145 days, to further assess the impact of hypochlorite pretreatment of WAS on the performance of continuously operated reactors. 1% $Ca(ClO)_2$ was added to WAS to improve its anaerobic digestion, and the common hydraulic retention time (HRT) (~20 days) was shortened to 5 days by introducing three loading shocks to each reactor to compare the performance stability and resilience between the digestion of $Ca(ClO)_2$ pretreated TWAS and untreated TWAS.

2) *Illustrate the role of micro-aeration pretreatment on the anaerobic digestion of blackwater in ASBRs at 20 ℃.*

Hydrolysis is limited in anaerobic blackwater treatment at low temperatures. Micro-aeration was applied in ASBRs as a pretreatment to facilitate the blackwater AD performances at ambient room temperature (20 ℃). The effect of different microaerophilic conditions on the hydrolysis, acidogenesis, and methanogenesis steps were studied for four operational stages with the HRT stepwise reduced from 5 days to 2 days.

3) *Design and operate a novel GAC-amended UASB that realizes phase separation.*

The optimal conditions for hydrolysis/acidogenesis and methanogenesis are different and can be optimized separately in a two-phase AD system to improve the overall performance. A floated-GAC UASB reactor was constructed to allow sufficient fermentation near the reactor inlet, and to promote methanogenesis in the upper reactor column zones. Three UASB reactors, supplemented with plastic biofilm carriers-only, GAC-only and the self-fluidized-GAC (plastic biofilm carriers combined with GAC) reactors were operated and compared under ambient temperature (20 ± 0.5 ^{o}C) for 120 days.

4) *Explore the microbial community and functionality changes in the enhanced AD systems.*

The microbial community structure and diversity were analyzed to provide ecological profiles for these economical treatment technologies. Microbial communities that developed in different stages or reactor zones (including the biofilm) were analysed and compared. Microbial community dynamics were quantified using a non-steady-state mass balance model to reveal the microbiome responses to disturbances. Co-occurrence networks were investigated to reveal the microbial interactions. The functional profiles of the microbial communities were predicted using PICRUSt.

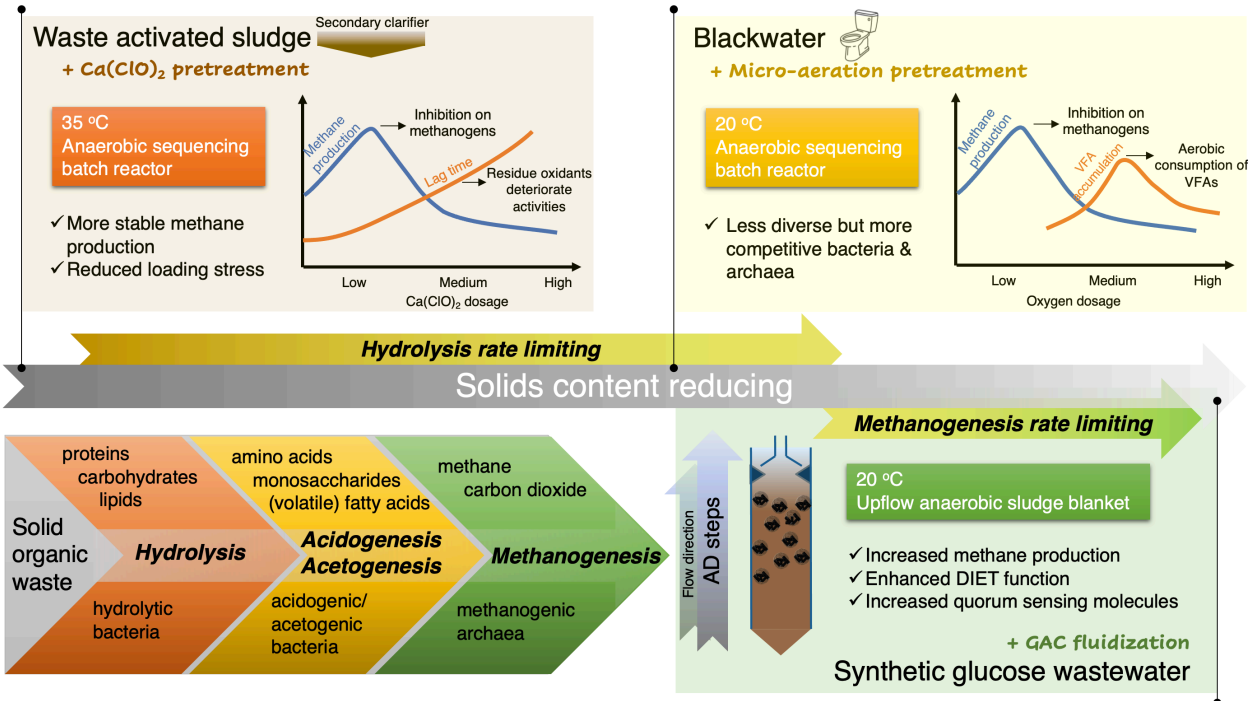

Fig. 1.1. Overview of thesis.

1.3 Thesis layout

This thesis is organized into eight chapters.

Chapter 1 gives a background and problem statement, and provides the motivation, objectives, and approaches of the research.

Chapter 2 provides sources and characteristics of the targeted wastes (*i.e.*, blackwater and WAS), summaries the available material in the literature about pretreatments in blackwater and WAS AD, identifies the limitations of previous studies, and proposes novel and cost-efficient strategies to improve hydrolysis and methanogenesis.

Chapter 3 investigates the feasibility of applying calcium hypochlorite as a WAS pretreatment strategy to improve AD treatment efficiency using laboratory reactors. The anaerobic digestibility

of WAS pretreated with low (5 – 20%) and high $Ca(ClO)_2$ doses (20 – 50%) was illustrated and compared with the AD of raw WAS. The development of fermentative and syntrophic bacteria in different reactors was elucidated by microbial community analysis. The dissolved organic compounds and the phosphorus content in liquid digestate were also included. This chapter is directed to objectives 1 and 4. This chapter validates $Ca(ClO)_2$ pretreatment in batch WAS AD and provides the optimum dosage that guided the continuously reactors operation in Chapter 4.

Chapter 4 investigates and compares the performances of two ASBRs, one fed with $Ca(ClO)_2$ pretreated thickened WAS (TWAS) and one with raw TWAS, at mesophilic conditions (35 °C) for 145 days. Three loading shocks were introduced to each reactor to compare the performance stability and resilience between the digestion of $Ca(ClO)_2$ pretreated TWAS and untreated TWAS. Microbial community shifts were quantified to reveal the microbiome responses to disturbances. This chapter is directed to objectives 1 and 4.

Chapter 5 investigates the impacts of micro-aeration on the performance of ASBRs for blackwater treatment. Different micro-aeration rates, 0, 5, 10, 50, and 150 mg O_2/L-reactor/cycle, and their effect on the hydrolysis, acidogenesis, and methanogenesis of blackwater were evaluated and compared at ambient temperature. The development of functional and oxygen-tolerant microbial communities was illustrated. This chapter is directed to objectives 2 and 4.

Chapter 6 presents a modified UASB reactor with self-fluidized GAC amendment that forms a semi-two-phase AD process treating synthetic high strength wastewater. Two control UASB reactors with only non-conductive or conductive materials were operated, monitored and compared with the novel UASB. The chemical and biological properties at different reactor heights were analyzed. This chapter demonstrates objectives 3 and 4.

Chapter 7 compares the microbial communities developed on settled or floated GAC biofilms in UASB reactors described from Chapter 6 to clarify the effect of the GAC biofilm to the methane production. DIET-related microbial functions in biofilms and surrounding sludge flocs in the settled GAC and floated GAC reactors were investigated along with the structure, diversity, and correlation of the microbial communities. This chapter demonstrates objectives 3 and 4.

Chapter 8 provides a concluding overall summary of the thesis. It includes the research summary and principal conclusions of the study, and sets recommendations for future studies in the similar fields.

Bibliographies from all chapter are combined and presented at the end.

CHAPTER 2 LITERATURE REVIEW

2.1 Wastewater management strategies

The global demand for clean water has been growing due to the rapid urbanization and industrialization (Kümmerer et al., 2018). However, large amount of wastewater is discharged without proper treatment due to the lack of sanitation services in developing countries, leading to the deterioration of water resources (Mara, 2013). Proper wastewater management strategies are essential to tackle the problems associated with the freshwater scarcity. The geographical, social, and economical properties should be taken into consideration during the planning of wastewater management systems to design sustainable wastewater infrastructure that adapts to local conditions (Abbassi and Baz, 2008). In general, wastewater management strategies can be categorized as centralized (*i.e.*, off-site management) or decentralized systems (*i.e.*, on-site management) (Wilderer and Schreff, 2000).

Centralized system

The conventional approach of wastewater treatment system collects wastewater by sewage network that leads to a centralized wastewater treatment plant (WWTP), where the organic material is removed by activated sludge processes (Oladoja, 2017). The centralized strategy offers the advantages including effective control of the effluent quality, and lower per capital cost, which has been widely applied in big cities serving large populations (Dodane et al., 2012). However, in small towns and rural areas, the implementation of centralized systems may face many difficulties (Hophmayer-Tokich, 2006). The cost of building and maintaining the collection system can be high, and without sufficient maintenance of the wastewater collection infrastructure, the chances of soil and ground water pollution would increase due to wastewater exfiltration (Roehrdanz et al., 2015). Further, treating municipal wastewater in centralized WWTPs is energy intensive due to

aeration, which consumes 35% to 75% of total energy input depending on the scale and processes of the plants (Otterpohl et al., 2008). Therefore, it is hardly feasible to build and operate a centralized sewer system in low- and middle-income countries for economic reasons.

Over 90% of the WWTPs use activated sludge process as the core technology to convert the organics in wastewater to carbon dioxide and water, with the production of significant amount of waste activated sludge (WAS), which requires further treatment before being suitable for land application or disposal (Campo et al., 2018; Liu, 2003). The goals of WAS processing include improving the dewaterability of raw WAS, converting the perishable organics to a stabilized form, and reduce the contaminants to meet the level for final disposal (Cao et al., 2021; Liang and Zhou, 2022).

Decentralized system

In low-density communities, *i.e.*, townships and rural aeras, the implementation of decentralized solutions is preferred from an economic perspective and has drawn increasing attention (Groh et al., 2015; Singh et al., 2015). The basic concept of decentralized wastewater management is to collect, treat, and dispose/reuse the wastewater at or near the wastewater producers so that the wastewater collection network is minimized, leading to a significant reduction of cost. As the collection component in decentralized systems is kept as minimum as possible, the challenge is to provide sufficient treatment to meet public health demands and water quality goals. Fortunately, unlike centralized systems, the decentralized systems can be designed for a specific site, which is more flexible in management than the centralized systems (del Castillo et al., 2022). The conventional centralized collection systems combine all kinds of household wastewaters, leading to a high wastewater volume with a wide variety of pollutants (Anglada et al., 2009; Bigda, 1995). This also results in the dilution of harmful components such as pathogens and toxicants, making it

difficult to be effectively treat. In comparison, within the framework of decentralized systems, a source-separated sanitation system allows for wider range of technologies to treat different wastewater streams (Butkovskyi et al., 2015; Ledezma et al., 2015; Maurer et al., 2006). Two waste streams, blackwater collected from the toilet, and greywater from the sink, shower, and laundry can be treated in dispersed treatment units with different processes according to their composition (Zeeman et al., 2008). This improves the recovery of water and nutrients, and the removal of pathogens and emerging pollutants. The development of novel technologies with minimum energy demand, low maintenance, and simple operation is needed for easy on-site applications.

2.2 Resource recovery from wastewater

Nowadays, the goals of wastewater management have moved beyond protecting public health and the aquatic environment to the reduction of energy input, reducing the waste, and recycling the nutrients due to the limits in resource availability (Mehta et al., 2015). Therefore, the focus of wastes handling has been changed from the treatment to resource recovery. Biotechnological processes are recognized as an economic and versatile way to transform waste/wastewater into value-added products such as biohydrogen, biopolymers, biogas, and VFAs (Ntaikou et al., 2009; Puyol et al., 2017). The development of environmentally and economically sustainable biotechnologies transforms sanitation from a costly service to a self-sustaining wastewater solution in a circular economy (Guerra-Rodríguez et al., 2020).

Waste activated sludge

In developed countries, approximately 80% of the municipal wastewater is treated by activated sludge process in the WWTPs to remove organic carbon and nitrogen compounds (Ghimire et al., 2021). Activated sludge process is an aerobic process that convert the organics to carbon dioxide

and water, with the production of new cells, a semi-solid waste or slurry known as waste activated sludge (WAS) or biosolids (Demirbas et al., 2017). WAS production is increasing with the expansion of industry and population, and its treatment can account for 25 – 65% of the total operation cost (Villamil et al., 2020). The appropriate disposal of WAS in an environmentally sound and cost-effective manner is necessary.

WAS from WWTPs has been recognized as a misplaced resource. Energy in WAS can be captured by producing renewable energy in useful forms (*e.g.*, electricity, methane, H_2, VFAs) through microbial energy conversion processes (Tao et al., 2020). The most implemented sludge handling technology is anaerobic digestion (AD) that generates biogas, a mixture of methane, carbon dioxide, and other trace compounds (Appels et al., 2008). Biogas is a sustainable alternative of natural gas and can be used to produce heat and electricity. The production of biogas considerably compensates the energy requirements (25 – 50%) in activated sludge process (Puyol et al., 2017). Another approach that can reduce sludge volume and destroy pathogens is biosolids incineration (Mo and Zhang, 2013). It generates energy through biosolids combustion and cuts down the disposal costs by reducing the WAS volume to minimum. However, the capital and energy cost are high, and the water content needs to be reduced to below 30% to achieve positive net energy (McCarty et al., 2011).

Stabilized biosolids can be applied as soil amendments or fertilizers since the sludge contains 20 – 30% of the N and up to 95% of the P from wastewater (Pritchard et al., 2010). Biosolids can be stabilized by several processes including aerobic and anaerobic digestion, alkaline treatment, composting, and heat drying (Turovskiy and Mathai, 2006). The fertilizers produced from biosolids release nutrients slowly than commercial fertilizers in land applications, and thus reduce the chances of groundwater or surface waters contamination. Except for the direct land

applications of WAS, the first step of P recovery is P releasing with sludge hydrolysis (Bi et al., 2014). Then, P can be recovered from the liquid phase as hydroxyapatite or struvite (Cichy et al., 2019). Finding an effective way to disintegrate sludge and release P is crucial to promote P recovery.

Blackwater

Blackwater stream is collected from the toilets, which mainly contains human feces, urine, toilet paper and the flushing water (Gao et al., 2019b). Human feces have the highest chemical energy content in the form of organic substances, and urine is rich in nutrients. In addition, the blackwater flow volumes are smaller than the greywater, leading to smaller footprint of the treatment facilities (Paulo et al., 2013). Therefore, source-separated blackwater offers great opportunities for on-site carbon and nutrients recovery. The most common form of energy that make the best use of the organic loads of wastewater is the methane-containing biogas, which is produced by anaerobic treatment (Wendland et al., 2007). A proven technology of blackwater anaerobic treatment is pilot scale upflow anaerobic sludge blanket (UASB) reactors, achieving 90 % of COD removal and 60 % of methane production (Slompo et al., 2019). Electrochemical processes have also been tested in laboratory reactors and showed great potential for source-diverted wastewater streams treatment (Zamalloa et al., 2013). The chemical energy was converted to electricity in microbial fuel cells, while organics were removed with the generation of hydrogen or methane with the applied voltage.

Nitrogen and phosphorus are also major targets for blackwater treatment. Blackwater contains 82% of the total N and 68% of total P in domestic wastewater (Kuramae et al., 2020; van Voorthuizen et al., 2008). Recovering these valuable nutrients is beneficial in the current context of the growing population and the diminishing of natural P reserves. The most intensively studied technology that can simultaneously recovery N and P from blackwater and produce fertilizers for agricultural use

is struvite ($MgNH_4PO_4 \cdot 6H_2O$) precipitation by magnesium dosage (Sun et al., 2020). Alternative additives such as aluminium, iron and calcium can also be used to precipitate P (Klimeski, 2007). Other available technologies include adsorption, air stripping, ion exchange, membrane bioreactors and electrochemical systems are also promising (Talekar and Mutnuri, 2021).

2.3 Anaerobic digestion

Anaerobic digestion is a very flexible technology that can be applied to the treatment of a wide range of different types of substrates (Mata-Alvarez et al., 2000). The organic components are degraded in the absence of oxygen, generating biogas and a residual stream (digestate). The energy value of biogas is widely recognized. It has almost identical characteristics to natural gas, which can be used as fuel for heating, lighting, and electricity production, on-site or transported elsewhere (Holm-Nielsen et al., 2009; Kleerebezem et al., 2015). AD realizes the bio-energy potential in organic materials and has advantages over other technological options such as flexible, easy to operate, no need for secondary processing, low energy requirement, and the residual digestate for agricultural reuse (Jensen et al., 2022).

AD undergoes four main phases, carrying out by different groups of microorganisms: hydrolysis, acidogenesis, acetogenesis and methanogenesis (Zamri et al., 2021). In the hydrolysis step, complex suspended compounds and colloidal matter are converted into soluble monomers and dimers by hydrolytic enzymes. Then, the soluble organics such as amino acids, sugars and long chain fatty acids are further converted into VFAs, alcohols and CO_2 by acidogenic bacteria. Acetogenic bacteria then convert VFAs and alcohols into acetic acids or H_2 and CO_2. Finally, methanogenic archaea use acetate or H_2 and CO_2 to produce methane.

AD performance varies for different types of substrates and the reactor configuration as well as the operational conditions (Kamali et al., 2016). Various biological conversion steps are required to be well balanced to prevent process failure due to the accumulation of intermediates. For instance, a loading rate exceeded the system capacity can result in the accumulation of VFAs, H_2 overproduction, and eventually lead to the deteriorated methane production performance (Mahmod et al., 2020). Research challenges remain in maximizing the energy recovery and digestate quality using effective approaches with low energy input.

2.3.1 Limitations in AD

AD is a muti-step complex process, the overall kinetics is controlled by the slowest step, *i.e.*, the rate-limiting step. It is crucial to determine the rate-limiting step before designing the AD process for a specific feedstock to maximize the efficiency and yields (Ma et al., 2013). Depending on the feedstock physic-chemical characteristics, two major steps can be rate limiting. For complex organic substrates with high solids content, hydrolysis is often considered as the rate-limiting step, while for soluble organic matter, the methanogenesis is rate-limiting (Tsigkou et al., 2022; Vavilin et al., 2008). The concentration, composition, and activities of anaerobic microbial communities involving in disparate metabolic steps are also crucial in achieving stabilized AD (Xu et al., 2021). AD process is accomplished by (i) fermentative bacteria secreting extracellular enzymes to solubilize particulate matters during hydrolysis; (ii) acid-forming bacteria metabolizing soluble organics; (iii) acetogenic bacteria that yield acetate; (iv) syntrophic acetate oxidizing bacteria (SAOB) that oxidize acetate to H_2 and CO_2; (v) hydrogenotrophic and acetoclastic methanogenic archaea that produce methane (Yuan et al., 2019). Stressful environmental conditions and toxicants such as low inoculum to substrate ratio, low temperature, VFAs accumulation, abnormal pH, high

free ammonia and H_2S often inhibit the activities of the microorganisms and lead to unsatisfactory AD performances (Yuan and Zhu, 2016).

Waste activated sludge

Among various WAS management approaches, AD is the most energy-efficient method for WAS treatment and stabilization. AD is widely favored as it stabilizes large volume of diluted sludge and reduces solid content, and substantially reduces the transportation cost. The pathogen levels are also reduced during AD. Further, the produced biogas can cover part of the energy requirements of the activated sludge process. However, the anaerobic biodegradability of WAS is often low due to its complex composition. It consists of mostly proteins (25 – 62.4%VS), humic substances (7.7 – 28.6%VS), bacterial cells (10 – 24%VS) and carbohydrates (7 – 19%VS) (Gonzalez et al., 2018). The organized structure of proteins and carbohydrates in WAS decreases the anaerobic biodegradability, while cells and humic substances are difficult to break down anaerobically. Therefore, pre-treatment methods have been applied to improve the AD treatment of WAS.

Blackwater

The feasibility of applying AD process to treat and recover energy from various backwater sources has been demonstrated in previous studies in different types of reactors under various operating temperatures (Gao et al., 2020b; Gao et al., 2019c). The highest organic loading rate (OLR) achieved is 4.1 kg COD/m^3/day treating vacuum toilet collected blackwater in a UASB reactor at 35 °C (Gao, 2020). Mesophilic (~35 °C) and thermophilic (~55 °C) conditions are preferred in AD to maintain high microbial activities and subsequently high treatment efficiencies (Zhang et al., 2021c; Zhang et al., 2020c). However, heating is great energy consumption especially in temperate and cold regions. Blackwater treatment under ambient room temperature (~20 °C) is attractive as

it reduces the capital cost and the heating energy consumption. Decomposing of the blackwater biomass is challenging at low temperatures because the hydrolysis rate is often limited, which may result in longer hydraulic retention time (HRT) and larger footprint (Huang et al., 2022). Pre-treatment techniques may offer solutions for such challenges.

High-strength soluble wastewater

The optimum pH for fermentation and methanogenic reactions falls into different ranges, being 5.5 and 6.5 for hydrolysis and acidogenesis, respectively, and 6.5 – 8.2 for methanogenesis (Kainthola et al., 2019). The acidogenesis phase can be overaccelerated during the AD treatment of easily hydrolysable substances such as food waste that contains high concentrations of soluble sugars or fats, leading to process instabilities and reactor acidification (Ma et al., 2021). Therefore, methanogenesis is the rate-limiting step in such cases since methanogenic microorganisms are extremely sensitive to acid accumulations. Conducting AD processes with phase separation is an interesting alternative to optimize the conditions separately for different groups of microorganisms, minimizing the impacts of VFAs accumulation and pH fluctuations on methanogenesis phase (Cohen et al., 1982). Two-phase AD process can be realized by connecting two independent reactors in series. However, it requires a large physical space and high capital cost (Baloch et al., 2007). Innovative reactors configurations that realize phase separation in a single reactor is attractive to improve the economic competitiveness of biomethane production in phased AD systems.

2.3.2 Pre-treatments to facilitate hydrolysis

Various pretreatment technologies (*i.e.*, chemical, mechanical, thermal treatments) have been previously evaluated to improve the hydrolysis of refractory wastes such as lignocellulosic biomass, sludge in wastewater treatment plants and organic solid wastes. Chemicals addition (*e.g.*

NaOH, H_2O_2, ozonation) is effective for enhancing the biodegradation of complex materials (Song et al., 2014; You et al., 2019), but can produce inhibitory compounds towards microorganisms, and may cause corrosion of the reaction vessels (Lee and Jeffries, 2011). Mechanical methods, *e.g.* milling and ultrasounds, can be used to improve the solubilization of extra- and intra-cellular organics (Kor-Bicakci and Eskicioglu, 2019; Zheng et al., 2013). Thermal pretreatment has also been shown to be effective in improving substrate hydrolysis, and the heating energy can be compensated with the combustion of produced methane (Toutian et al., 2020). It can be noted that pretreatments often require high operational costs and intensive energy input, energy and cost-efficient technologies are still in demand to facilitate AD performance when treating WAS and blackwater.

$Ca(ClO)_2$ addition in WAS treatment

WAS have low bioavailability to functional microbes, largely due to the presence of excessive extracellular polymeric substances (EPS) (Sari Erkan and Onkal Engin, 2020). Ultrasonication, hypothermal, and microwave treatments, enzymes, acids, and alkalis addition (Cosgun and Semerci, 2019; Hou et al., 2020; Ma et al., 2019; Zhou et al., 2019a) have been used to enhance sludge disintegration. However, high energy demand, operational complexity, and secondary environmental pollution limit the large application of these approaches.

A recent study showed that hypochlorite, a safe and economic oxidant, could cause intracellular oxidation and cell lysis, achieving simultaneous deep-dewatering and pathogens inactivation. Key contributors to pollutant decomposition include hypochlorite (ClO^-), hypochlorous acid (HOCl), and the hydroxyl radical (·OH), all of which are generated when hypochlorite dissociates in water (Zhang et al., 2020b). When added to WAS fermentation reactors, calcium hypochlorite ($Ca(ClO)_2$) induced a high volatile fatty acids (VFA) production at a lower dose and in a shorter time than

sodium hypochlorite (Luo et al., 2020). On the other hand, the anaerobic digestion of WAS results in high orthophosphate (PO_4^{3-}-P) concentrations in the fermentation liquor, which is often recycled to the parent activated sludge process, providing carbon sources for the denitrification process and subsequently increases the PO_4^{3-}-P loads in enhanced biological phosphorus removal (EBPR) systems (Bi et al., 2013). Adding metal ions (*e.g.*, calcium and iron) can form insoluble metal phosphates and has been developed to enhance phosphorus removal (Bunce et al., 2018).

Previous studies have reported improved performances of anaerobic fermentation (Luo et al., 2020; Zhang et al., 2020b) and dewaterability of WAS using calcium hypochlorite (Zhu et al., 2018b). However, because of its potential impact on the archaeal community, whether $Ca(ClO)_2$ can be applied to improve methane recovery from WAS remains unknown. Moreover, no information is currently available on the optimum pretreatment time of WAS using $Ca(ClO)_2$. Given the advantages of $Ca(ClO)_2$ pretreatment, which include low cost, easiness to apply, and the effectiveness for improving WAS hydrolysis, VFA production, phosphorus removal and pathogens reduction, the feasibility of applying $Ca(ClO)_2$ as a WAS pretreatment strategy for improving AD performance should be investigated (Dai et al., 2017; Kanazawa et al., 2020; Li et al., 2019b).

Micro-aeration for blackwater treatment

Introducing a small amount of oxygen (*e.g.* micro-aeration) was recently proven to be beneficial to the AD treatment by promoting hydrolysis rates (Fu et al., 2016), and was considered as a promising environment-friendly pretreatment strategy to enhance methane recovery from recalcitrant wastes (Nguyen and Khanal, 2018). Previous studies have found that anaerobic digestion of blackwater without micro-aeration can only recover upwards of less than 40% of chemical oxygen demand (COD) to methane at room temperature due to the low hydrolysis rate

of biomass content in blackwater. Oxygen injection can also help to reduce the accumulation of volatile fatty acids (VFA), especially when the loading rate is high (Nguyen et al., 2019). Further, micro-aeration treatment can reduce levels of toxic H_2S from the biogas, which is a more cost-effective (62% cost reduction) approach as compared to chemical absorption (Ramos et al., 2014). Micro-aeration has been applied to different kinds of feedstocks including highly recalcitrant feedstock such as corn straw (Fu et al., 2015), primary sludge (Diak et al., 2013), and co-digestion of brown-water and food-waste (Lim and Wang, 2013), where hydrolysis is critical to solubilize complex organics for downstream conversion. To our best knowledge, no studies to date have investigated the application of micro-aeration for low-temperature anaerobic treatment of blackwater.

Previously oxygen-based applications were often avoided during AD operation because of their potential inhibitory effects on obligate anaerobes. However, recent studies suggested that some strict anaerobes can also adapt to microaerophilic conditions by producing anti-oxidative enzymes or co-existing with facultative microorganisms quickly scavenging oxygen (Angle et al., 2017; Botheju and Bakke, 2011). The balance between these syntrophic microorganisms needs to be maintained by precise oxygen dosage control to prevent over aeration that exceeds the anti-oxidation capacities in a defined system. The effects of micro-aeration vary with regards to enhancing hydrolysis, controlling VFA accumulation, removing hydrogen sulfide, and maintaining suitable conditions for methanogenesis, depending on the amount of oxygen input (Deng et al., 2009; Lim et al., 2014). Previous studies have primarily focused on the comparison between anaerobic and microaerobic conditions (Ruan et al., 2019; Yin et al., 2016). Many of these studies were conducted in batch reactor mode (less than 60 days), unable to evaluate the impact of

micro-aeration on the AD process in long-term operation, especially with respect to the microbial community structures after long-term acclimation (Nguyen and Khanal, 2018).

2.3.3 Conductive materials stimulate DIET and methanogenesis

Efforts have been made to develop strategies to improve AD performance for high-strength soluble/easily hydrolysable wastewater treatment in harsh environments, such as under low temperature or high organic loading conditions (Gao et al., 2019c; Rotaru et al., 2014; Zhang et al., 2020d). The addition of conductive materials to AD systems has been shown to improve methane production (Yang et al., 2017; Zhang et al., 2020d), possibly due to its stimulation of direct interspecies electron transfer (DIET) between fermentative bacteria and methanogens.

The conversion of fermentation intermediates (especially propionate) to methane can only happen when produced hydrogen is maintained at a very low level (H_2 partial pressure lower than 100 ppm) due to the thermodynamics limit (Barua and Dhar, 2017; Yin and Wu, 2019). The transportation of electrons from intracellular or extracellular electron donors to acceptors across the cell membrane is a process referred to as extracellular electron transfer (EET) (Feng et al., 2020). There are two main types of EET mechanisms: mediated electron transfer (MET) and direct interspecies electron transfer (DIET) (Baek et al., 2018). Compared to MET, DIET is considered to be a more efficient electron transfer pathway through cell components such as e-pili or c-type cytochrome without relying on the diffusion of electron carriers such as hydrogen (Barua and Dhar, 2017; Park et al., 2018). However, the effective range of DIET between different species is often low (Igarashi et al., 2020). The proposed mechanism for long-range DIET is through cellular appendices such as pilus-like structures or forming filamentous multicellular structure, which allows electron transport at centimeter scales (Liu et al., 2018; Yin and Wu, 2019). Unfortunately, the biosynthesis of these conductive cell components requires significant energy investment by

microbes (Xu et al., 2018). Several conductive or semi-conductive materials such as granular activated carbon (GAC), biochar, carbon nanotubes, and magnetite have been reported to greatly enhance the methanogenesis in AD (Dang et al., 2016; Lee et al., 2016; Martins et al., 2018; Zhang et al., 2018). Park et al. (Park et al., 2020) reported that under lower temperature conditions (25 ^{o}C), GAC supplementation reduced the lag time and increased the maximum methane production rate in rural wastewater anaerobic digestion. These stable and electrically conductive materials promote DIET between electron-donating and electron-accepting cells via a conduction-based mechanism, which compensates for the lack of pili and other cell components involved in DIET.

Mechanisms underlying the GAC benefits

In general, GAC supplementation offers great advantages in AD as reported by many researchers (Florentino et al., 2019; Guo et al., 2020b; Yang et al., 2017), and the effects of GAC may go beyond the stimulation of DIET (Yin and Wu, 2019). Another crucial factor that can affect EET and methanogenic processes is the oxidation-reduction potential (ORP), which can be decreased to an ideal level for methanogenesis with the addition of redox materials such as carbon nanotubes (Gu et al., 2019; Salvador et al., 2017). Moreover, the formation of biofilm or granular sludge allows for different bacteria to spatially group together, which remarkably benefits biomass mutual cooperation (Marsili et al., 2008; Richter et al., 2009; Wang et al., 2019a; Xu et al., 2016; Zhang et al., 2019c). GAC provides high surface area for bacteria to attach to and shortens the cell-cell distance to achieve efficient interspecies electron transfer. However, the amount of GAC applied in anaerobic reactors is often low, ranging from 0.5 to 50 g/L, and the attached biomass makes up less than 10% of the total biomass yet is responsible for more than 30% of the methane production (Lee et al., 2016). In a recent study, a relatively small volumetric ratio of GAC (7% volume) enhanced the organic loading capacity by 4-times and methane production by 1-time (Guo et al.,

2020b). It was revealed that even not directly in contact, GAC enhanced the sludge microbial activity and stimulated microbial community changes based on RNA analysis (Guo et al., 2020b). Yin et al. (Yin et al.) and Lv et al. (Lv et al., 2018) proposed that quorum sensing (QS), which regulates the microbial density and structure by excreting signal molecules, was affected by the addition of conductive materials. Several signal molecules such as acyl-homoserine lactone (AHL) and 3'-5' cyclic diguanosine monophosphate (*c*-di-GMP) were reported to regulate the genera that participated in DIET (Bordeleau et al., 2015; Jenal et al., 2017; Lv et al., 2018), indicating that QS may play an important role in adjusting the microbial community to induce syntrophic interactions. Further, the secretion of signal molecules may potentially contribute to sludge granulation, allowing the microbes to stay in close proximate and promotes syntrophic interactions (Ding et al., 2015). Limited number of studies have applied GAC in a continuous AD reactor operated under low temperature conditions (10 – 20 ^{o}C), which is an aera of interest for AD operation in temperate regions (Park et al., 2020).

Further improve AD by GAC fluidization

Due to the heavy nature of GAC, it settles at the bottom of a continuous UASB reactor and limits the contact between GAC and biomass; therefore, it is potentially beneficial to fluidize the GAC. Conventional fluidization of GAC requires maintaining a high up-flow velocity (at least 200 mL/min), as seen in conventional fluidized-bed biofilm reactors (FBBR) (Islam et al., 2014; Puyol et al., 2015). To reduce operation costs, other attempts in GAC-fluidization in bioreactors have been investigated. For instance, Park et al. (Park et al., 2018) suggested fabricating moving-bed biomass-support media from conductive materials, which prevented the formation of thick biofilms and stimulated DIET more efficiently than fixed-bed media. Recently, Liu et al. (Liu et al.) demonstrated enhanced AD performance by gluing graphite on high-density polyethylene

(HDPE) as an electron mediator, however, mechanical mixing was still required. The introduction of low-density carriers to decrease the overall density and increase GAC distribution in the reactor may help to provide better mixing conditions in GAC-based UASB reactors, further improving reactors performances.

2.4 Research gaps

Blackwater and waste activated sludge are attractive renewable bioenergy sources that are abundantly found in human habitats. Anaerobic digestion has been extensively studied for the effective utilization of blackwater and WAS for biogas production. The initial solids hydrolysis is considered as a rate-limiting step in blackwater and WAS treatment especially at low operational temperatures in temperate regions. Various pretreatment technologies (physical, chemical, and biological) have been tested in previous studies. However, these pretreatments often involve expensive chemicals, biological enzymes, or mechanical equipment, making them not economically feasible. A cost-effective and efficient method is lacking to increase AD efficiency especially at low-temperature (winter) conditions. Another potential limiting step is methanogenesis in the treatment of easily hydrolysable or low-solid-content substances. Connecting two independent reactors in series can eliminate intermediates inhibition on the methanogenesis phase. However, it requires a large physical space and high capital cost. Innovative reactors configurations that realize phase separation in a single reactor is attractive for economic reasons yet have not been demonstrated.

CHAPTER 3 CALCIUM HYPOCHLORITE ENHANCES THE DIGESTIBILTY OF AND THE PHOSPHORUS ROVERY FROM WASTE ACTIVATED SLUDGE[1]

A version of this chapter has been published in Bioresource Technology.

3.1 Introduction

Within the framework of the conventional centralized wastewater collection systems, large amount of waste activated sludge (WAS) generated from wastewater treatment plants (WWTP) contains abundant carbon and nutrients, making it a good source for bioenergy recovery (Adeleke et al., 2019; Appels et al., 2008; Kim et al., 2003). Anaerobic digestion (AD) is an effective process for energy recovery and WAS reduction (Ikumi et al., 2014). However, the poor digestibility and hydrolysis of WAS limit AD applications.

Hypochlorite has been found to aid pollutant removal and to contribute to sludge dewatering (Zhu et al., 2018a). Compared to other advanced oxidation methods (*e.g.*, Fenton oxidation, ozonation, electro-oxidation), the advantages of hypochlorite-based technologies include low cost, easy application, few safety concerns, and the ability to function over a wide range of pH values (Yu et al., 2019). Sodium hypochlorite deteriorates the dewatering performance in the presence of sodium ion, but calcium hypochlorite is stable when kept dry; and calcium ions can act as coagulants, improving sludge settleability. Applying calcium hypochlorite in WAS disposal has been found effective in terms of enhancing the performance of WAS fermentation, P removal, dewaterability,

[1] Yu, N., Sun, H., Mou, A. and Liu, Y. 2021b. Calcium hypochlorite enhances the digestibility of and the phosphorus recovery from waste activated sludge. Bioresource Technology 340, 125658.

and pathogens removal, while its effects on WAS digestibility remains unknown (Dai et al., 2017; Kanazawa et al., 2020; Li et al., 2019b).

The current study investigated the feasibility of applying calcium hypochlorite to the anaerobic digestion of WAS in terms of biodegradability promotion, phosphorous fixation, methane recovery, and microbial community response. Values of the sludge solubilization degree and variations in calcium and phosphate concentrations in WAS after adding different amounts of $Ca(ClO)_2$ under aerobic pretreatment conditions were compared to values obtained in WAS with no $Ca(ClO)_2$ addition. The methane recovery from untreated WAS and WAS pretreated with hypochlorite were determined. Microbial communities were analyzed to provide ecological profiles for this economical WAS treatment technology.

3.2 Materials and methods

3.2.1 WAS source and characterization

Waste activated sludge was collected from a secondary sedimentation tank in a local WWTP (Edmonton, Canada), and was stored at 4 °C until use. WAS characteristics were: total suspended solids (TSS) 4.9 ± 0.2 g/L, total chemical oxygen demand (TCOD) 5.8 ± 0.4 g/L, volatile suspended solids (VSS) 3.6 ± 0.1 g/L, soluble chemical oxygen demand (SCOD) 0.2 ± 0.08 g/L, pH 6.6 ± 0.2, and total phosphorous (TP) 135 ± 0.2 mg P/L.

3.2.2 Batch experiments design

WAS pretreatment with different dosages of $Ca(ClO)_2$

Ten-day WAS pretreatment tests were performed using serum bottles. In this study, 15 serum bottles, with a working volume of 120 mL, were operated at room temperature (20 – 24 °C) to examine the changes of WAS characteristics after pretreatment with five different $Ca(ClO)_2$

dosages in triplicate. Firstly, 50 mL of WAS was transferred to each bottle. Then, calcium hypochlorite ($Ca(ClO)_2$) with 65% available chlorine from Sigma Aldrich (Canada) was added to the serum bottles at 0%, 5%, 10%, 20%, and 50% dosages (0, 0.05, 0.1, 0.2, and 0.5 g per g TSS in WAS), respectively. After gently shaking to mix, the bottles were sealed using butyl rubber caps, putted in an incubator, and shaken at 120 rpm in dark. The caps were opened every two days to assure aerobic conditions. Mixed liquor samples were collected immediately after the $Ca(ClO)_2$ addition, and 9, 23, 46, 141.5 and 239 hours after the $Ca(ClO)_2$ addition. The liquid characteristics including SCOD, pH, calcium and phosphate concentrations were monitored to illustrate the impact of $Ca(ClO)_2$ on WAS.

Anaerobic digestion of pretreated WAS

Anaerobic digestion of the $Ca(ClO)_2$ pretreated WAS (at 5 different $Ca(ClO)_2$ pretreatment doses) was performed in 120 mL serum bottles to study the impact of $Ca(ClO)_2$ on methane recovery from WAS. The inoculum sludge with around 10 g/L of VSS was taken from a mesophilic anaerobic digester. In serum bottles, 25 mL of the pretreated WAS (with 0%, 5%, 10%, 20%, and 50% (of WAS TSS) $Ca(ClO)_2$ addition and mixed for 30 mins until uniform suspension was obtained) was mixed with 25 mL anaerobic digested sludge. Deionized water was mixed with the seed sludge as blank reactors to determine its endogenous methane production. The bottles were flushed with nitrogen gas for 10 mins to create anaerobic conditions and sealed with rubber stoppers and aluminum caps. The bottles were shaken at 120 rpm at room temperature. The methane production was continuously monitored in 240 days. Triplicated bottles were set up for all batch tests.

3.2.3 Analytical methods

WAS characteristics—TCOD, SCOD, TSS, VSS—were determined following the standard methods of the America Public Health Association (APHA, 1985). COD was measured by sealed

digestion and spectrometry method. The samples were filtered, dried, and weighed to determine suspended solids content. Total phosphorus (TP) and PO_4^3-P were determined using Hach TNT vial tests (Hach, USA). A pH meter (B40PCID, VWR, SympHony) was used to measure the sludge pH.

An EEM fluorescence spectrophotometer (Agilent, Australia) was used to obtain the fluorescence spectra of the sludge supernatant. The mixed liquor was filtered through 0.45 μm filter and diluted with deionized water before each measurement.

Methane generation in the head space of the bottles was determined by analyzing the biogas composition as well as the pressure. A manual pressure meter (GMH 3151, Germany) was used to measure the gas pressure in headspace before and after each biogas sampling. Headspace biogas (2 mL) was taken from each bottle and analyzed using a 7890B gas chromatograph (Agilent Technologies, USA). Temperatures of the oven, injector, and detector were 100, 150, and 200 °C, respectively. At the end of the anerobic digestion, the sludge was sampled, and the sample was dried at 105 ºC. Ca, Mg, and P in the dried sludge were analyzed using inductively coupled plasma mass spectrometry (ICP-MS) (Elan 6000, Perkin Elmer, Canada).

3.2.4 Modified Gompertz model

To compare the maximum rates of methane production (R_{max}), the lag phase (λ), and the biomethane potential (P), the methane production curves were fitted to a modified Gompertz model using OriginPro®.

3.2.5 Microbial community analyses

Sludge samples (2 ml mixed liquor) were taken from the bottles for DNA extraction after 140 d anaerobic digestion. After centrifuged for 10 min at 5000 *g*, the supernatant of the sample was

discarded. Then, the sludge pellet was used to perform DNA extraction using the DNeasy PowerSoil kit (QIAGEN, Toronto, Canada) following the manufacturer's protocol. The microbial 16S rRNA genes (V4 hypervariable regions) were amplified, barcoded and sequenced at the Génome Québec Innovation Centre (Illumina Miseq PE250 platform, Montréal, QC, Canada).

Raw sequences were analyzed with the QIIME2 DADA2 algorithm (Callahan et al., 2016). The reference database was the Greengenes database, version 13_8 (99% similarity) (McDonald et al., 2012; Werner et al., 2012). Alpha diversity was computed in RStudio, version 3.4.1, using the "vegan" package (Jari Oksanen et al., 2017).

3.2.6 Statistical analysis

Three replicates of each condition were set up and the results were reported as mean ± standard deviation. The means were compared using an analysis of variance (ANOVA) to determine the significance level using Microsoft Excel® software Version 16.51. The effect of $Ca(ClO)_2$ is considered significant when the p-value is less than 0.05.

3.3 Results and discussion

3.3.1 Solubilization of WAS under aerobic conditions

The disintegration of WAS was reflected in an increase in SCOD. The concentration of SCOD at different $Ca(ClO)_2$ doses pretreated WAS is shown in Fig. 3.1. The $Ca(ClO)_2$ pretreatment of WAS resulted in an significant increase in SCOD ($F = 13.59$, $DF = 4$, $P < 0.01$) from 222.7 ± 14.8 mg/L in the control (without $Ca(ClO)_2$ addition) to 366.2 ± 9.9 mg/L, 415.7 ± 0 mg/L, and 430.6 ± 4.9 mg/L in the 0.1, 0.2, and 0.5 g $Ca(ClO)_2$/g TSS pretreated samples, respectively. For the lowest $Ca(ClO)_2$ dosed samples (5% $Ca(ClO)_2$, TSS basis), there was no observed immediate SCOD release. With $Ca(ClO)_2$ pretreatment, the SCOD of WAS increased to up to 945.3 mg/L in the

following 23 hours. With no $Ca(ClO)_2$ addition to WAS, the SCOD decreased rapidly in 9 hours and remained at a low level (< 100 mg/L) for 10 days. Additions of 0.05, 0.1, 0.2, 0.5 g $Ca(ClO)_2$/g TSS caused SCOD concentrations to peak in 23, 46, 96, 239 hours, respectively. A SCOD concentration of 1009.6 mg/L was obtained with 10% $Ca(ClO)_2$ addition to a WAS sample. SCOD concentrations of 970.0, 910.7, and 826.5 mg/L were obtained with 20%, 50% and 5% $Ca(ClO)_2$ (TSS basis), respectively, which were 3.7 to 4.5 folds changes as compared to the control sample where no $Ca(ClO)_2$ was added. The results demonstrated that $Ca(ClO)_2$ addition did not solubilize WAS instantaneously, but might have weakened the cell walls and enhanced the biodegradability of WAS. However, high $Ca(ClO)_2$ doses deteriorated the microbial activity and slowed the biological solubilization progress.

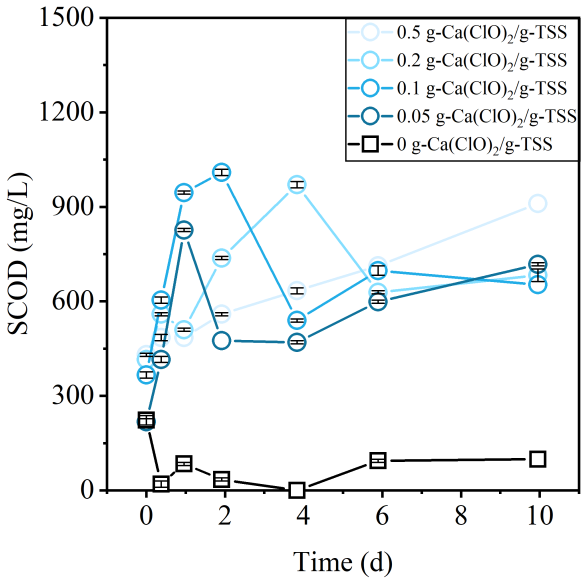

Fig. 3.1. SCOD release from WAS after different dosages of $Ca(ClO)_2$ addition. Error bars were the standard deviations, which were calculated from triplicate tests.

3.3.2 Calcium and phosphate precipitation from WAS conditioned with calcium hypochlorite

Untreated WAS had a pH of 6.57 ± 0.01. The pH in WAS samples increased to 6.67 ± 0.01, 6.71 ± 0.01, and 6.77 ± 0.01 with dosages of 5%, 10%, and 20% $Ca(ClO)_2$ (TSS basis), respectively, as shown in Fig. 3.2A. WAS treated with 50% $Ca(ClO)_2$ (TSS basis) recorded an initial pH of 7.57 ± 0.01. As $Ca(ClO)_2$ dissociated in water, the ClO^- anion accepted a proton from a water molecule, leaving a hydroxyl anion in solution and led to the pH increase. Then, the pH rapidly decreased to 6.81 ± 0.01 in 9 hours, indicating the rapid consumption of the generated hypochlorous acid.

Fig. 3.2B and 2C illustrates the calcium (Ca^{2+}) and phosphate (PO_4^{3-}) variations in WAS measured after $Ca(ClO)_2$ addition. The total calcium concentration (including the Ca^{2+} in raw WAS and the Ca^{2+} from $Ca(ClO)_2$ dissociation) in each group is represented by the dashed lines of corresponding color. High $Ca(ClO)_2$ addition (0.2 and 0.5 g $Ca(ClO)_2$/g TSS) immediately triggered calcium precipitation, as indicated by the lower Ca^{2+} concentrations compared to the corresponding total calcium concentrations. This was more evident at the highest $Ca(ClO)_2$ additions (645 mg/L total calcium and 326 ± 2 mg/L Ca^{2+}). The calcium precipitate was partially solubilized in one day due to pH decrease of the sample. Initially, the level of soluble PO_4^{3-} was similar in the samples without $Ca(ClO)_2$ and with low $Ca(ClO)_2$ addition (62.09 ± 0.02 to 65.76 ± 0.07 mg/L PO_4^{3-} in samples with 0 to 20% $Ca(ClO)_2$ (TSS basis) addition). However, a low level of soluble PO_4^{3-} (11.37 ± 0.03 mg/L) was detected after adding 50% $Ca(ClO)_2$ (TSS basis) to WAS, indicating the co-precipitation of PO_4^{3-} and Ca^{2+}. The concentrations of PO_4^{3-} increased slightly in hypochlorite pretreated WAS in 1 day, whereas phosphate concentrations in the control (no $Ca(ClO)_2$ addition) sharply decreased to 0 mg/L in 9 hours, then slowly recovered to 87.14 ± 0.16 mg/L in 142 hours. The phosphorus reduction observed in the control might be explained by the aerobic metabolism

of polyphosphate accumulating organisms (PAOs) (Kristensen et al., 2021; Palatsi et al., 2021). Higher SCOD concentrations in the hypochlorite treated WAS might benefit glycogen accumulating organisms and compromise the competitive advantage of PAOs (Panswad et al., 2007). WAS treated with low $Ca(ClO)_2$ (5 – 10% $Ca(ClO)_2$, TSS basis) exhibited the highest phosphate release (103.15 – 105.53 mg/L PO_4^3-P) after 10 days culture, whereas WAS pretreated with high $Ca(ClO)_2$ (0.5 g $Ca(ClO)_2$/g TSS) showed 39% phosphate removal compared to the control. This could be explained by the oxidative effect of ClO^- and its derivates enhanced phosphorus release from WAS, and a high calcium concentration triggered calcium-phosphate precipitation, removing Ca^{2+} and PO_4^{3-} simultaneously.

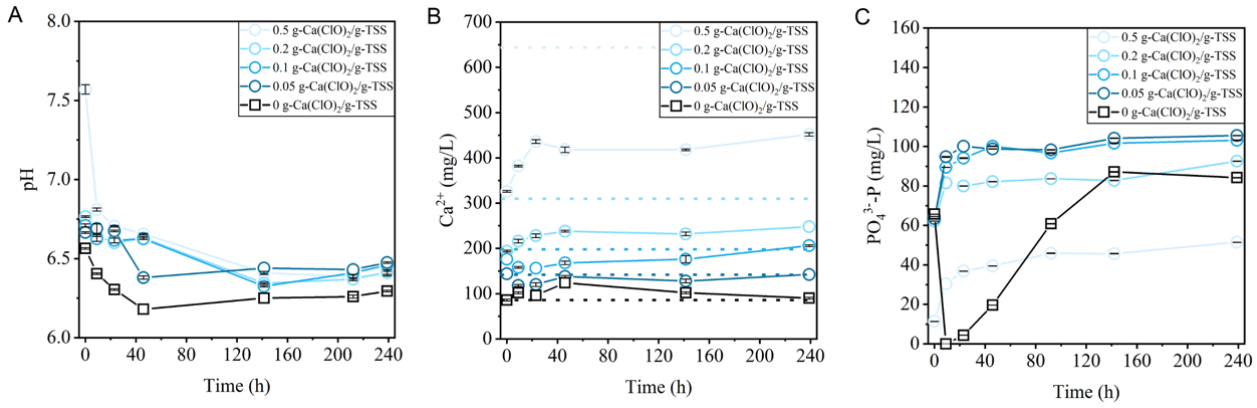

Fig. 3.2. Variations in pH (A), levels of calcium (B) and phosphate (C) after different doses of $Ca(ClO)_2$ were added to WAS (F = 142.55 and 12.52 for Ca and P, respectively, DF = 4, $P < 0.01$ for both Ca and P). The dashed lines with the same color as the solid lines represent the total calcium concentrations in the corresponding hypochlorite dosages. Error bars were the standard deviations, which were calculated from triplicate tests.

The dissolved organic matter in WAS pretreated with calcium hypochlorite was characterized using 3D-EEM spectroscopy (Fig. 3.3). Raw WAS has three peaks in Regions I, II, and IV

(representing aromatic protein, aromatic protein II, and soluble microbial by-products, respectively), as shown in Fig. 3.3A-0, illustrating that aromatic protein as well as tryptophan and protein-like substances were dominant among the DOM with fluorescence characteristics in WAS. As $Ca(ClO)_2$ was increased, the peaks belonging to the protein-like regions (Regions I, II, and IV) decreased. However, the fluorescence intensity in Regions V and III (humic acid-like substance and fulvic acid-like substance, respectively) first increased and then decreased. The results illustrated that $Ca(ClO)_2$ addition stimulated the degradation of protein-like substances, releasing humic acids and fulvic acids. Further, excessive $Ca(ClO)_2$ might contribute to the degradation of non-biodegradable humic acid and fulvic acid, as indicated by the lowest fluorescence intensity detected in WAS with the highest $Ca(ClO)_2$ addition. After 10 days of cultivation, the fluorescence intensity of Regions I, II, and IV disappeared in raw WAS, indicating that protein-like substances were consumed. In comparison, two peaks in Regions II and IV appeared with 5% $Ca(ClO)_2$ (TSS basis) addition; these were protein-like compounds, indicating biodegradability (BOD_5) (Jimenez et al., 2014). However, a further increase of $Ca(ClO)_2$ to 20% (TSS basis) lead to an increase in recalcitrant humic and fulvic substances. WAS pretreated with 50% $Ca(ClO)_2$ (TSS basis) exhibited the weakest fluorescence intensity of all the hypochlorite pretreated samples, indicating the lowest microbial activity. The results indicate that low $Ca(ClO)_2$ addition improved the WAS biodegradability. In comparison, higher levels of $Ca(ClO)_2$ pretreatment possibly promote WAS disintegration and the accumulation of humic acid, which inhibits sludge biodegradation (Azman et al., 2017a; Guo et al., 2014).

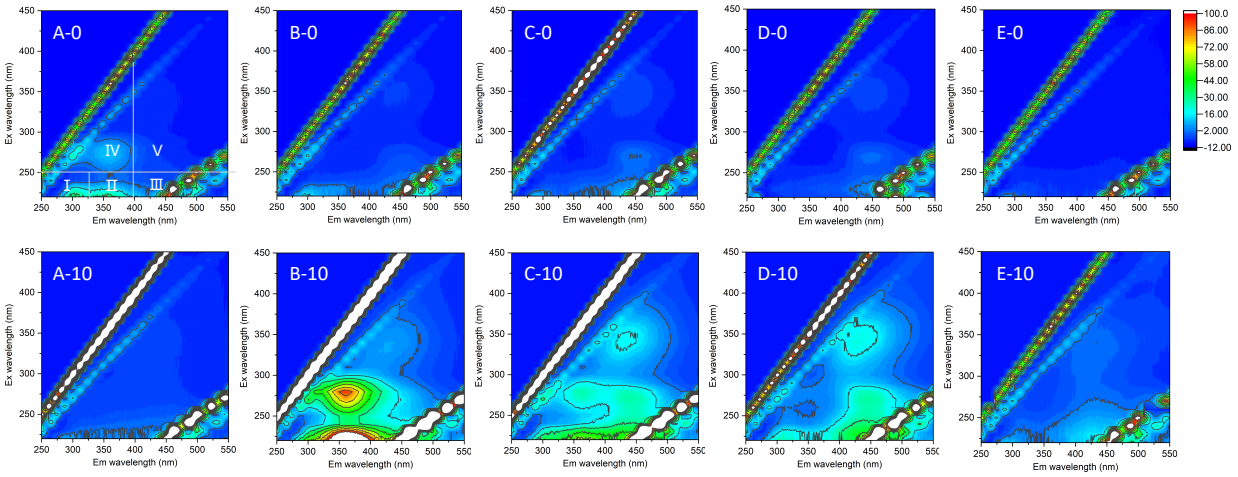

Fig. 3.3. Fluorescence spectra of liquid obtained in WAS pretreated with 0 (A), 0.05 (B), 0.1 (C), 0.2 (D), 0.5 (E) g $Ca(ClO)_2$/g TSS at day 0 (-0) and day 10 (-10). Fluorescence regions of the EEM spectrum are illustrated in A-0.

3.3.3 Impact of $Ca(ClO)_2$ pretreatment levels on WAS methane production

$Ca(ClO)_2$ pretreatment significantly altered the methane production pattern of WAS AD ($F = 13.14$, $DF = 4$, $P < 0.01$). According to the modified Gompertz model, values of the methane potential were 106.15 ± 4.20, 109.33 ± 4.01, 117.07 ± 3.00, and 111.51 ± 3.57 mg COD at $Ca(ClO)_2$ pretreatment dosages of 0, 5%, 10%, and 20% (TSS basis), respectively (Fig. 3.4). Untreated WAS converted only 42.05 ± 0.01% of the total COD to methane in 233 days, with a maximum methane production rate of 0.85 ± 0.10 mg COD/reactor/d. After pretreated with 0.05 to 0.2 g $Ca(ClO)_2$/g TSS, the methanation rate was elevated to 46.12 ± 4.59%, 51.57 ± 2.23%, and 45.18 ± 1.07%, respectively. The maximum methane production rate increased by 30.25%, 89.89%, and 54.51% when pretreated with 5%, 10%, and 20% of $Ca(ClO)_2$ (TSS basis), respectively (these numbers were obtained from the modified Gompertz model fitting results). However, a $Ca(ClO)_2$ dosage greater than 10% of TSS resulted in an extended lag phase (6 d, 49 d, and 177 d in 0.1, 0.2, and 0.5 reactors, respectively (according to the modified Gompertz model). As mentioned in section

3.1, the activities of functional microorganisms in $Ca(ClO)_2$ pretreated WAS decreased when the $Ca(ClO)_2$ dosages were increased. The strong oxidative ability of $Ca(ClO)_2$ and the reactive oxygen species generated, such as •OH, have been reported to largely reduce the number of fermentative bacteria (Zhang et al., 2020b). Further, a high oxidation-reduction potential (ORP) in the substrate (WAS) can shock obligate anaerobic seed microbes, especially methanogens. It has been reported that Ca^{2+} can form a bridge between macromolecular organic molecules and hinder the hydrolysis of particulate organic matter (Yin et al., 2020a). This binding effect of Ca^{2+} may cause flocculation of the cells and the EPS damaged by ClO^- and its derivatives; large flocs can negatively affect the hydrolysis kinetics and prolong the lag phase of WAS digestion at high hypochlorite doses (Chen et al., 2016). A small amount of calcium can stimulate the growth of microorganisms and upgrade biogas by CO_2 sequestration, whereas high calcium concentrations (> 2 g/L) can negatively affect methanogenic activity (Chen et al., 2020; Czatzkowska et al., 2020).

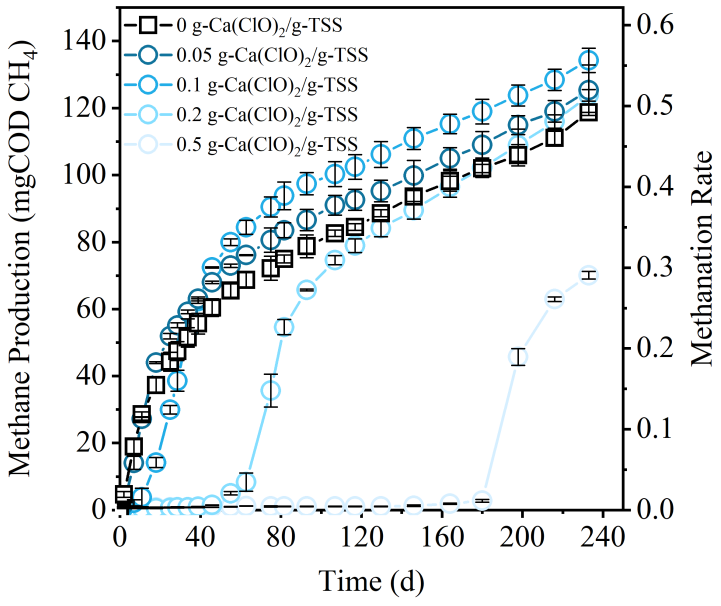

Fig. 3.4. Methane production from WAS pretreated with different doses of calcium hypochlorite. The $Ca(ClO)_2$ conditioned WAS was seeded with anaerobic digested sludge. Error bars were the standard deviations, which were calculated from triplicate tests.

3.3.4 Metal contents in the sludge

Fig. 3.5 shows the levels of magnesium, calcium, and phosphorus in sludge pretreated with different concentrations of calcium hypochlorite. Calcium in the sludge increased as the calcium hypochlorite in the pretreatment increased, reaching 1.28 mol/kg dry solids with 50% $Ca(ClO)_2$ (TSS basis). With a sludge pretreatment of 10% $Ca(ClO)_2$ (TSS basis), magnesium and phosphorus reached 0.45 mol and 1.07 mol, respectively per kg dry solids.

Previous studies reported that calcium hypochlorite can remarkably reduce soluble PO_4^{3-} in fermentation liquids and precipitate into sludge as apatite (a group of phosphate minerals, *e.g.*, hydroxyapatite, fluorapatite and chlorapatite) with the combination of Ca^{2+}, illustrating the positive effects of $Ca(ClO)_2$ in PO_4^{3-} fixation (Zhang et al., 2020b). Here, $Ca(ClO)_2$ at 0.1 g/g TSS achieved highest phosphorus recovery, 1.1 mol/kg dry solids. This $Ca(ClO)_2$ dosage also promoted a P fraction in the Ca/Mg-P precipitations, as indicated by the lowest Ca and Mg to P molar ratios (1.27). Calcium phosphate crystallizations in anaerobic digesters have been observed previously (Zhang et al., 2021a; Zhang et al., 2021b), which were induced at high pH. It has been reported that the biological consumption of H^+ during methanogenesis is critical for internal CaP precipitation (Cunha et al., 2018). This was in line with the highest bulk pH (Fig. 3.6) and methane production (Fig. 3.4) measured in the anaerobic digestion of WAS pretreated with 0.1 g $Ca(ClO)_2$/g TSS in this study.

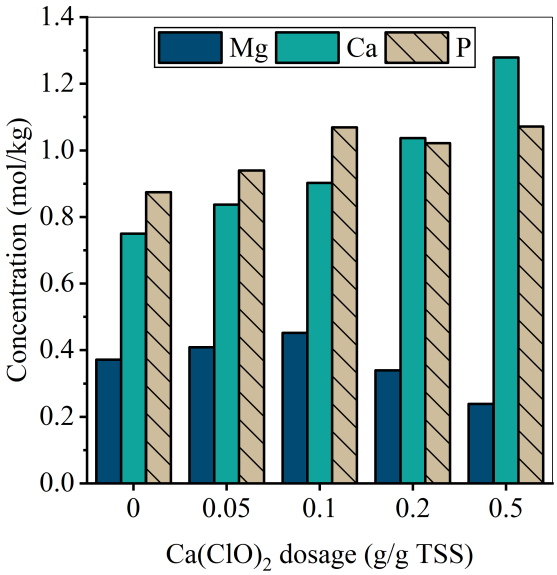

Fig. 3.5. Metal elements (calcium and magnesium) and phosphorus in anaerobic digestion of WAS with 30 min of different doses of calcium hypochlorite pretreatment.

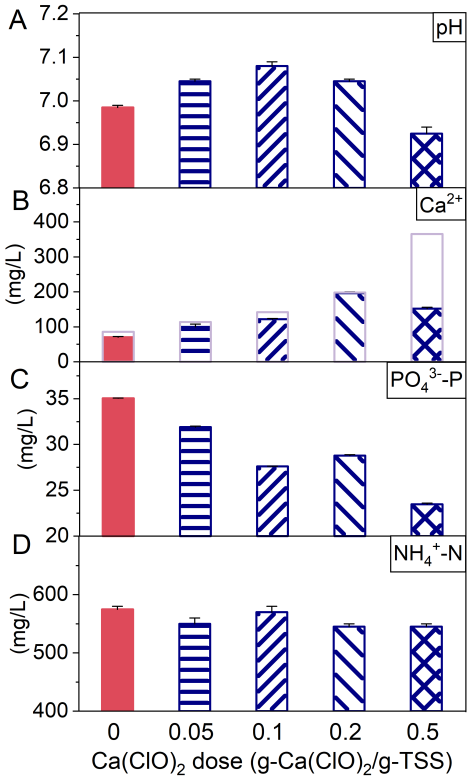

Fig. 3.6. The pH (A), Ca^{2+} (B), phosphate (C), and ammonia (D) concentrations in sludge supernatant after 80 days anaerobic digestion of WAS pretreated with different doses of calcium hypochlorite.

3.3.5 Microbial community analysis

According to the increased Shannon diversity index (Fig. 3.7A), bacterial community diversity increased when WAS was pretreated with low to medium doses of hypochlorite (3.38 to 3.75 for 0 to 20% $Ca(ClO)_2$ basing on TSS). The bacterial community diversity decreased with a higher hypochlorite dosage of 50% (TSS basis). This can be attributed to the oxidation effect of $Ca(ClO)_2$, which elevates the oxidation-reduction potential of the digestion systems and allows more facultative bacteria to inhabit the low to medium dose niches; higher doses of $Ca(ClO)_2$ might inhibit strictly anaerobic bacteria.

At the family level, all samples shared some abundant microorganisms, such as *[Cloacamonaceae]*, *Anaerolinaceae*, and an unidentified family in the order *Bacteroidales*. In AD reactors fed with untreated WAS and at low doses of hypochlorite (less than 10% basing on TSS), microorganisms in the order *Bacteroidales* and the order *GW-28*, and in the families *Syntrophaceae*, *Comamonadaceae*, *Xanthomonadaceae*, *Syntrophorhabdaceae*, and *Saprospiraceae*, showed higher abundances than the same microorganisms developed under medium and high doses of hypochlorite pretreatment conditions (0.2 g and 0.5 g $Ca(ClO)_2$/g TSS). These fermentative bacteria might play important roles in breaking down complex organic compounds in WAS, but they were sensitive to oxidative conditions. Further, the enrichment of syntrophic bacteria, such as *Syntrophaceae* (4.72 – 6.06%) and *Syntrophorhabdaceae* (0.76 – 0.98%), might contribute to an unimpeded electron flow between bacteria and archaea, which was correlated to the higher methane generation and shorter lag phase (Fig. 3.4) observed in reactors with low hypochlorite

dosages. Certain families, including *Porphyromonadaceae*, *Ruminococcaceae*, and an uncultured family in class *Pla3*, were higher in abundance in AD reactors fed with WAS pretreated with medium and high hypochlorite dosages, inferring their high tolerance to oxidative stress.

The relative abundances of archaeal genera in AD of WAS pretreated with different dosages of $Ca(ClO)_2$ are shown in Fig. 3.7B. *Methanosaeta* and one unclassified genus in the family *WSA2* dominated reactors fed with untreated WAS and WAS treated at low doses of hypochlorite (22.1 – 32.1% and 19.2 – 30.8%, respectively, in 0, 5%, and 10% $Ca(ClO)_2$ (TSS basis) samples), but decreased to 8.8% and 3.1%, respectively, in the medium hypochlorite dose sample (20% $Ca(ClO)_2$, TSS basis), and to 11.0% and 8.4%, respectively, in the high hypochlorite dose sample (50% $Ca(ClO)_2$, TSS basis). This indicated the low oxidative stress tolerance of *Methanosaeta* and the unclassified genus in the family *WSA2*, consistent with previous studies (Tang et al., 2004; Wu and Conrad, 2001; Yu et al., 2020a). *Methanosarcina* predominated in the medium $Ca(ClO)_2$ dosage sample (69.6%), and one unidentified genus in the order *WCHD3-30* predominated in high $Ca(ClO)_2$ dosage sample (36.1%). High substrate concentrations in the medium $Ca(ClO)_2$ dosage sample (Fig. 3.8) might have induced the growth of *Methanosarcina*, a genus with a high maximum specific growth rate as well as a high half-saturation coefficient; both factors play an important role at high organic loading conditions (Lins et al., 2014). The order *WCHD3-30* has mainly been found in a mineralized aquifer (Coral et al., 2018) and on the microbial mats in a hypersalinity condition (Wong et al., 2017), which might be enriched by high calcium concentration in the 0.5 g $Ca(ClO)_2$/g TSS reactor.

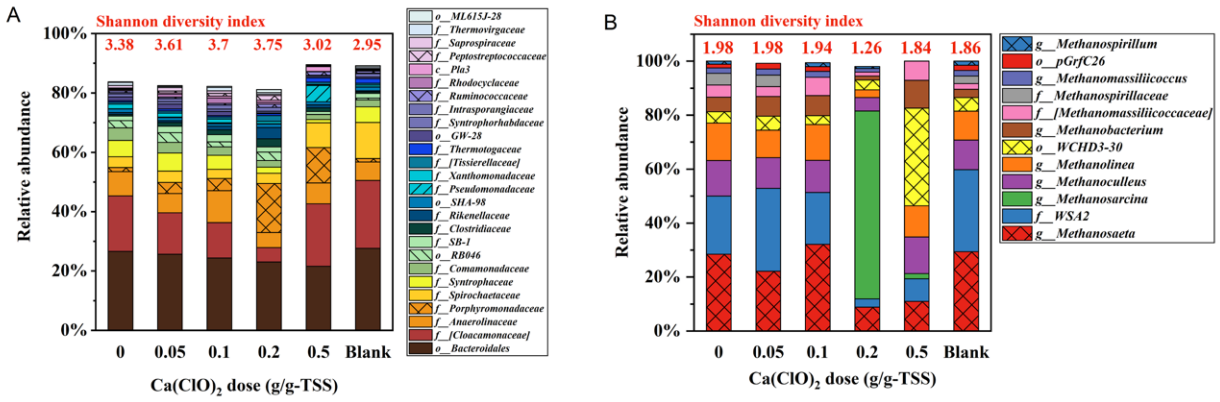

Fig. 3.7. Bacterial communities at the family level (A, >1% in any sample, shown as f_) and archaeal communities at the genus level (B, > 1% in any sample, shown as g_). Taxon names are shown at a higher level if not identified at family and genus levels, *i.e.*, order level (o_) and class level (c_). The Shannon diversity index is shown on top of each bar in red text.

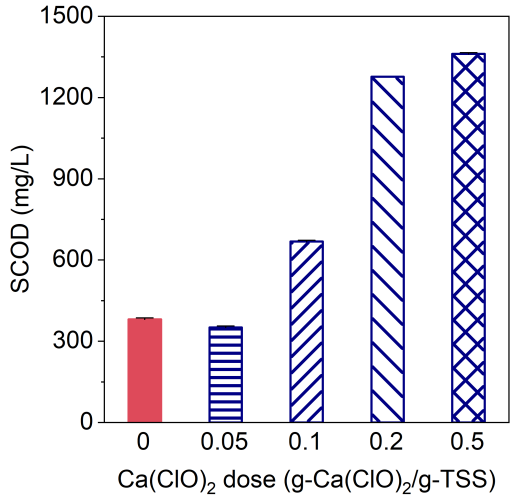

Fig. 3.8. The soluble COD concentrations in sludge supernatant after 80 days anaerobic digestion of WAS pretreated with different doses of calcium hypochlorite.

3.3.6 Implications in WWTP

The hydrolysis of large molecules related to microbial cells was considered as a rate-limiting step during WAS anaerobic digestion. A small amount of calcium hypochlorite (5% – 10% basing on TSS) promoted the solubilization of WAS under aerobic pretreatment conditions. The retention time of WAS in the chemical dosing pool should be less than 2 days to minimize the aerobic organics consumption before entering the digester. Comparing to other WAS pretreatment technologies, applying $Ca(ClO)_2$ offers several major advantages including low transport and operational costs (*i.e.*, $Ca(ClO)_2$ are available in solid forms; and are easy to mix) (Tyagi and Lo, 2011; Zhang et al., 2020b), and its effectiveness in improving biogas production and effluent quality, as demonstrated in the present study.

3.4 Conclusion

Waste activated sludge (WAS) was pretreated with $Ca(ClO)_2$ (5% – 50% basing on TSS) and then fed to the anaerobic digesters. Good microbial activity was maintained at lower $Ca(ClO)_2$ dosages. Calcium phosphate precipitated at high levels of $Ca(ClO)_2$ but microbial activity was compromised. Prolonged methane production lag phases were observed at high hypochlorite doses, but WAS pretreated with 10% $Ca(ClO)_2$ (TSS basis) achieved the highest methane production rate and 22.6% more methane production than untreated WAS. Results from this study indicate that conditioning with calcium hypochlorite is an economic and effective way to improve the WAS treatment efficiency.

CHAPTER 4 ANAEROBIC DIGESTION OF THICKENED WASTE ACTIVATED SLUDGE UNDER CALCIUM HYPOCHLORITE STRESS: PERFORMANCE STABILITY AND MICROBIAL COMMUNITIES[2]

A version of this chapter has been published in Environmental Research.

4.1 Introduction

Hypochlorite pretreatment has been proven effective in enhancing waste activated sludge (WAS) anaerobic digestion performances in batch reactors as demonstrated in the last chapter. In this chapter, two semi-continuous anaerobic sequencing batch reactors (ASBRs), one fed with $Ca(ClO)_2$ pretreated thickened WAS (TWAS) and one with raw TWAS, were operated at mesophilic conditions (35 °C) for 145 days, to further assess the impact of hypochlorite pretreatment of WAS on the performance of continuously operated reactors.

1% $Ca(ClO)_2$ was added to WAS to improve its anaerobic digestion, and the common hydraulic retention time (HRT) (~20 days) was shortened to 5 days by introducing three loading shocks to each reactor to compare the performance stability and resilience between the digestion of $Ca(ClO)_2$ pretreated TWAS and untreated TWAS. Microbial community shifts were quantified to reveal the microbiome responses to disturbances. Sludge samples were removed from the reactors at different operational stages to determine the microbial community dynamics. A non-steady-state mass balance model was applied to quantify the microbiome responses to chemical and environmental

[2] Yu, N., Mou, A., Sun, H. and Liu, Y. 2022. Anaerobic digestion of thickened waste activated sludge under calcium hypochlorite stress: Performance stability and microbial communities. Environmental Research 212, 113441.

disturbances, and co-occurrence network analysis was performed to determine microbial interactions and shifts in microbial clustering patterns at each stage of the WAS digestion.

4.2 Materials and methods

4.2.1 Sludge source

Thickened waste activated sludge (TWAS) was collected from a waste activated sludge thickener in a local (Edmonton, Canada) wastewater treatment plant. Waste activated sludge thickeners receive solids from a secondary clarifier and use gravity to separate solids from liquids. The TWAS was stored at 4 °C until use. TWAS characteristics were: total suspended solids (TSS) 46.9 ± 2 g/L, volatile suspended solids (VSS) 36.6 ± 2 g/L, total chemical oxygen demand (TCOD) 50.8 ± 0.4 g/L, soluble chemical oxygen demand (SCOD) 0.2 ± 0.08 g/L, pH = 6.5 ± 0.2. The inoculum sludge (VSS ~ 14 g/L) used in the continuously operating reactors was taken from an anaerobic digester in the same wastewater treatment plant.

4.2.2 $Ca(ClO)_2$ pretreatment and batch tests

Calcium hypochlorite ($Ca(ClO)_2$) powder with 65% of available chlorine was purchased from Sigma Aldrich (Canada). $Ca(ClO)_2$ was added to the TWAS at dosages of 1%, 5%, 10%, 20%, and 50% of the total suspended solids in the TWAS, yielding 0.01, 0.05, 0.1, 0.2, and 0.5 g $Ca(ClO)_2$/g TWAS TSS. The mixing time was 30 min at room temperature to allow sufficient time for the chemical pretreatment reaction. TWAS alone (control) and $Ca(ClO)_2$ conditioned TWAS were added to serum bottles (working volume 120 mL) with the inoculum for anaerobic digestion test. The serum bottles were flushed with nitrogen gas, sealed with rubber stoppers and aluminum caps, and shaken at 120 rpm under mesophilic conditions (35 °C). The methane yield from the anaerobic

digestion of TWAS was monitored until stationary methane production was achieved. The test for each condition was performed in triplicate.

4.2.3 ASBR operation

Two anaerobic sequencing batch reactors (ASBRs), each with a working volume of 2 L were operated at 35 °C for five months. The control reactor contained untreated raw TWAS, and the experimental reactor contained TWAS + $Ca(ClO)_2$. At the end of each treatment cycle, the sludge was allowed to settle for 30 min. Then, 20% of the sludge was discharged from the top of the reactors and replaced by TWAS (control reactor) and TWAS treated with $Ca(ClO)_2$ (experimental reactor). The reactors were flushed with nitrogen gas for 10 min, then sealed. The hydraulic retention time (HRT) was progressively reduced from 20 to 15 to 10 to 5 days. Reactor performances with respect to methane production, TCOD, SCOD, TS, and effluent pH were compared. The fraction of influent COD that was converted to methane was calculated and shown as methanation rate.

4.2.4 Analytical methods

The total chemical oxygen demand (TCOD), the total solids (TS), and the volatile solids (VS) in the TWAS were measured according to the standard methods of the American Public Health Association (APHA, 1985). The pH was measured with a B40PCID pH meter (VWR, SympHony). A 10 L gas bag was connected to each reactor to collect the produced biogas. At the end of each treatment cycle, 2 mL of biogas was extracted from the gas bag and analyzed with a 7890B gas chromatograph (Agilent Technologies, Santa Clara USA) to determine the levels of CH_4, N_2, O_2, and CO_2 in the biogas.

4.2.5 Bioinformatics analysis and the mass balance model

To measure microbial community responses to the organic loading shock brought about by changes in the HRT, 2 mL of sludge samples were taken from the reactors after each treatment cycle. Samples were centrifuged at 5000 *g* for 10 min and DNA was extracted from the pellet with a DNeasy PowerSoil kit (QIAGEN, Toronto, Canada) according to the manufacturer's protocol. The DNA was sent to the Génome Québec Innovation Centre (Montréal, QC, Canada) for sequencing of the V4 hypervariable regions in amplicons of the microbial 16S rRNA using the Illumina Miseq PE250 platform. Raw DNA sequences were analyzed using the QIIME2 DADA2 algorithm (Callahan et al., 2016) with reference to the GreenGenes database, version 13_8 (99% similarity) (McDonald et al., 2012; Werner et al., 2012). Principal Coordinate Analyses (PCoA) of archaea and bacteria was performed using the "vegan" package (Jari Oksanen et al., 2017) in RStudio version 4.0.2. Three co-occurrence networks were constructed for three different stages after the loading shock, using "igraph" and "psych" packages in RStudio (correlations between genera were considered significant when Spearman's correlation coefficient $r > 0.6$, $p < 0.05$) (Yu et al., 2021a). To quantify microbiome responses to hydraulic retention time (HRT) decreases, a newly developed non-steady-state mass balance model (Sun et al., 2021) was applied.

4.3 Results and discussion

4.3.1 Anaerobic digestion of TWAS treated with different concentrations of $Ca(ClO)_2$ at different food/inoculum (F/I) ratios

Methane production versus time in samples containing TWAS treated with $Ca(ClO)_2$ is shown in Fig. 4.1. Anaerobic digestion was continued for 220 d for F/I = 1 and 70 d for F/I = 0.33. Lag phase values in the methane production increased with an increase in $Ca(ClO)_2$ concentration. The methane production results for raw TWAS had a minimal lag time, whereas the addition of calcium

hypochlorite introduced inhibition and led to delayed and stepped methane production. TWAS treated with 0.05, 0.1, and 0.2 g $Ca(ClO)_2$ showed lag times of 14.2, 24.2, and 40.4 days, according to the modified Gompertz model at F/I = 1, respectively. Lag times were reduced to 2.7, 10.2, and 14.1 days at lower F/I (0.33). This was likely due to residual $Ca(ClO)_2$ and its derivates which reduced methane production by inhibiting the activities of strict anaerobes, such as methanogens (Braguglia et al., 2006; Kim and Kim, 2020; Ware and Power, 2017; Yu et al., 2020a). Treatment of TWAS with 0.01 g $Ca(ClO)_2$ increased the methane yield by 4.8% and 8.3%, respectively, at F/I = 1 and F/I = 0.33. These results illustrated that the AD performance of TWAS was enhanced with the addition of a trace amount (0.01 g/g TSS) of $Ca(ClO)_2$ with controlled F/I ratios of below 0.33. Further, the pretreatment reduced the TWAS COD by 8%, which substantially reduced the organic loading pressure in the following treatment units.

The calcium hypochlorite dosage, temperature, and the operating procedures (such as treatment duration, reactor type, and HRT) exhibit great impact on WAS AD performance. Yu et al. reported the influences of $Ca(ClO)_2$ dosages on WAS (TSS 4.9 ± 0.2 g/L) digestibility at room temperature (20 – 24 °C) (Yu et al., 2021b). After 30 mins of pretreatment with 0.05, 0.1, and 0.2 g $Ca(ClO)_2$ per g TSS in WAS, the methanation rate increased from 42.05 ± 0.01% in the untreated WAS to 46.12 ± 4.59%, 51.57 ± 2.23%, and 45.18 ± 1.07%, respectively, while severe inhibition was observed for 0.5 g/g TSS $Ca(ClO)_2$ pretreated WAS. The study of Wu et al. showed that the methane production significantly increased with 48 h of $Ca(ClO)_2$ pretreatment at dosages of 0 – 240 mg/g VS under mesophilic condition (WAS TS 14.52 ± 0.5 g/L, VS 6.09 ± 0.4 g/L) (Wu et al., 2021). Hu et al. achieved 73% higher methane yield than that of the control (from 156 ± 4.3 to 269.9 ± 5.2 mL) with 1.6 g/L $Ca(ClO)_2$ addition in two-phase anaerobic digestion systems (4 days for the acidogenic phase and 45 days for BMP experiments) treating WAS (TSS 20.5 ± 0.2 g/L)

at 35 °C (Hu et al., 2022). However, the methane yield reduced to 235.4 ± 5.5 mL at 2 g/L of $Ca(ClO)_2$. These studies indicated that long pretreatment time (or utilizing two-phase AD) with moderate $Ca(ClO)_2$ dosage promote the methane recovery from WAS, while negative effects are expected with excessive dosages. Additionally, as an easily accessible disinfecting agent with low price, the application of $Ca(ClO)_2$ is feasible for wide industry application as AD pretreatement. Pilot-scale demonstrations and life cycle environmental and economic assessment of this technology should be investigated in future study.

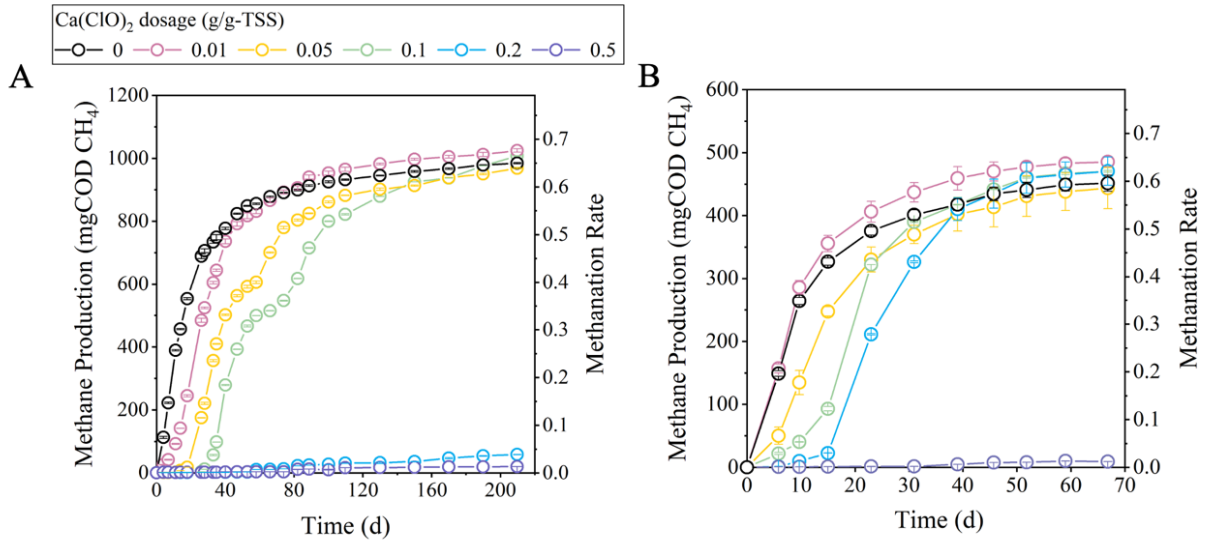

Fig. 4.1. Cumulative methane production from TWAS treated with different doses of $Ca(ClO)_2$ at food/inoculum (F/I) ratios of 1.0 (A) and 0.33 (B) as a function of time. Error bars represent standard deviations calculated from triplicate samples.

4.3.2 Time course of methane production in AD reactors

The methane productions in two ASBRs digesting raw and $Ca(ClO)_2$-treated TWAS are shown in Fig. 4.2. The methane yield was continuously monitored for 145 days, which was divided into four phases according to the HRT. In Phase 1, the start-up phase, the organic loading rate (OLR) was

2.3 to 2.5 kg COD/m^3/d (HRT 20 d). Both reactors maintained a stable methane production after a 20 d adaptation period. The methanation rate in the absence of $Ca(ClO)_2$ was 41.15 ± 3.50%, which increased to 47.03 ± 3.31% with $Ca(ClO)_2$ addition in Phase 1. Then, the HRT was decreased to 15 days on day 48, introducing the first loading shock to the reactors. The methane production was reduced to 17.21% of the influent COD (1147.61 mg CH_4-COD/reactor/d) in the control reactor (no $Ca(ClO)_2$), and it took 32 days for the reactor to restore methanogenic activity. Methanogenic activity remained stable at 45.52 ± 2.70% (2791.99 ± 165.61 mg CH_4-COD/reactor/d) throughout Phase 2 in the reactor containing $Ca(ClO)_2$. Similar results were observed following the second shock—the methane production from the control reactor was severely affected for 16 days, dropping to only 6.19%. In comparison, the experimental reactor acclimated to the higher organic loading rate in 8 days, achieving a methane yield of 4287.29 ± 335.70 mg CH_4-COD/reactor/d (46.60 ± 3.65%). The enhanced methane production resilience and stability probably stemmed from an enhanced destruction of microbial cells and the release of intracellular materials caused by the $Ca(ClO)_2$. However, when the HRT was further reduced to 5 days, both reactors crashed in 15 days; the experimental reactor deteriorated sooner than the control reactor. This could be explained by the increased number of dead cells in the experimental reactor resulting from the $Ca(ClO)_2$ treatment and the reduced microbial activity due to a shorter HRT. The results suggested that improved methane production rate and stability can be achieved with $Ca(ClO)_2$ pretreatment (1%), as long as sufficient HRT was maintained (at least 10 days). The batch results also showed that $Ca(ClO)_2$ addition inhibited the methane production at first (increased methane production lag phase), while the benefit of the pretreatment can be observed with long enough incubation time. Similarly, Wu et al. reported that $Ca(ClO)_2$ pretreatment (10 – 240 mg/g VS) inhibited the methane production for the first 12 days of anaerobic digestion, but

eventually increased the methane production by 3.6 – 59.7% as compared to the reactor without pretreatment (Wu et al., 2021). Further, this study demonstrated that lowering the F/I ratio (exchange ratio in semi-continuous ASBRs) can help to mitigate the inhibitory effect of $Ca(ClO)_2$.

The present work demonstrated that mesophilic TWAS digestion in semi-continuous ASBRs achieved satisfactory performance at high organic loading rate (OLR) of 4.6 – 5 kg COD/m^3/d, which was comparable to reported pretreatment studies using different pretreatment strategies. Calderon et al. applied ferric and nitrite combined pretreatment to TWAS, and achieved 160 ± 14 mL CH_4/g VS methane production and 39 ± 4% of VS destruction at 4.2 kg COD/ m^3/d OLR (Calderon et al., 2021). Microwave/alkali pretreatment has also been reported to effectively increase the anaerobic biodegradability of sludge at OLR of 3.4 kg COD/m^3/d with 41.8 ± 0.9% of VS removal and 226 ± 15 mL CH_4/g VS methane production (Jang and Ahn, 2013).

Given the low chemical dose and the chemical cost, the cost benefit for applying calcium hypochlorite pretreatment can be expected. Based on the experimental results, the cost for treating 1 m^3 TWAS with calcium hypochlorite is estimated to be < $ 0.6 (based on 0.47 kg $Ca(ClO)_2$ usage/m^3 TWAS, and $ 0.8–1.2/kg $Ca(ClO)_2$ from Henan Sinowin Chemical Industry Co., Ltd.), which leads to a 22.9% increase in methane production and $ 6.9 revenue generation (4.8 m^3 increase in CH_4 production/m^3 TWAS treated, and $ 1.42/m^3 CH_4 (Hu et al., 2022)), and reduced digested TWAS management costs. Further, $Ca(ClO)_2$ can be combined with other processes to achieve optimal treatment performance as a sustainable option. For instance, $Ca(ClO)_2$ oxidation followed by rapid sand filtration (iron rust aided) showed complete removal of color and over 95% removal of COD in textile wastewater treatment (Khandaker et al., 2020). The combined treatment of $Ca(ClO)_2$, ferric coagulant, and walnut shell effectively improved the sludge dewaterability (Liang et al., 2019). Simultaneously sludge dewaterability, stabilization, and P fixation can be

achieved when combining electrochemical process with $Ca(ClO)_2$ oxidation (Hu et al., 2021). The results from long-term semi-continuous operations in the present study and the cost-benefit analysis suggest the great potential of applying calcium hypochlorite for TWAS treatment in engineering practice.

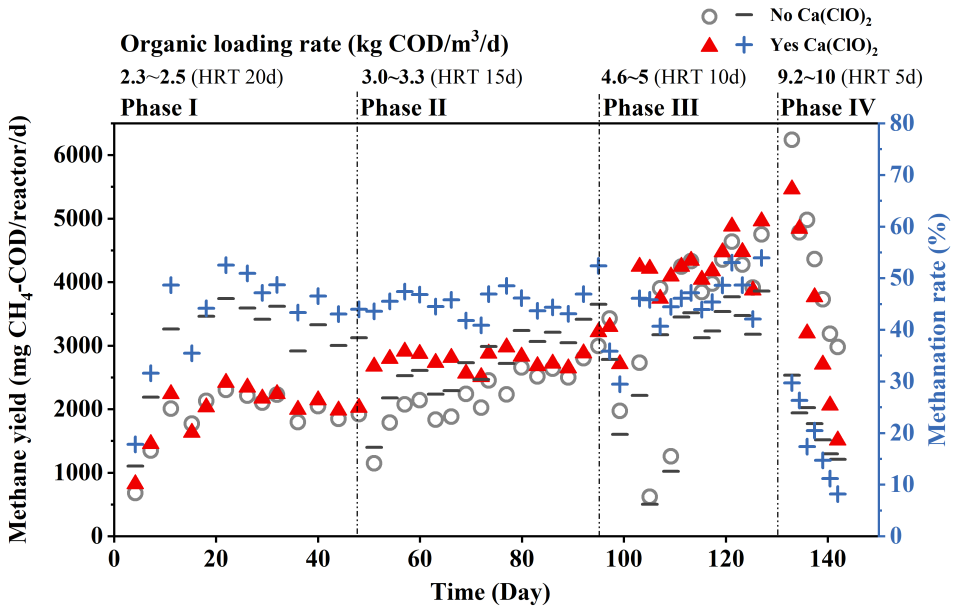

Fig. 4.2. Methane production in ASBRs treating TWAS with or without $Ca(ClO)_2$ treatment at four HRTs.

4.3.3 Microbial community responses to the loading shocks

Microbial communities in the anaerobic digesters were analyzed by principal coordinates analysis (PCoA) (Fig. 4.3). The archaeal communities in the TWAS influent were distinctly different from the seed, the effluent, and the sludge settled in the reactors. When loading shocks were introduced to the reactors, the archaeal communities were initially similar between the seed and the sludge from reactors, and shifted away from the seed later in each operational phases. Unlike the archaeal

communities, the bacterial communities shifted from the seed towards the influent (especially in the last phase) with increasing organic loading rates. Further, the bacterial communities in the two ASBRs diverged immediately after the loading shock and this difference was reduced later in each phase. The results suggest that changes induced by higher organic loading rates affected the microbial communities, and increased the AD performance of the reactors. Bacterial community differences between the reactors decreased as the reaction time increased.

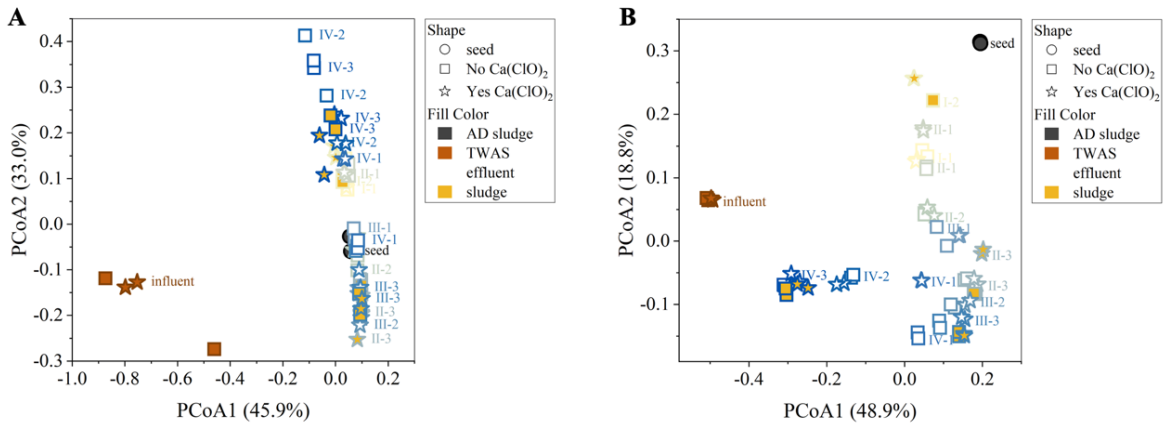

Fig. 4.3. Beta diversity of archaeal (A) and bacterial (B) communities in the two ASBRs over time. Phases I, II, III, and IV represent HRTs of 20 d, 15 d, 10 d, and 5 d, respectively. 1, 2, and 3 represent the first, second, and third sampling points (*i.e.*, initial, acclimation, and stabilization stages after the disturbance), respectively.

The microbial communities in the two ASBRs are shown in Fig. 4.4. The highest abundance of archaea in the two reactors included unidentified genera in the families *WSA2* and *Methanospirillaceae*, *Methanosaeta*, and *vadinCA11*. Acetoclastic *Methanosaeta* was the dominant archaea at the first two and the last two sampling points in both reactors, whereas *WSA2* predominated in both reactors in the middle of the operation. *Methanosaeta* have a low specific growth rate and a low half-saturation coefficient, and the predominance of which could be

associated with the low methanogenesis efficiency at extreme HRT conditions. Members of the family *WSA2* have been reported to produce methane through methylated thiol reduction, with acetate, malonate, and propionate as carbon sources; this activity might play an important role in bridging the carbon and sulfur cycles in a stable anaerobic digestion environment (Nobu et al., 2016). *Blvii28* and one unidentified genus in the order *Bacteroidales* were the two most abundant bacteria in the TWAS anaerobic digestion reactors. The relative abundances of *Blvii28* increased in two stable operational phases (Phase II and Phase III) and decreased between phases in both reactors. In the control reactor, *Bacteroidales* followed the same trends as *Blvii28*. The relative abundance of *Bacteroidales* increased in Phase II but slightly decreased in Phase III (possibly due to the significant increase in *Blvii28*). Both genera decreased in the Phase IV, with the development of other genera, such as microorganisms in the families *Comamonadaceae*, *Saprospiraceae*, *Xanthomonadaceae* and *Cytophagaceae*, and genera *Simplicispira* and *Lutispora*. *Blvii28* was classified as a strictly anaerobic fermenter that utilizes carbohydrates but not amino acids and fatty acids. Members in the order *Bacteroidales* are well known hydrolytic microbes that hydrolyze a wide range of substrates and produce short chain fatty acids. Their enrichment in our experiments indicates that microbial populations became acclimated to the increased organic loading.

Significant differences between the two reactors in terms of composition and abundance in the microbial community were not observed. Further analysis is required to determine the microbial community responses to loading shock and to compare the difference between the reactor containing TWAS and the reactor containing TWAS + $Ca(ClO)_2$. Therefore, a non-steady-state mass balance model was applied, as discussed in the following section.

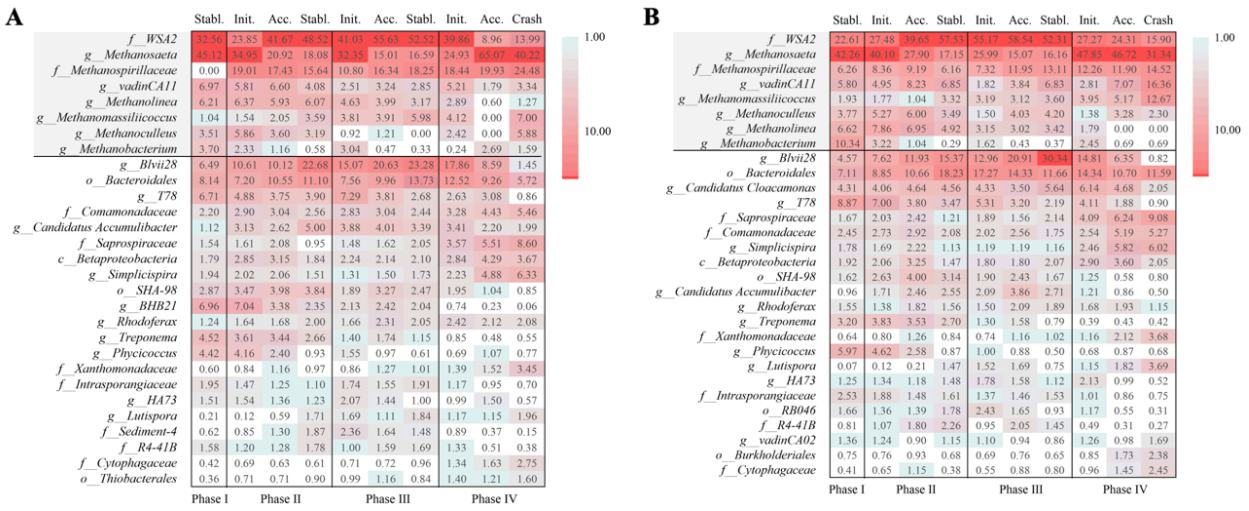

Fig. 4.4. Relative abundance of genera with average abundance > 1% in sludge taken from the control reactor (A) and experimental reactor (B) at different hydraulic retention times. Unidentified genera were named at family (f_), order (o_), and class (c_) levels.

Fig. 4.5 illustrates the growth rate of the dominant microbes (average relative abundance > 1%) in response to the change in organic loading rates (OLRs). The hydraulic retention times (HRTs): 20 days (Phase I), 15 days (Phase II), 10 days (Phase III), and 5 days (Phase IV), can each be divided into three stages, including initial (Init.) (the disturbance), acclimation (Acc.), and stabilization (Stabl.). The dominant archaea—one unidentified genus in the family *WSA2*, *Methanosaeta*, and one unidentified genus in the family *Methanospirillaceae*—had negative growth rates immediately after the first loading shock in the reactor containing TWAS alone, whereas active growth of these archaea was observed in the reactor containing TWAS + $Ca(ClO)_2$, as indicated by the positive μ values. Higher μ values were observed for *Blvii28*, *T78*, *Treponema*, *HA73*, and *Lutispora*; for microorganisms in the families *Saprospiraceae*, *Intrasporangiaceae*, *R4-41B*, and *Cytophagaceae*; and for the orders *Bacteroidales* and *SHA-98* in the reactor containing TWAS + $Ca(ClO)_2$ compared to the control reactor with no $Ca(ClO)_2$. This phenomenon was even more evident

immediately after the second shock (Phase III), when most archaea and the two most abundant bacteria (*Blvii28* and an unclassified genus in the order *Bacteroidales*) responded negatively to the loading stress. Net growth rates were as low as -0.1 d^{-1} in the control reactor, but the reactor containing $Ca(ClO)_2$ was less affected. In Phase II and Phase III, the microbial population changed right after the shock (*i.e.*, most microbes were negatively affected at the initial stage of each phase, but slowly recovered at the acclimation stage). According to their deteriorated performances, microbial communities in both reactors experienced a progressive crash after the third loading shock. At a short HRT (Phase IV), archaea in the reactor containing $Ca(ClO)_2$ lost their resistance to the loading shock sooner than archaea in the control reactor, perhaps because the presence of $Ca(ClO)_2$ substantially increased the oxidative stress in the reactor. On the other hand, the coexistence of aerobic and anaerobic micro-environments may boost the microbial activity and build a robust microbial community to form a buffer against organic loading shocks (Jari Oksanen et al., 2017).

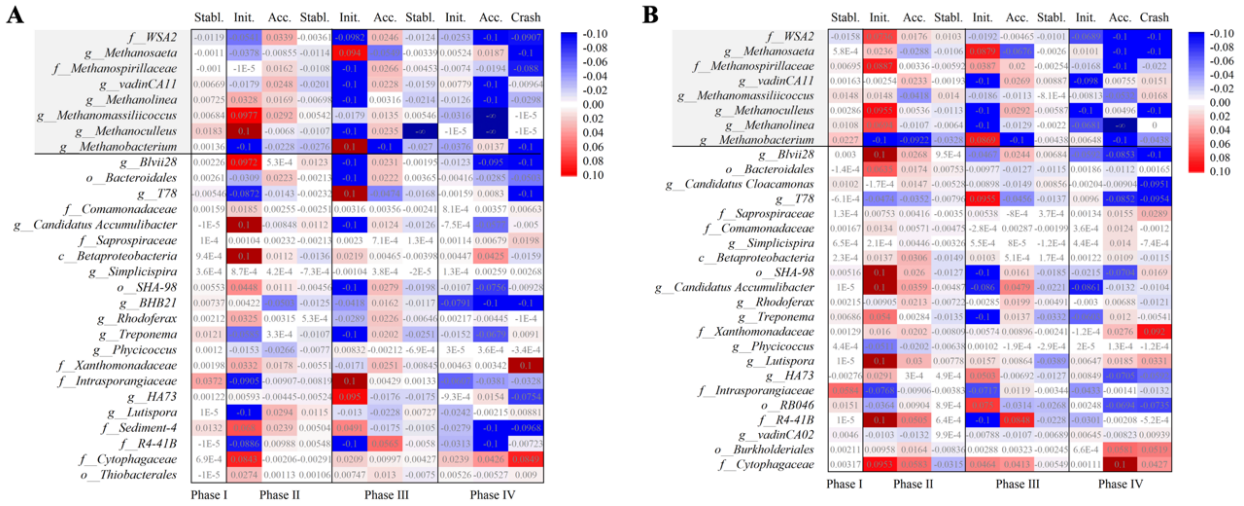

Fig. 4.5. Net growth rates of genera with average abundances of > 1% in sludge taken from the reactor containing TWAS alone (A) and the reactor containing TWAS + $Ca(ClO)_2$ (B) at different

hydraulic retention times (HRTs). Unidentified genera were named with respect to family (f_), order (o_), or class (c_) levels; "– ∞" represents negative infinity.

Three microbial community groups were used for co-occurrence network analysis based on the three reaction stages: initial disturbance, acclimation, and stabilization. The microbial networks in Fig. 4.6 indicate significant correlations among the genera in the three microbial community groups. The clustering patterns and characteristics of the microbial networks (Table 5.1) varied in each group. The connections (interactions) realized between microbial species represent the complexity of the microbial network. The microbial network showed the highest connectivity (0.38) at the stabilization stage, indicating that the strongest microbial interactions were established at the stable operational stage of the AD reactor. The clustering coefficient, the average degree, and the betweenness centralization were highest, and the average path length was the lowest at the stabilization stage, indicating that the microbial community was the most dynamic and compact at this stage, consistent with previous studies (Guo et al., 2022). Higher cluster coefficients and shorter average path lengths were reported to present in thermophilic and mesophilic anaerobic co-digestion networks with both high hydrolysis and methanogenesis rates, inferring high activities and interdependence among the microorganisms.

There was one main cluster in the immediately after the disturbance network, with some less predominant archaea (the family *Methanospirillaceae, Methanobacterium, Methanolinea, Methanoculleus*, and others) closely encircling the cluster. During the acclimation stage after the loading shock, the cluster started to divide, finally becoming two sub-clusters at the stabilization stage. Two dominant archaea, *Methanosaeta* and the family *WSA2*, were included in a newly formed cluster, implying that they might be playing important roles during the reactor response to the loading shocks.

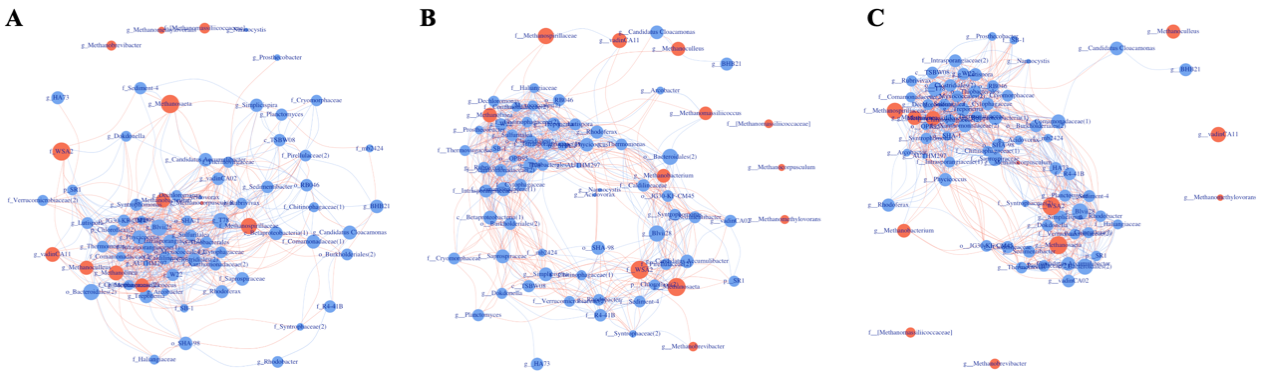

Fig. 4.6. Network analysis of microorganisms at the initial stage (A), the acclimation stage (B), and the stabilization stage (C) after the loading disturbance.

Table 4.1. Network key characteristics of three groups including initial after the disturbance (Init.), Acclimation (Acc.), and stabilization (Stabl.).

	No. of vertices	No. of edges	Connectivity	Clustering coefficient	Ave. degree	Betweenness centralization	Ave. path length
Init.	73	789	0.30	0.65	21.62	0.24	1.70
Acc.	73	780	0.30	0.64	21.37	0.24	1.70
Stabl.	68	875	0.38	0.70	25.74	0.27	1.62

4.4 Conclusion

Calcium hypochlorite pretreatment enhanced methane production from TWAS at a low dosage and F/I ratio. Compared to the control (no $Ca(ClO)_2$ treatment), the addition of 1% $Ca(ClO)_2$ to TWAS increased the methane yield by 27.7% (from 35.65 ± 9.29% to 45.53 ± 4.42%) in continuously operated ASBRs. The dominant microbes in the reactor containing TWAS only were

negatively affected by the loading shocks, whereas the dominant microbes in the reactor containing TWAS + $Ca(ClO)_2$ showed better resilience, as indicated by the positive net microbial growth rates observed; this was consistent with the more stable performance in the reactor containing $Ca(ClO)_2$. Therefore, $Ca(ClO)_2$ is an effective and promising additive in TWAS AD processes.

CHAPTER 5 DIFFERENT MICRO-AERATION RATES FACILITATE PRODUCTION OF DIFFERENT END-PRODUCTS FROM SOURCE-DIVERTED BLACKWATER[3]

A version of this chapter has been published in Water Research.

5.1 Introduction

The application of AD for municipal wastewater streams is limited by the low methanogenesis rates due to low organic concentrations and low temperatures (Huang et al., 2019). Recent studies applied AD for source-diverted blackwater (*i.e.*, toilet wastewater) treatment which takes advantage of the high organic content of blackwater in the absence of other domestic wastewater streams, *i.e.*, greywater (Florentino et al., 2019; Zhou et al., 2019b). Thermophilic (50 – 60°C) and mesophilic temperatures (30 – 40 °C) have been shown to be suitable for blackwater AD (Gao et al., 2019a), while at ambient temperatures, challenges still remain with regards to the chemical oxygen demand (COD) removal efficiency and methane production (Oarga Mulec et al., 2016; Pedrouso et al., 2019). Hydrolysis is considered as the rate-limiting step in the blackwater treatment process since the blackwater biomass-content is high (25 – 54 wt% of total solids) (Rose et al., 2015).

This study aims to illustrate the role of micro-aeration pretreatment on the anaerobic digestion of blackwater. The effect of different microaerophilic conditions on the hydrolysis, acidogenesis, and methanogenesis steps were studied. Microbial networks were also investigated to reveal the fundamental impacts of long term continuously oxygen input on AD performance.

[3] Yu, N., Guo, B., Zhang, Y., Zhang, L., Zhou, Y. and Liu, Y. 2020a. Different micro-aeration rates facilitate production of different end-products from source-diverted blackwater. Water Research, 115783.

5.2 Materials and methods

5.2.1 Blackwater collection and characterization

Blackwater (toilet wastewater) was collected from conventional toilets (9 liters of water per flush) from the University of Alberta Campus. Influent and effluent samples were filtered through 0.45 μm nylon membrane filters (Fisher Scientific, CA) for soluble component analyses. Total COD and soluble COD (after filtration) concentrations, total solids (TS) and volatile solids (VS) were measured according to the Standard Methods of the American Public Health Association (Rand et al., 1976). Acetate, propionate, and butyrate, being the primary VFAs, were analyzed on a DIONEX ICS-2100 Ionic chromatography (IC) system (Thermo Fisher Scientific, Waltham MA, USA) equipped with a conductivity detector and IonPac AS18 Analytical Column (2 x 250 mm). Samples were diluted and filtered through 0.2 μm nylon membrane filters before VFA analysis.

5.2.2 Experimental setup and inoculum

Five semi-continuous anaerobic sequencing batch reactors (ASBR) were made using glass with a diameter of 101 mm and a height of 225 mm and a polypropylene cap (inner neck diameter 30 mm). The cap had three ports that were fixed with two longer silicone rubber tubing in the liquid phase and one short silicone rubber tubing in the gas phase. One of the tubes was connected to a gas diffuser submerged in the liquid phase for aeration, the second was used to take liquid samples, and the third for pressure detection and gas sampling. All ports were fixed with plastic valves at the upper end.

The semi-continuous ASBRs were inoculated with 0.5 g VS/reactor (100 mL/reactor) of digested sludge and 0.5 g VS/reactor (130 mL/reactor) of waste activated sludge to ensure both anaerobes and aerobes were present in the system. Reactors were operated at room temperature (22 ^{o}C). All

reactors were placed in a shaker at 120 rpm. There were five parallel reactors, including AnR, 5-MaR, 10-MaR, 50-MaR and 150-MaR, representing the anaerobic reactor (AnR with no O_2 treatment) and micro-aerobic reactors with gradient aeration levels (MaR with 5, 10, 50, and 150 mg O_2/L-reactor/cycle, respectively). The reactors were operated for 100 days, during which time the performance was evaluated at four different HRTs (5, 4, 3, and 2 days, corresponding to Stages I – IV, respectively). Each cycle consisted of the following steps: filling (5 min, including feeding and air injection), reaction (from 2 to 5 days), settling (30 min) and discharging (5 min). The gas composition analysis was conducted at the end of settling. The exchange ratio was 70 % of the working volume.

5.2.3 Analysis methods

The oxidation reduction potential (ORP) level was measured in the reactors right after air injection to determine the tendency of the aqueous solution in the reactors to accept or donate electrons. ORP can reflect small changes in oxygen concentration which are below the detection limit of dissolved oxygen (DO) probes (0.1 mg/L, which corresponds to -50 mV), and was therefore used in place of DO. ORP was measured by a portable ORP meter (Milwaukee MW500). The pH was measured with a pH meter (B40PCID, VWR, SympHony). Methane production was assessed by measuring the headspace pressure using a pressure meter (GHM 3151, Germany) and the composition of biogas using gas chromatography (GC) (7890B Agilent Technologies, USA). For each gas detection, biogas in reactor headspace was mixed and then withdrawn with a gas-tight syringe. T-test was applied to determine the significance level using Microsoft Excel® software. A p-value smaller than 0.05 is considered as statistically significant difference.

5.2.4 Microbial analysis

DNA extraction was performed for the inoculum sludge and sludge in all ASBRs at the end of the experiment using the DNeasy PowerSoil Kit (QIAGEN, Hilden, Germany), according to the manufacturer's protocol. Sludge was sampled three times in one cycle, well mixed, and then centrifuged at 4000 *g* for 10 min to obtain representative sludge samples (Rosenkranz et al., 2013). The pellet was used for DNA extraction. The extracted DNA concentration and quality were examined by NanoDrop One (ThermoFisher, Waltham MA, USA) and gel electrophoresis. PCR was performed followed by sequencing on the Illumina MiSeq platform. The 16S rRNA genes were amplified using the universal primer pair 515F (GTGCCAGCMGCCGCGG) and 806R (GGACTACHVGGGTWTCTAAT). Sequence analysis was performed using the Qiime2 DADA2 pipeline (Caporaso et al., 2010) with 99 % similarity with reference to the Greengenes database version 13_8 . Alpha and Beta diversities and principal coordinates analysis (PCoA) using Bray-Curtis distance were performed using the "vegan" package (Jari Oksanen et al., 2017) in RStudio version 3.4.1. The predicted metagenome and functional genes were determined using the Phylogenetic Investigation of Communities by Reconstruction of Unobserved States (PICRUSt) (Langille et al., 2013). Correlation was computed using the R "corrplot" package using Pearson's product-moment correlation test (Wei and Simko, 2017).

5.3 Results

5.3.1 Blackwater characterization and reactor performances

The characteristics of blackwater from toilets on campus varied slightly in every collection. The total chemical oxygen demand (TCOD) of the blackwater was 1000 ± 70 mg/L and the corresponding soluble chemical oxygen demand (SCOD) of the fresh blackwater was 296 ± 74 mg/L, accounting for 20 – 30% of TCOD. The blackwater pH varied from 7.2 to 8.0, depending

on the storage time and the solubilization of the feedstock. The total ammonia nitrogen (TAN), total nitrogen (TN) and total phosphorus (TP) concentrations are shown in Table 5.1. The five ASBRs operated with different levels of air injection were operated for 100 days, under four different HRT conditions (initially set as 5 days then gradually shortened one day at a time to 2 days).

Table 5.1. Characterization of conventional flush toilets blackwater

Index (mg/L)	TCOD[a]	SCOD[b]	pH	TAN[c]	TN[d]	TP[e]
Blackwater	1000 ± 70	296 ± 74	7.2-8.0	80 ± 7	200 ± 20	20 ± 4

[a] total chemical oxygen demand

[b] soluble chemical oxygen demand

[c] total ammonia nitrogen concentration

[d] total nitrogen concentration

[e] total phosphorus concentration

The impact of micro-aeration treatment on hydrolysis is shown in Fig. 3.1A. Despite the relatively large standard deviation observed due to the fluctuate blackwater quality, statistical analysis results demonstrated the impacts of micro-aeration on blackwater digestibility ($P < 0.05$). For all HRT conditions, the low-dose micro-aeration in 5-MaR (5 mg O_2/L-reactor/cycle) resulted in the highest hydrolysis rates when compared to the no micro-aeration condition (AnR), and micro-aeration at higher dosages (10-MaR, 50-MaR, and 150-MaR); this indicates that low-dose micro-aeration can

enhance hydrolysis efficiency. As the micro-aeration dose increased, there was a decreasing trend in the hydrolysis rate. In particular, under Stage IV (HRT of 2 days), the 5-MaR and 10-MaR reactors had significantly higher ($P < 0.01$) hydrolysis efficiencies (48.7 ± 3.3 % for 5-MaR and 39.9 ± 5.8 % for 10-MaR), as compared to the AnR (34.7 ± 3.7 %). Under this condition, the 50-MaR exhibited a comparable hydrolysis efficiency (37.7 ± 5.6 %), as compared to AnR ($P < 0.01$), while higher micro-aeration doses (*i.e.*, 150-MaR with 25.1 ± 6.5 %) led to a significant reduction in hydrolysis efficiency ($P < 0.01$).

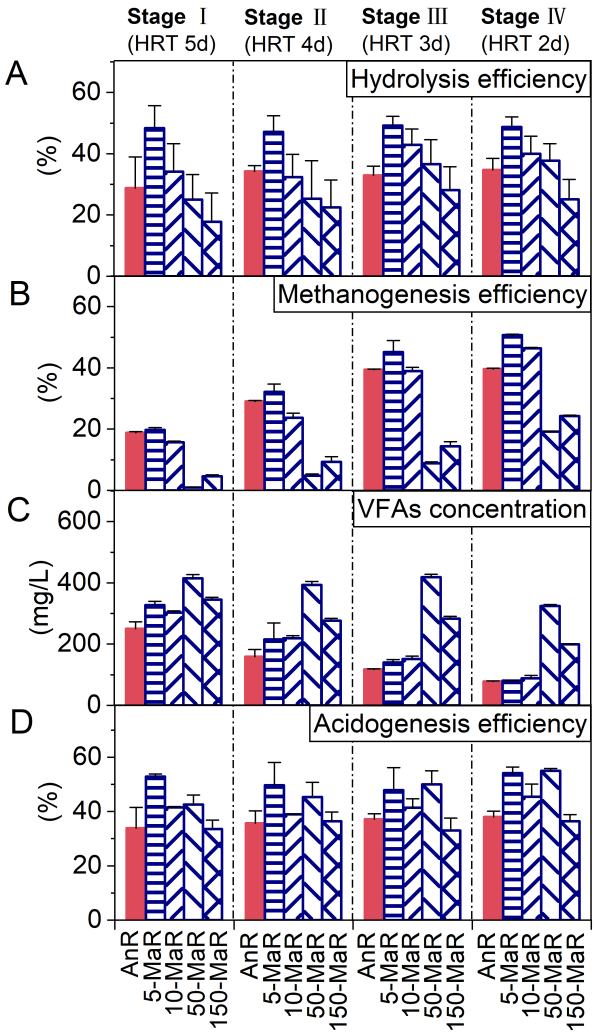

Fig. 5.1. Reactor performances including (A) hydrolysis efficiency, (B) methanogenesis efficiency, (C) total VFAs production, and (D) acidogenesis efficiency. Error bars represent standard deviation calculated from the stabilized cycles in each stage.

The stabilized methanogenesis efficiency in each stage of the operation is shown in Fig. 5.1B. Reactor ORP values are provided in Fig. 5.2B. For all five reactors, the methanogenesis rate increased with a reduction in HRT. This observation may be attributed to the establishment of more efficient methanogen communities at higher organic loading rates, similar to results reported previously (Lim and Wang, 2013; Ramos and Fdz-Polanco, 2013). At the end of Stage IV, the methanogenesis efficiency reached 50.5 % and 46.1 % in 5-MaR and 10-MaR, respectively, higher than that in AnR (39.9%). However, significantly lower methanogenesis efficiencies were observed in the 50-MaR (19.3%) and 150-MaR (24.6%) reactors, likely due to the inhibitory effect of increased oxygen dosage to methanogens. Although the effluent ORP of all five reactors was maintained below -300 mV under all conditions, the reduced methanogenesis rates at higher micro-aeration dosages indicate relatively higher ORP (as shown in Fig. 5.2B) had a considerable impact on methanogen activities.

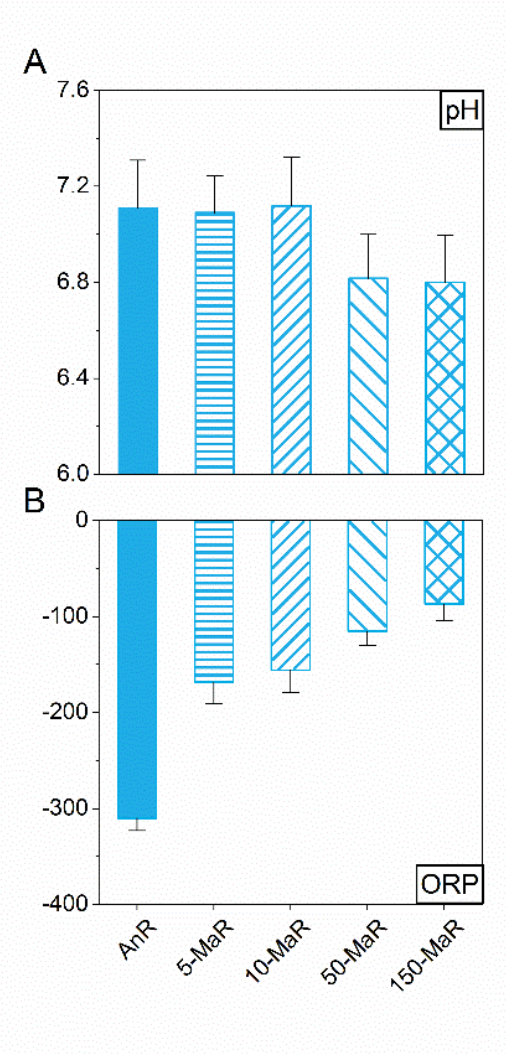

Fig. 5.2. Effluent pH and ORP measured immediately after air injection. (A) pH. (B) ORP.

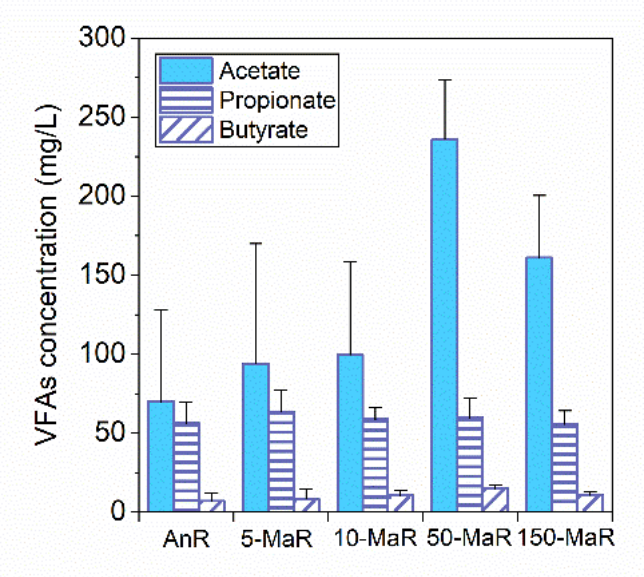

Fig. 5.3. VFAs composition.

The effects of micro-aeration intensity on effluent VFA concentrations are shown in Fig. 5.1C. Detailed information on VFA compositions and reactor pH changes are provided in Fig. 5.3 and 5.2A. As shown in Fig. 5.1C, effluent VFA concentrations exhibited decreasing trends as the HRT was reduced from Stage I to IV, correlating with the increasing methanogenesis efficiencies discussed above. The 50-MaR condition showed the highest VFA accumulatio in all stages, also correlating to the lowest methanogenesis activities in 50-MaR (Fig. 5.1B), possibly due to the VFA inhibition of methanogens. In Stage IV, 50-MaR had the highest VFA concentration (324.5 ± 4.5 mg/L), which was more than three times higher than that observed in AnR, 5-MaR, and 10-MaR, and was slightly higher than the VFAs produced from 150-MaR (199 ± 1 mg/L). As compared to the 150-MaR, 50-MaR had higher hydrolysis efficiency, but lower methanogenesis efficiency, both contributing to the higher VFA accumulation.

The acidogenesis efficiency (accounting for the proportion transformed to methane) is shown in Fig. 5.1D. The acidogenesis efficiency was significantly higher ($P < 0.01$) in 5-MaR, 10-MaR, and

50-MaR (54.1 ± 2.3 %, 45.4 ± 4.7 % and 55.0 ± 0.9 % in last stage, respectively), as compared to AnR (38.0 ± 2.2%). This indicates that micro-aeration at relatively lower dosages improved acidogenesis. Further, since the different component is mainly acetate (Fig. 5.3), it reveals that the acetogenesis step of anaerobic digestion can also be enhanced.

5.3.2 Microbial community analysis

The microbial community alpha-diversity and number of different genera, which indicates community richness, is shown in Fig. 5.4A for bacteria and archaea. Both bacterial and archaeal communities exhibited a decreasing trend with the increasing oxygen dosage, which may be explained by the inhibitory effects of oxygen on some of the obligate anaerobic microorganisms. The PCoA of Bray-Curtis distance (Fig. 5.4B) shows that bacterial and archaeal communities were clustered into an AnR, 5-MaR, and 10-MaR group, and 50-MaR and 150-MaR group, and shifted away from the inoculum community. The clustering pattern is in close relation to the methanogenesis efficiency pattern (Fig. 5.1B) where AnR, 5-MaR, and 10-MaR showed similar values while 50-MaR and 150-MaR showed impaired levels of methanogenesis. The total abundance ratios of archaea and bacteria showed a decreasing trend with increasing oxygen dosage (Fig. 5.4B), which further confirmed that oxygen has an inhibitory effect on methanogens.

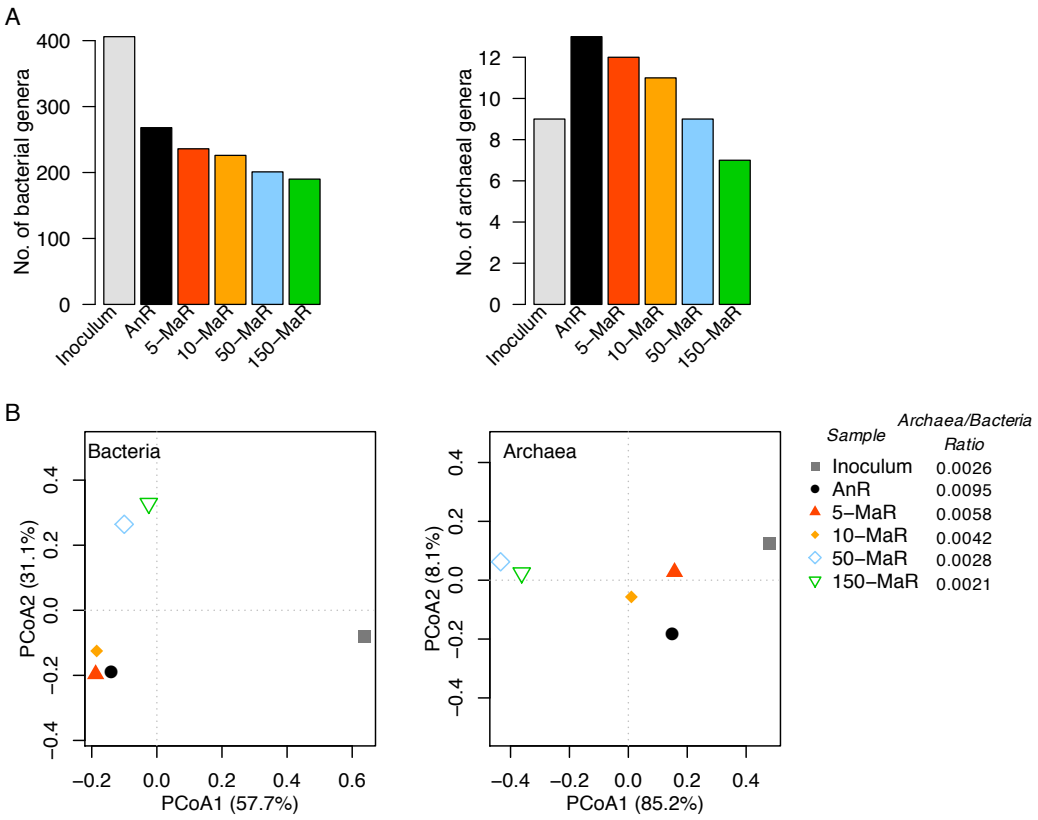

Fig. 5.4. Microbial community diversity. (A) community richness indicated by the number of genera. (B) PCoA of Bray-Curtis distance.

The comparison of archaeal genera composition is shown in Fig. 5.5A. The AnR, 5-MaR, and 10-MaR were dominated by *Methanosaeta*, which is an acetoclastic methanogen. The abundance of *Methanosaeta* was remarkably lower at higher micro-aeration dosage conditions (50-MaR and 150-MaR). In comparison, *Methanosarcina*, which can utilize both acetate and H_2/CO_2 to produce methane, was less affected by the oxygen dosage. The decreasing order of the sum of *Methanosaeta* and *Methanosarcina* abundances in 5-MaR, 10-MaR, AnR, 150-MaR, and 50-MaR is well correlated with methanogenesis efficiencies at the final steady state. On the other hand, *Methanospirillum*, a hydrogenotrophic strain, had a higher abundance in the higher oxygen dosage reactors (50-MaR and 150-MaR), indicating that hydrogenotrophic methanogens may have a

higher tolerance to oxygen and thus become the dominant methane-production pathway under higher oxygen levels. Further, *f_Methanomassiliicoccaceae* was present in all reactors but also higher in these two reactors (41 % in 50-MaR and 35 % in 150-MaR), indicating that obligately methylotrophic may proliferate under higher oxygen conditions.

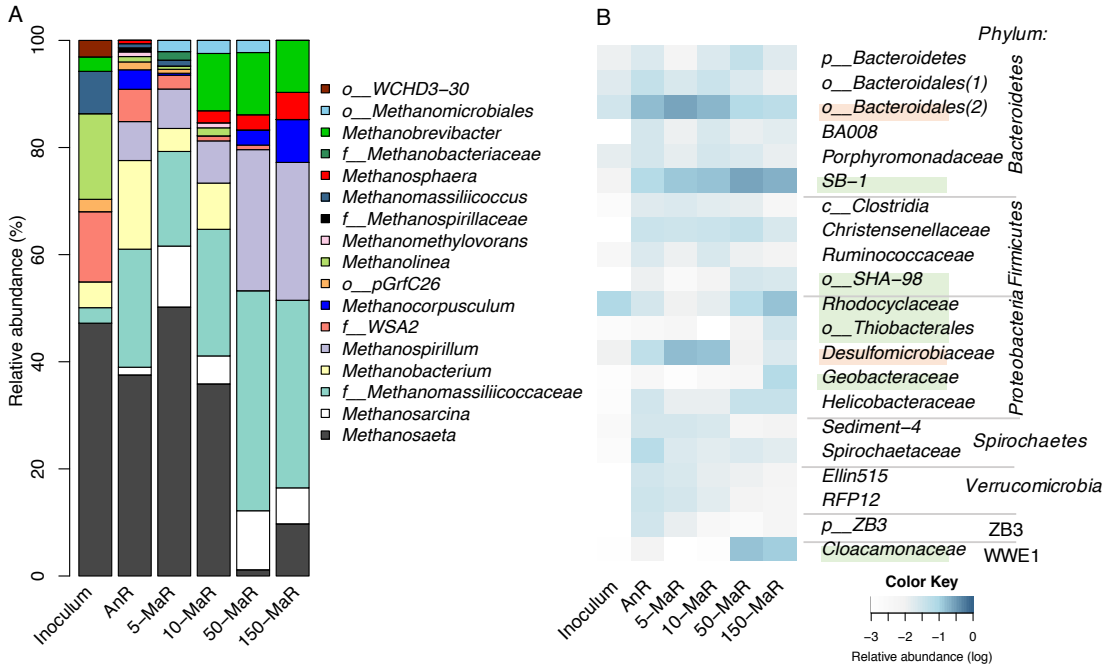

Fig. 5.5. (A) The relative abundance of archaeal genera (B) The most abundant 10 bacterial families in samples of inoculum, AnR, 5-MaR, 10-MaR, 50-MaR, and 150-MaR. The orange shade indicates higher abundance in 5-MaR, the green shade indicates higher abundance in 50-MaR or 150-MaR.

The bacterial composition at the family level of the most abundant 10 families in each reactor is shown in Fig. 5.5B. 5-MaR and 10-MaR shared similar abundances of bacterial families, while the 50-MaR and 150-MaR shared similar abundances. One unidentified family in the order *Bacteroidales* (*o__Bacteroidales[2]*) and *Desulfomicrobiaceae* were highly enriched in 5-MaR

(26 % and 17 %, respectively) and 10-MaR (18 % and 16 %, respectively). *Bacteroidales* makes up a significant portion of fecal bacterial population (Ridley et al., 2014) and have been reported to function as hydrolytic/fermentative bacteria of large macromolecules such as cellulose and protein (Azman et al., 2017b; Yi et al., 2014) The enrichment of these fermenters and sulfate-reducing bacteria in low micro-aeration intensity reactors may be attributed to enhanced substrate provided by hydrolysis. At higher oxygen dosages, certain families showed increased abundance, including *SB-1* from the phylum *Bacteroidetes*, one unidentified family in the order *SHA-98* from the phylum Firmicutes, *Rhodocyclaceae*, one unidentified family in the order *Thiobacterales*, *Geobacteraceae* from the phylum *Proteobacteria*, and *Cloacamonaceae* from the phylum *WWE1*. *Bacteroidetes* is a broad group of microorganisms that mainly ferment polysaccharides or carbohydrates (Braz et al., 2019). 5-MaR, 10-MaR, and 50-MaR all showed higher *Bacteroidetes* levels (45 %, 44 % and 43 %, respectively) compared to AnR (37 %), which correlates well with the hydrolysis activities observed. The increase of *Cloacamonaceae* may be related to the VFA accumulation in 50-MaR and 150-MaR since these microorganisms may ferment amino acids and syntrophically oxidize propionate (Braz et al., 2019; Goux et al., 2015). Decreasing trends in abundance with increasing oxygen dosage were observed in the families *Sediment-4* and *Spirochaetaceae* (phylum *Spirochaetes*), *Ellin515* and *RFP12* (phylum *Verrucomicrobia*), and one unidentified family in the phylum *ZB3*, indicating their inhibited activity under high oxygen dosage.

The metagenome and functional genes were predicted from the 16S rRNA gene amplicon data using a reference database (Langille et al., 2013). Different oxygen dosages promoted different functional groups as shown in Fig. 5.6. In the metabolism function group, 50-MaR showed the highest prevalence of the biosynthesis and metabolism of glycan, and the metabolism of

carbohydrates, nucleotides, terpenoids, polyketides, cofactors, vitamins, and lipids, which can be associated with the high VFA production and accumulation in 50-MaR. The 50-MaR reactor also exhibited the highest prevalence of genetic information processing functions of replication and repair, translation, folding, sorting, and degradation, which could be triggered by the acidic environment resulting from VFA accumulation. The highest oxygen dosage (150-MaR) improved functions of xenobiotics biodegradation and metabolism as well as signal transduction and membrane transport, which require sufficient energy and maybe promoted at higher ORP (Fig 3.2B). Moreover, cell mobility, growth, and death functional genes were the highest in 150-MaR, indicating active growth of cells, which may have resulted from the promoted activity of aerobic microorganisms.

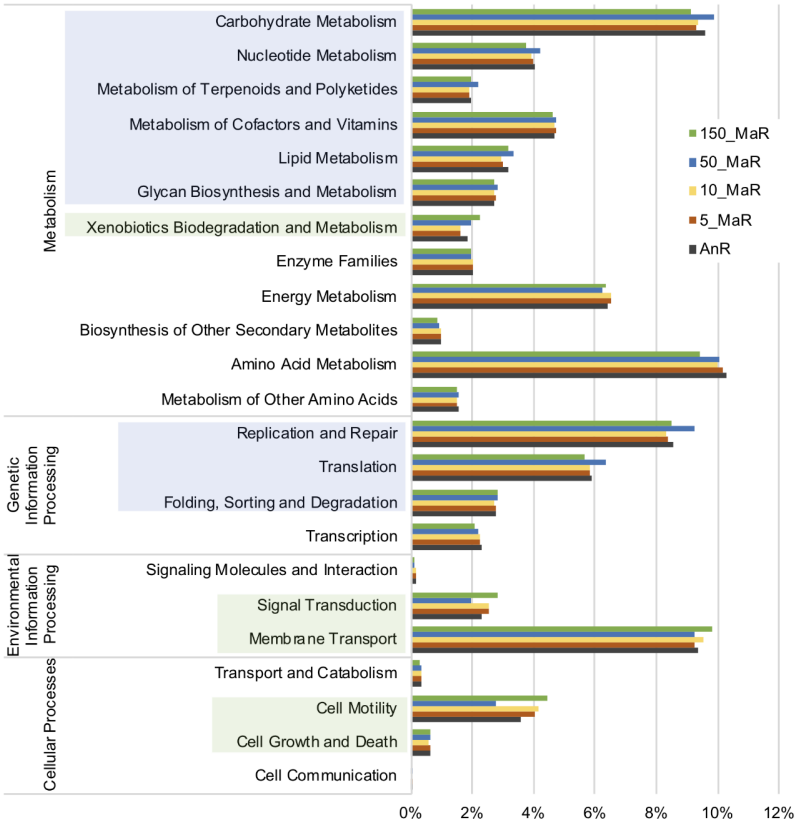

Fig. 5.6. Predicated metagenome functions. The blue shade indicates a higher abundance in 50-MaR, and the green shade indicates a higher abundance in 150-MaR.

5.3.3 Correlation between parameters

Fig. 5.7 depicts the Pearson's product-moment correlation matrix between oxygen dosage and reactor performance (effluent VFAs, effluent SCOD, methanogenesis, hydrolysis, and acidogenesis), pH and archaea/bacteria ratio, and the significance level ($P < 0.05$) of the correlation. Oxygen dosage had a significant negative correlation with the hydrolysis and acidogenesis efficiencies. Further, higher oxygen dosages were significantly negatively correlated with methanogenesis, pH, and archaea ratio, resulting in higher effluent VFAs and SCOD since the methanogenesis was inhibited and organic substrates were accumulated. Fig. 5.7 shows a significant positive correlation between effluent VFAs and SCOD since the SCOD was primarily

composed of fermented substrates. Methanogenesis was significantly negatively correlated with effluent VFAs and SCOD, because the VFAs and SCOD were either transformed to methane or accumulated in the reactor. A positive correlation cluster between methanogenesis, hydrolysis, acidogenesis, pH and archaea ratio is shown in the lower part of Fig. 5.7, indicating that the biochemical reactions in anaerobic digestion process are interrelated; this emphasizes the importance of maintaining an appropriate pH and archaea ratio.

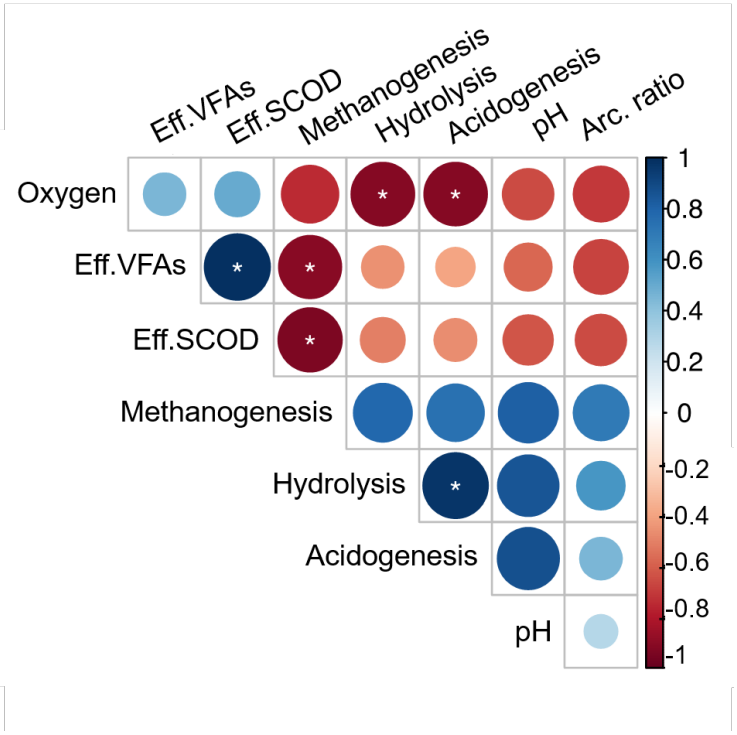

Fig. 5.7. Correlogram of reactor parameters and archaea ratio in the total community (star denotes significance $P < 0.05$).

5.4 Discussion

5.4.1 Balance between anaerobic and aerobic activities

Low oxygen dosages could promote hydrolysis and acidogenesis bacterial activity. The growth of *Bacteroidetes* was enhanced at lower oxygen dosages compared to anaerobic conditions (Fig. 5.5B). Large molecules were broken down into smaller molecules such as tyrosine (Fig. 5.8). By manipulating the oxygen level in the extracellular environment, intracellular metabolic pathways and oxidation related gene expressions of microbes can also be changed (Liu et al., 2013). The predicted metagenome functions of medium oxygen dosages (Fig. 5.6) exhibited higher functional genes of large-molecule metabolism (carbohydrate, nucleotide, terpenoids, polyketides, cofactors, vitamins, lipids, and glycan). However, too much oxygen may promote aerobic microorganism growth, *e.g. Rhodocyclaceae* grow under high oxygen dosages (Fig. 5.5B), and inhibit methanogens, especially *Methanosaeta* (Fig. 5.5A). In micro-aerobic environment, anti-oxidative enzymes are produced to protect cells. *Bacteroides fragilis* (*p__Bacteroidetes*), *Desulfovibrio gigas* (*p__Proteobacteria*), and *Methanosarcina barkeri* (*g__Methanosarcina*) were reported to show 2 to 30 times overexpression of genes encoding anti-oxidative enzymes under an oxidative stress as compared to anaerobic conditions (Brioukhanov and Netrusov, 2007; Brioukhanov et al., 2006).

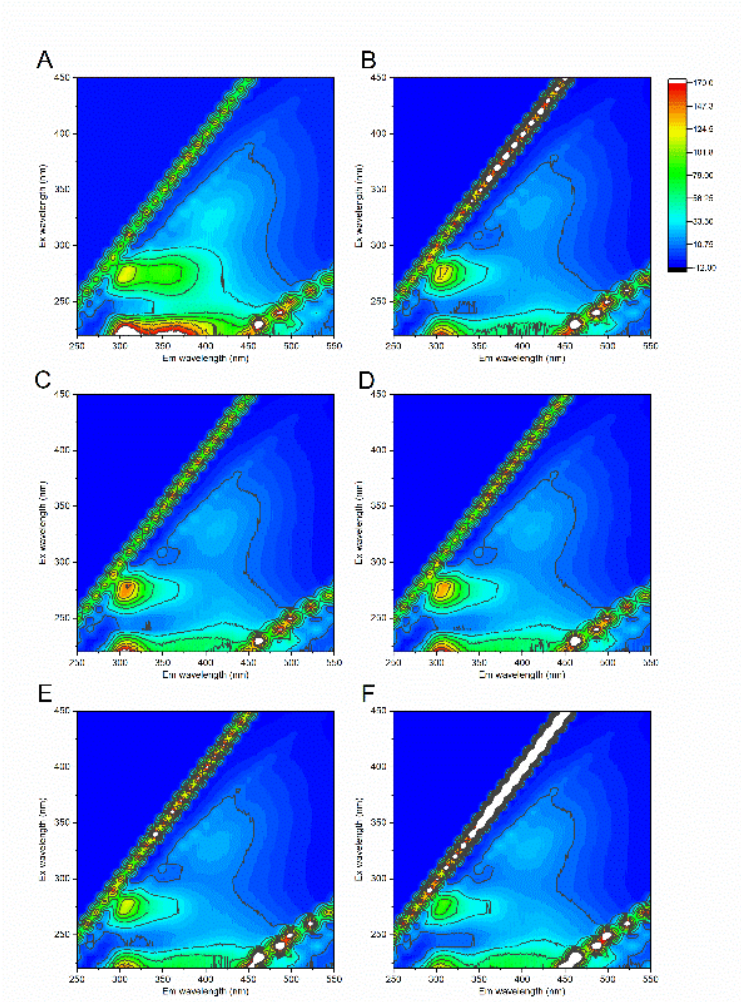

Fig. 5.8. EEM A-influent blackwater; B-F AnR, 5-MaR, 10-MaR, 50-MaR, 150-MaR.

5.4.2 End product-oriented oxygen dosage control

The micro-aeration intensity varies depending on specific purpose and feed composition. There are four interdependent steps during anaerobic degradation of organic waste, and the products excreted by one step serve as the substrates for another group of microbes and thus should be kept kinetically constant. To avoid the inhibition of methanogens and harvest the highest methane yield, low oxygen dosages should be applied when designing a micro-aeration-based AD system. However, the hydrolytic acidification process is also considered an economical and effective

pretreatment method, especially for wastewater containing highly recalcitrant and complex pollutants (Braz et al., 2019; Tsapekos et al., 2017). A medium oxygen dosage (50 mg O_2/L-reactor/cycle, 5 % of influent COD) is the threshold oxygen level for methanogen inhibition, cutting off the methanogenesis step for VFA production (Duan et al., 2017; Xu et al., 2014). The syntrophic anaerobic oxidation of VFAs to acetate and H_2 is inhibited under medium micro-aerobic condition, as indicated by the lowest *Proteobacteria* level (13 %), which include glucose and VFAs utilizing bacteria (Ariesyady et al., 2007). Further, higher oxygen level (150 mg O_2/L-reactor/cycle) is sufficient to facilitate the highly energetic metabolism of aerobic VFAs oxidation by heterotrophs (Zhu et al., 2009). Previous studies showed that in order to enhance hydrolysis, micro-aeration rates can be calculated based on 2 – 10 % of substrate COD (Botheju and Bakke, 2011), while in our study a much lower oxygen dosage (0.5 % of influent COD) was needed to boost hydrolysis, offering a cost-efficient strategy.

5.5 Conclusion

This study evaluated the effects of five micro-aeration intensities (0, 5, 10, 50, and 150 mg O_2/L-reactor/cycle) on the hydrolysis, acidogenesis, and methane yield of blackwater in five ASBRs. The optimum micro-aeration intensity was 5 mg O_2/L-reactor/cycle (5-MaR), which accelerated COD solubilization (hydrolysis efficiency 48.7 ± 3.33 %) and enhanced methane production (methanogenesis efficiency 50.7 ± 0.20 %) by 40.3 % and 28.1 %, respectively, when compared to no aeration (hydrolysis efficiency 34.7 ± 3.75 % and methanogenesis efficiency 39.6 ± 0.28 %). However, excessive oxygen (150 mg O_2/L-reactor/cycle) had a negative effect on the AD process. Aerobic respiration consumes some organics which were supposed to be recovered as energy. Further, strict anaerobes were inhibited before oxygen was consumed. VFAs accumulated in the 50 mg O_2/L-reactor/cycle reactor (ranging from 324.5 mg/L to 418.3 mg/L) due to the lack of

downstream VFA conversion, so medium-dose micro-aeration offers an operational strategy for a two-stage anaerobic digestion system. Oxygen impaired the diversity of bacteria and archaea but enriched more competitive microorganisms which can recover higher methane compared to the fully anaerobic reactor.

CHAPTER 6 SELF-FLUIDIZED GAC-AMENDED UASB REACTOR FOR ENHANCED METHANE PRODUCTION[4]

A version of this chapter has been published in Chemical Engineering Journal.

6.1 Introduction

Supplementation of GAC was found to enhance the AD efficiency in wastewater treatment possibly by stimulating DIET-based syntrophy and methanogenic kinetics (Park et al., 2020; Ryue et al., 2019). Methanogens act as an electron sink for electrons generated by the fermentative bacteria, and this syntrophic partnership ensures favorable conditions for efficient AD. Previous GAC applications in continuously operated UASB reactors have GAC settled at the reactor bottom, which limits the sludge-GAC contact and clogs the reactor inlet. Fluidizing GAC at the reactor upper layers can overcome these drawbacks and leaves the bottom zone for solids hydrolysis.

This study aimed to examine the effect of GAC fluidization on AD reactor performance efficiency. Three UASB reactors, supplemented with plastic biofilm carriers-only, GAC-only and the self-fluidized-GAC (plastic biofilm carriers combined with GAC) reactors were operated and compared under ambient temperature (20 ± 0.5 ºC) for 120 days. Fundamental mechanisms with respect to the impact of GAC addition on reactor performance were evaluated and discussed.

6.2 Materials and methods

6.2.1 Experimental setup and inoculum

Three up-flow anaerobic sludge blanket (UASB) reactors with a working volume of 2.0 L each were operated continuously at room temperature (20 ± 0.5 ºC) for 120 days. The inoculum sludge

[4] Yu, N., Guo, B., Zhang, Y., Zhang, L., Zhou, Y. and Liu, Y. 2020b. Self-fluidized GAC-amended UASB reactor for enhanced methane production. Chemical Engineering Journal, 127652.

(VS 7.4 g/L) was obtained from a full-scale anaerobic digester at a local wastewater treatment plant (Edmonton, Alberta, Canada). The Control reactor was supplemented with fifty polyethylene (PE) plastic media of 1-inch diameter (Powkoo, Canada) as shown in Fig. 6.1. The GAC-only reactor was supplemented with 25 g/L activated carbon pellets (Acurel®, USA), which settled at the bottom of the reactor due to the relatively higher density of GAC (~2 g/mL) than the sludge blanket. The SF-GAC (self-fluidized GAC) reactor was filled with the same amount of GAC in the GAC-only reactor evenly packed into fifty plastic media. The multiple-channel structure in the bio-balls provides water flow and nutrient access for the bacteria colonization on and captures the produced biogas, allowing carriers move to the upper layer of the sludge blanket by means of buoyancy.

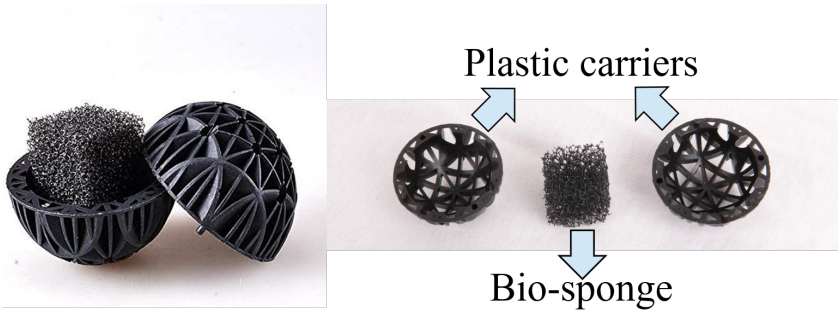

Fig. 6.1. The bio-balls added to the control reactor.

6.2.2 Synthetic wastewater and analytical methodology

The composition (per liter) of this synthetic wastewater was as follows: glucose (3.0 g); $CaCl_2 \cdot 2H_2O$ (0.026 g); $MgCl_2 \cdot 7H_2O$ (0.05 g); NH_4Cl (0.23 g); K_2HPO_4 (0.031 g); KH_2PO_4 (0.027 g); $NaHCO_3$ (2.0 g); and trace nutrient solution (0.3 mL) as described in our previous work (Guo et al., 2020b). The chemical oxygen demand (COD) of this high-strength synthetic wastewater was 3000 mg/L. The feeding was flushed with nitrogen gas for 15 mins to deoxygenate before it was

fed to the reactors. COD, total solids (TS), volatile solids (VS), and volatile suspended solids (VSS) were determined based on the protocols from Standard Methods of American Public Health Association (Rice et al., 2012). The pH was measured with a pH meter (B40PCID, VWR, SympHony). The biogas was collected in a 10 L foil gas bag (CHROMSPEC™, Brockville, Canada) and the methane production was assessed twice a week by measuring the gas volume in the gas bag with a 500 mL syringe, and the composition of biogas was determined using gas chromatography (GC,7890B Agilent Technologies, USA) equipped with a Hayesep Q column and a thermal conductivity detector. Helium gas with a 99.999% purity was used as the carrier gas in the system. The operation temperature of the oven and the detector was 100 ^{o}C and 200 ^{o}C, respectively. The dissolved methane was measured using a NaCl saturation method according to Zhang et al. (Zhang et al., 2013), and the results of which are shown in Fig. 6.2. Volatile fatty acids (VFA) including acetate, propionate, and butyrate were analyzed using ionic chromatography (IC) (DIONEX ICS-2100, ThermoFisher, USA) equipped with a conductivity detector and IonPac AS18 Analytical Column (2 x 250 mm) after being filtered through 0.22 μm membrane filters (Fisher Scientific, CA).

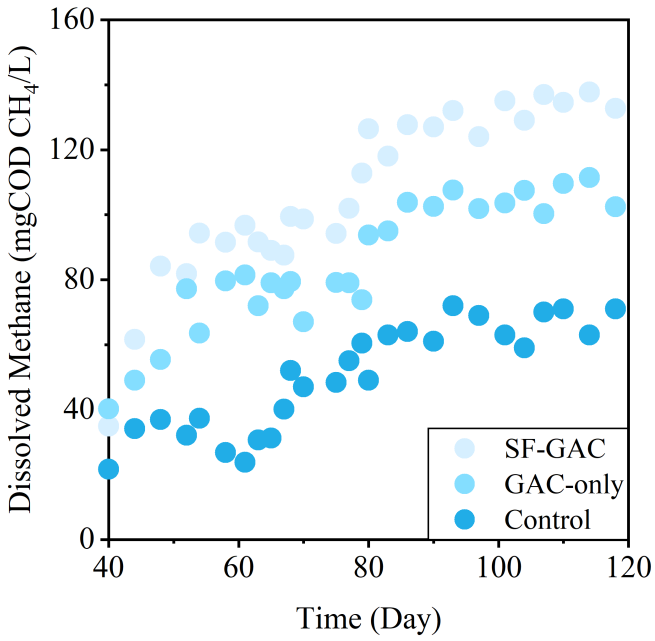

Fig. 6.2. Dissolved methane in three UASB reactors.

6.2.3 Sludge characterization and hydrogen inhibition tests

Specific methanogenic activity (SMA) tests were conducted for sludge from all three reactors at steady state to determine the maximum methane production rate of the incubated sludge for different reactor configurations in different parts of the reactors (up and low layers of the sludge blanket, sampling locations were shown in Fig. 6.3). For each SMA test, 5 mL of sludge from the reactor was diluted with 15 mL deionized water and added to 38 mL serum bottles. Sodium acetate (1 g/L) and H_2/CO_2 (volumetric ratio 4:1) were fed into the bottles to determine the activities of acetoclastic and hydrogenotrophic methanogens, respectively. The headspace of the bottles was filled with nitrogen gas in the SMA tests for acetate or H_2/CO_2-mixed gas in the SMA test for H_2/CO_2 and then sealed with rubber stoppers and aluminum caps.

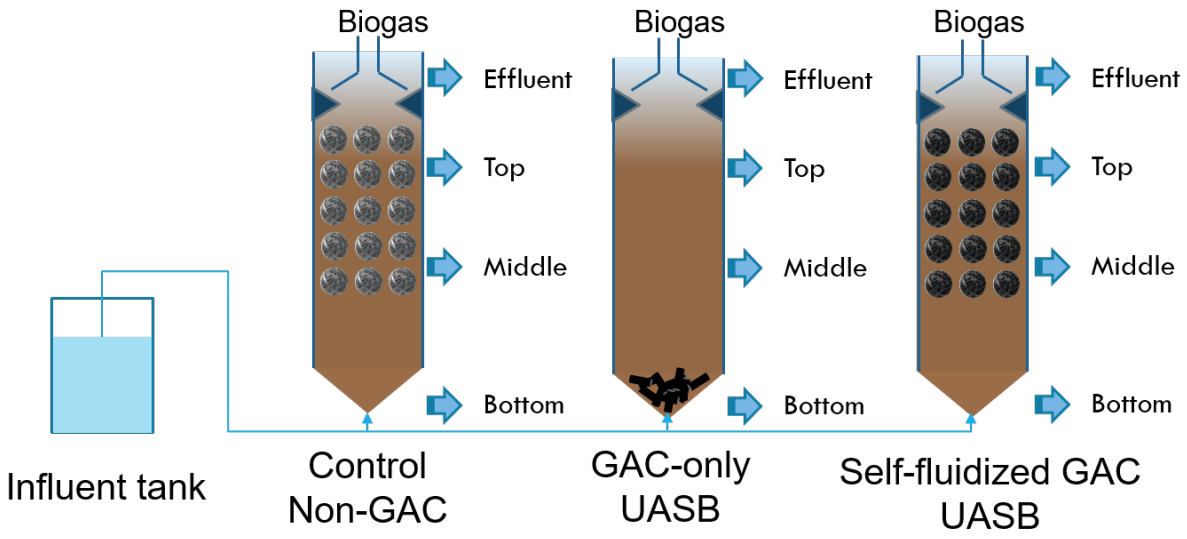

Fig. 6.3. The schematic layout and sampling depth of the UASB reactors.

To determine whether DIET-functioning microbes were enriched in the reactors, a high hydrogen partial pressure (about 10 kPa) was applied to inhibit the hydrogen-producing pathway during propionate and butyrate degradation. The seed sludge was taken from the middle port of the three UASB reactors during steady state operation. 1 to 2 mL of seed sludge was added to 38 mL serum bottles to inoculate with the same amount of sludge VSS. Sodium propionate was used as the sole carbon source. Dipotassium phosphate and monopotassium phosphate were supplied as buffer in lieu of sodium bicarbonate in the nutrient solution to prevent the generation of carbon dioxide from inorganics. The COD concentration of the nutrient solution was 1 g/L and each bottle contained 10 mL of the nutrient solution (De Kreuk and van Loosdrecht, 2006; Sheng et al., 2018). The high hydrogen partial pressure conditions were achieved by replacing the nitrogen headspace with hydrogen gas. Nitrogen-flushed bottles, with or without GAC, were used as control. Three kinds of activated carbon with different particle sizes, including GAC (activated carbon pellets as applied in the UASB reactors), SAC (small granular activated carbon from Sigma-Aldrich, 4-12 mesh

Oakville, ON, Canada) and PAC (powdered activated carbon obtained by grinding SAC), were supplemented (0.055 g/bottle) to serum bottles to investigate the impacts of the carbon-based material size. Batch assay bottles were incubated at room temperature in a shaking incubator at 120 rpm in the absence of light. All batch tests were conducted in triplicates.

6.2.4 AHL extraction and analysis

AHL in the sludge and water phases was measured by liquid chromatography tandem-mass spectrometer (LC-MS/MS) (Wang et al., 2017). The following AHLs (> 97%) were purchased from Sigma-Aldrich (Canada) and measured in this study: C4-HSL, C6-HSL, 3O-C6-HSL, C8-HSL, 3O-C8-HSL, C10-HSL, 3O-C10-HSL, C12-HSL, 3O-C12-HSL, C14-HSL, and 3O-C14-HSL. Briefly, mixed liquor was collected from the middle of the UASB reactors three times in one day then centrifuged at 9500 *g* for 10 min, and sludge pellets were re-suspended in 5 mL methanol with 50 μL protease inhibitor C (Sigma-Aldrich, CA). The mixture was ultrasonicated at 200 W for 30 min and centrifuged again at 9500 *g* for 10 min. The supernatant was then filtered through 0.45 μm membrane filters (Fisher Scientific, CA) and recorded as sludge phase. Similarly, 100 mL of the reactor effluent was centrifuged, filtered, and recorded as water phase. Finally, all the samples were concentrated by solid-phase extraction (SPE) with HLB tubes and then evaporated to dryness with a nitrogen evaporator. The samples were dissolved in methanol spiked with 20 μg/L of C4-HSL-d5 as an internal standard before analysis by the LC-MS/MS.

6.2.5 Modified Gompertz model

A modified Gompertz model (Eq. 1) was applied to compare the biogas production potential (P), maximum rates of methane production (R_m), and the duration of lag phase (λ, in days) using OriginPro® (Li et al., 2012). The equation is as follows and the fitted curves are shown in Fig. 6.9.

$$M = P \times exp\left\{-exp\left[\frac{R_m \times e}{p}(\lambda - t) + 1\right]\right\} \quad \text{(Eq. 1)}$$

6.2.6 Microbial community analysis

To compare the microbial communities enriched in reactors with different configurations, suspended biomass samples (account for more than 90% of the total VS) were collected from the top, middle and bottom ports of the reactors (as shown in Fig. 6.3) at the end of the experiment and were centrifuged at 4000 *g* for 10 min. DNA extraction was performed for the sludge pellets using the DNeasy PowerSoil Kit (QIAGEN, Hilden, Germany), according to the manufacturer's protocol. The 16S rRNA genes were amplified through the polymerase chain reaction (PCR) using the universal primer pair 515F (GTGCCAGCMGCCGCGG) and the 806R (GGACTACHVGGGTWTCTAAT). Sequencing was performed on the Illumina Miseq platform and analyzed using the Qiime2 DADA pipeline with 99% similarity with reference to the Greengenes database version 13_8. Prediction of microbial functions was done using the Phylogenetic Investigation of Communities by Reconstruction of Unobserved States (PICRUSt) referring to the Kyoto Encyclopedia of Genes and Genomes (KEGG) database (Langille et al., 2013). Co-occurrence network analysis was conducted for microbial communities developed from different seeds, using "igraph" and "psych" packages in R. The correlation matrix was obtained by using the "corr.test" function of the "psych" package, and the species were considered statistically significant correlated when $P < 0.01$ and $r > 0.6$.

6.2.7 Extreme gradient boosting (XGboost) regression models

XGboost regression is an estimator to solve supervised multi-output problems. The experimental conditions including seed source (NG, GDS, GMix), substrate (glucose, propionate, butyrate), before or after batch cultivation, and batch cultural conditions including headspace gas (H_2 or N_2)

and with or without fresh AC addition were the input, which were used to predict the relative abundance of top bacterial and archaeal taxa (average relative abundance > 1%) from 33 samples using the XGboost regressor with python package "xgboost" (version 1.6.1). The samples were randomly separated into training datasets and validation datasets with a ratio of 4:1. Mean decrease in impurity (MDI) was used to determine the feature (experimental conditions) importance with the function permutation importance in the python package "sklearn" (version 1.0.2). All the packages were running in python version 3.9.12.

6.2.8 Statistical analysis

A student's T-test using Microsoft Excel® was performed to determine the level of significance between means. A P-value less than 0.05 was considered as statistically different results.

6.3 Results and discussion

6.3.1 Anaerobic digestion of TWAS treated with different concentrations of $Ca(ClO)_2$ at different food/inoculum (F/I) ratios

COD removal and methane production

Three UASB reactors, including the carriers-only reactor (Control), GAC-only reactor (GAC-only) and the self-fluidized GAC reactor (SF-GAC) were fed with 3 g COD/L glucose and operated at room temperature of 20 ^{o}C for 120 days. The GAC in the GAC-only reactor was settled at the bottom of the reactor throughout the experiment and occupied 3% of the total reactor volume; while the GAC in SF-GAC reactor was dispersed along the sludge bed, thus the design enhanced the sludge/GAC contact. The final VSS in the Control, GAC-only and SF-GAC reactor were 12.1, 11.5 and 15.1 g, respectively, indicating that the SF-GAC configuration benefits biomass growth and retaining in a UASB reactor.

The organic loading rate was step-wise increased from 500 g COD/m^3/d (from days 1 to 54 including 40 days of reactor start-up) to 1000 g COD/m^3/d (from days 54 to 68) then to 1500 g COD/m^3/d (from days 68 to 120). The addition of GAC (in both GAC-only and SF-GAC reactors) remarkably enhanced reactor performances in terms of COD removal and methane production (Fig. 6.4). During steady state operation (from day 100 to the end of experiment), the effluent COD was 137 ± 45 mg/L in the SF-GAC reactor (with GAC well mixed in the reactor sludge blanket), 201 ± 31 mg/L in the GAC-only reactor (with GAC settled at the bottom of the reactor), while the effluent COD in non-GAC reactor remained high at 1013 ± 50 mg/L. Overall, GAC-amendment in reactors reduced the lag phase for methane production and led to a two-fold higher methane recovery. The methanation rate was 0.66 ± 0.02 g CH_4-COD/g influent COD in the GAC-only reactor and 0.77 ± 0.02 g CH_4-COD/g influent COD in the SF-GAC reactor, both of which were significantly higher ($P < 0.01$) than that of the non-GAC reactor, being 0.33 ± 0.08 g CH_4-COD/g influent COD. There was no significant difference in methane production between the GAC-only reactor and the SF-GAC reactor ($P > 0.05$) until day 79, while after which SF-GAC reactor exhibited a 16.9% higher methanation rate ($P < 0.01$) compared to the GAC-only reactor. This observation indicates a successful energy recovery system established through the novel SF-GAC UASB reactor design.

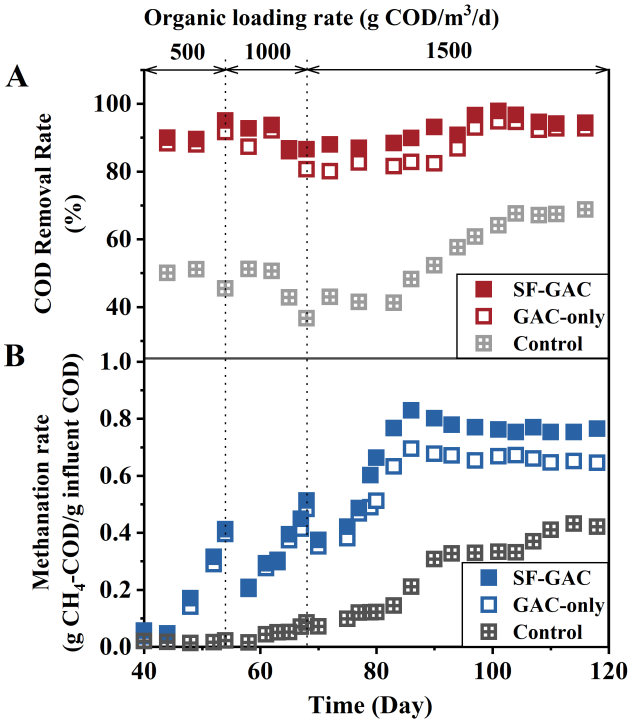

Fig. 6.4. Reactor performances: (A) COD removal rate (%) and (B) methanation rate (g CH_4-COD/g influent COD).

COD balance

The influent COD has three fates: being converted to methane or accumulating in the sludge bed or effluent. As shown in Fig. 6.5, without the GAC amendment, the non-GAC reactor had high COD accumulation in the sludge (35.4 ± 6.7%), only 32.9 ± 8.3% influent COD was converted to methane, and 40.5 ± 9.0% influent COD ended up in the effluent. In comparison, the GAC-amended reactors exhibited remarkably higher methane conversion percentage, with 66.1 ± 1.7% and 77.3 ± 2.2% influent COD converted to methane in the GAC-only and SF-GAC reactors, respectively. As a result, improved effluent quality (10.6 ± 5.1% influent COD for the GAC-only reactor and 6.4 ± 3.0% influent COD for the SF-GAC reactor) and reduced sludge accumulation

(21.6 ± 2.6% in GAC-only reactor and 19.0 ± 2.9% in SF-GAC reactor) were observed for GAC-amended reactors. Comparing the two GAC-amended reactors, it was clear that more energy was harvested as biomethane from the SF-GAC reactor.

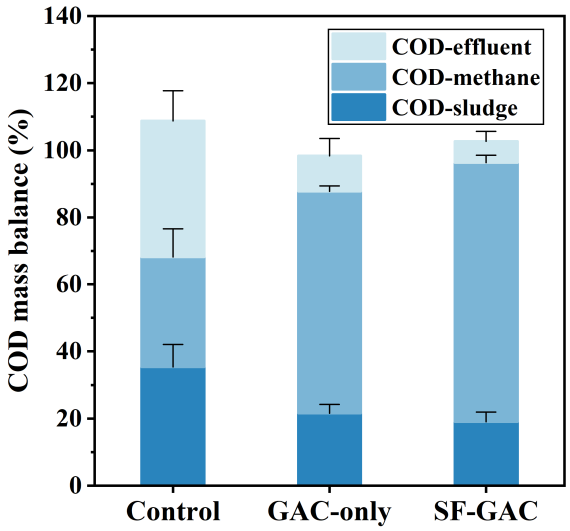

Fig. 6.5. COD mass balance. Error bars represent the standard deviation from triplicate measurements.

6.3.2 Spatial variation of volatile fatty acids (VFAs) and activity

Mixed liquor samples were taken from the top, middle, and bottom layers of the sludge blanket in the UASB reactor, along with the effluent to determine the spatial distribution of VFA under steady state conditions. As shown in Fig. 6.6, effluent VFA was the highest in the non-GAC reactor and was the lowest in the SF-GAC reactor. This result corresponds to the high methane production and COD reduction in the SF-GAC reactor. Further, for all three UASB reactors, the bottom layers of the reactors exhibited the highest VFA concentrations and lowest pH, as compared to the middle and top layers of each reactor. This observation indicates that fermentation was the dominant process at the bottom of the reactors.

Interestingly, for the SF-GAC reactor, although VFAs concentrations remained as the lowest among the three reactors in reactor effluent and in the middle and top layers of the reactor, the SF-GAC reactor had the highest VFAs accumulation at the bottom layer of the reactor as compared to GAC-only and non-GAC reactors. This result indicates that the conversion of VFAs to methane was mainly promoted at the mid and upper layer of the reactor (*i.e.*, middle to top layer of the sludge bed), while a fermentation zone existed at the bottom layer of the SF-GAC reactor. Hence, it can be concluded that the GAC addition not only accelerated the methanogenesis process, but also the acetogenesis rates in the reactor, which may be attributed to the improved syntrophic degradation activities, as described by (Xu et al., 2018), who found that GAC greatly increased the abundance of syntrophic bacteria such as *Syntrophomonas*, *Symbiobacterium*, and *Desulfotomaculum* species and enhanced the syntrophic methanogenic pathway. The observed low VFA accumulation at the bottom layer of the GAC-only reactor may be attributed to the high methanogenic activities at the bottom layer of the GAC-only reactor (as GAC accumulated at the bottom layer of the reactor). The segregation of fermentation and methanogenesis as observed in SF-GAC reactor provided more principal electron donors (*i.e.*, short-chain fatty acids and alcohols) for DIET-functioning bacteria such as *Geobacter* species, allowing them to thrive under the competing pressures of various microorganisms in complex organic wastes treatment (Zhao et al., 2017). On the contrary, the highest VFA and COD accumulation were observed throughout the control reactor, indicating the lowest system stability (Gao et al., 2020c). Overall, our observations demonstrated that the SF-GAC reactor configuration enhanced the performance of anaerobic digestion by fluidizing GAC and promoting the fermentation and VFA conversion efficiency throughout the reactor, as compared to the conventional GAC-amended (GAC-only) reactor.

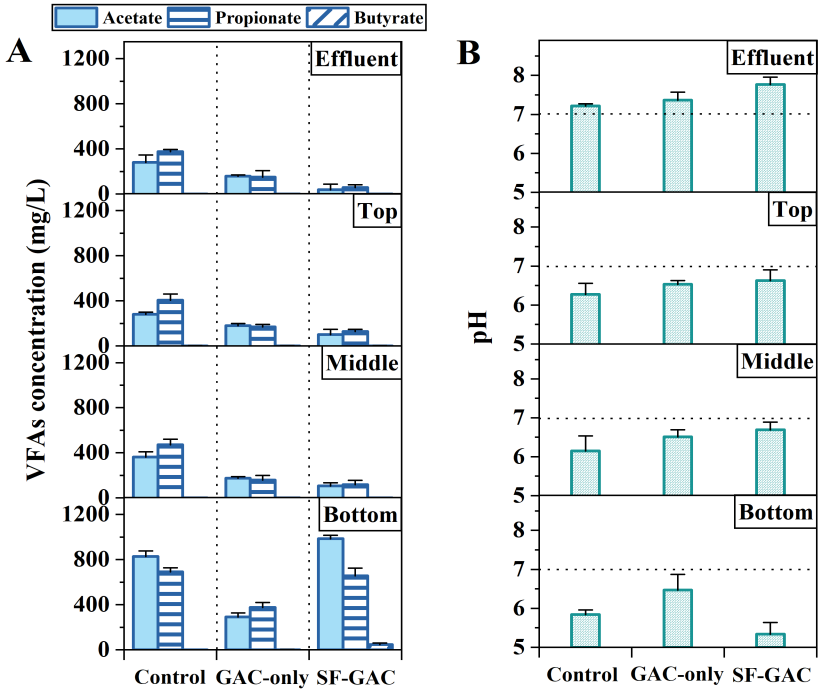

Fig. 6.6. Spatial variation of (A) VFA concentrations (mg/L) and (B) pH. Error bars represent for the standard deviation from triplicate measurements.

Fig. 6.7 illustrated the sludge SMA variations with the supplementation of H_2/CO_2 or acetate, which were reflected as hydrogenotrophic (SHMA) and acetogenotrophic methanogen activities (SAMA), respectively. The overall methanogenic activities for H_2/CO_2 were remarkably higher than those for acetate in all three reactors, which indicates that hydrogenotrophic methanogenesis was the predominant pathway. At the bottom layer of the reactors, the SHMA was the highest in the GAC-only reactor (0.052 ± 0.003 g COD/g VSS/d), as compared to the SF-GAC (0.034 ± 0.002 g COD/g VSS/d) and the non-GAC (0.017 ± 0.001 g COD/g VSS/d) reactors. In comparison, at the top layer of the reactor, the SHMA was the highest in the SF-GAC reactor (0.052 ± 0.004 g COD/g VSS/d), as compared to the GAC-only (0.037 ± 0.000 g COD/g VSS/d) and non-GAC (0.037 ± 0.001 g COD/g VSS/d) reactors. The settled-GAC (GAC-only) reactor promoted the

hydrogenotrophic methanogenic activity of the bottom sludge, but not for the top sludge where the biomass cannot get close contact with GAC. The SF-GAC reactor exhibited higher SHMA at both the bottom and top layers, as compared to the non-GAC reactor.

It was interesting to observe that SAMA was relatively high in the GAC-only reactor, where no clear spatial variation was observed. The relatively lower SAMA in the top layer of the SF-GAC reactor may be attributed to the high SHMA and syntrophic activities enriched in the SF-GAC reactor. Overall, GAC addition led to a 3 to 6 times SAMA increase, as compared to that in the non-GAC reactor.

Comparing to the methane-producing capability that calculated from SMA and the corresponding VSS, the observed methane yield of the control, GAC-only and SF-GAC reactors accounted for 65.4%, 62.5% and 68.8%, respectively. The observed 30% difference may be attributed to the methanogenic activity of the biofilm in each reactor, which was consistent with previous findings (Lee et al., 2016).

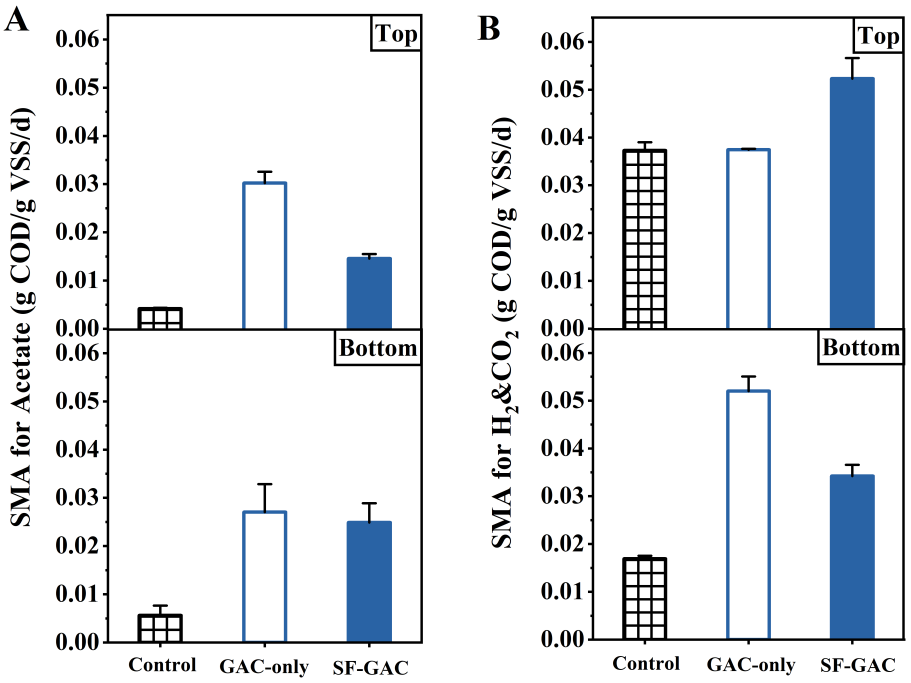

Fig. 6.7. Spatial specific methanogenic activity for (A) acetate (g COD/g VSS/d) and (B) H_2 and CO_2 (g COD/g VSS/d). Error bars represent standard deviations from triplicate experiments.

6.3.3 Batch tests under high hydrogen partial pressure

To examine if the sludge developed DIET-function, high hydrogen partial pressure was introduced to the sludge to hinder the hydrogen producing pathways involved in propionate and butyrate degradation. DIET offers an alternative to the conventional hydrogen interspecies transfer which can still function under hydrogen inhibitory conditions. Different sizes of activated carbon (*i.e.*, GAC, SAC, PAC) were added to the seed sludge taken from three UASB reactors (*i.e.*, the non-GAC UASB (NG), settled-GAC amended UASB (GDS), and the floated-GAC UASB (GMix)). The conversion of propionate and butyrate to methane under different gas compositions and with or without activated carbon conditions were shown in Fig. 6.8 and Fig. 6.10, respectively. Under

such high hydrogen partial pressure conditions, only with direct interspecies electron transfer (DIET) can methane produced (Muller et al., 2010).

Adding small-sized activated carbon (SAC and PAC) to the GAC enriched sludge (*i.e.,* seed sludge taken from GAC-only and SF-GAC reactors) enabled methane recovery from propionate under the high hydrogen partial pressures. In contrast, this process was suppressed under hydrogen inhibitory conditions without the supplement of activated carbon, and the addition of pellet activated carbon (GAC) failed to help mitigate the hydrogen inhibition in the serum bottles during the 40 days experiment. Sludge taken from the non-GAC reactor showed little methane production under high hydrogen partial pressure even with the addition of SAC and PAC, indicating a lack of DIET-functional microbial communities. The microbial consortium enriched in the GAC-only reactor started to generate methane in about 25 days with the supplement of SAC and PAC and reached final methane production of 12.12 ± 0.34 and 11.55 ± 0.14 mg-COD, respectively. The high hydrogen concentration showed less impact on the SF-GAC sludge with the addition of SAC and PAC compared to sludge enriched in other reactors. Specifically, 11.75 ± 0.60 and 15.20 ± 0.27 mg-COD methane production was observed for serum bottles seeded with sludge from SF-GAC reactor with SAC and PAC addition, respectively, which was comparable to the N_2 and N_2 + GAC conditions (12.57 ± 0.32 and 12.65 ± 0.30 mg-COD methane) in these reactors.

The maximum gas production rate in the SF-GAC consortium (0.7 and 0.9 mg-COD CH_4/d with SAC and PAC, respectively) was more than triple that of the GAC consortium (0.2 mg-COD CH_4/d) according to the modified Gompertz model Fig. 6.9. Eliminating hydrogen inhibition with the supplementation of small-sized activated carbon, as observed in the microbial consortium enriched with GAC-addition in UASB reactors, indicated the establishment of DIET between microbes. Further, more syntrophic partners that participated in DIET may have been enriched in the SF-

GAC reactor compared to the GAC-only reactor, as suggested by the higher methane production rate. GAC fluidization created a better mixing condition that facilitated DIET by acting as an electrical conduit between propionate-oxidizing bacteria and methanogens with higher electron transfer efficiency. In comparison, lower DIET-active microbes were enriched in the GAC-only reactor as indicated by the lower methane recovery rate.

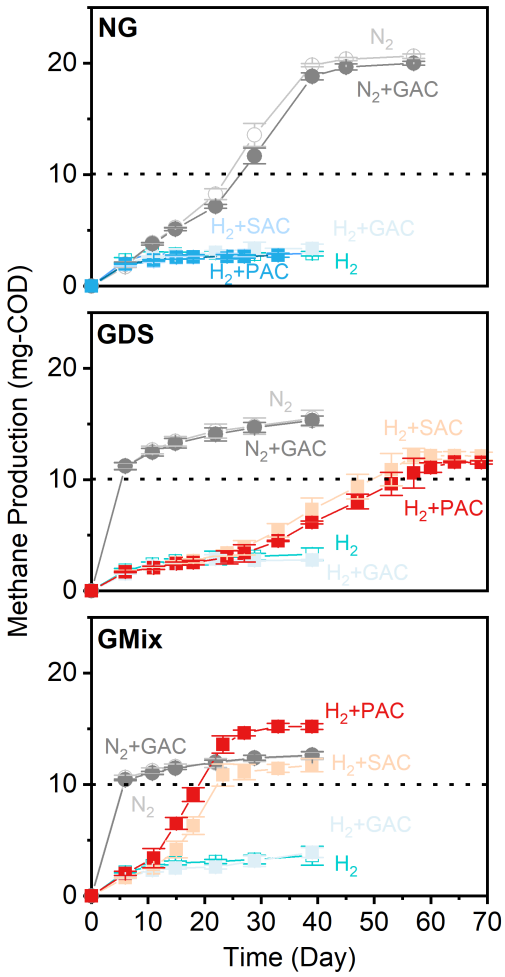

Fig. 6.8. Accumulated methane production from propionate seeded with sludge from the (NG) non-GAC control reactor, (GDS) GAC-only reactor, and (GMix) self-fluidized GAC reactor. Error bars represent the standard deviation from triplicate experiments.

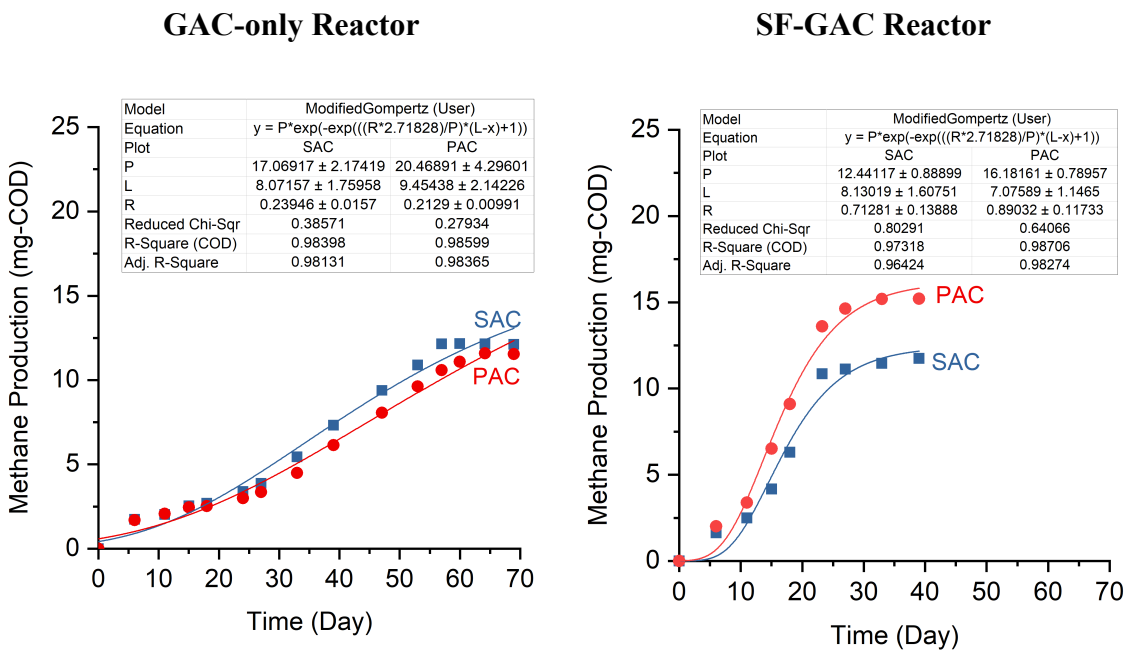

Fig. 6.9. The modified Gompertz model fitted methane production curves of seed sludge from GAC-only and SF-GAC reactors supplied with SAC and PAC.

Different sizes of fresh activated carbon particles were supplemented to the bottles in propionate degradation test, and the small-sized activated carbon exhibited the potential of mitigating hydrogen inhibition. Therefore, only the powdered activated carbon (PAC) was applied in the butyrate test. The microbial consortia enriched in the reactor without conductive material addition showed two methane production patterns during the batch incubation with butyrate as shown in Fig. 6.10. The conversion of butyrate to methane was observed after a lag phase of 21 days (according to the modified Gompertz model) under a conventional non-inhibitory anaerobic environment (N_2, N_2 + PAC). However, when high H_2 partial pressures were applied, the methane production was inhibited for 50 days, and the addition of fresh PAC did not alter the methane production pattern. This result illustrated the strong dependency on IHT pathway of a conventional

anaerobic consortia, which was incapable of degrading propionate/butyrate under high hydrogen partial pressure due to the lack of a DIET-functioning microbial community.

In comparison, the sludge collected at the GAC downstream and surrounding GAC exhibited a shorter methane production lag phase (3 days) under N_2 conditions. Moreover, the addition of PAC (H_2 + PAC) successfully mitigated the hydrogen inhibition in 19 days and 7 days with the GDS and GMix seed, respectively, and the final methane production was slightly higher than the N_2-filled reactors (11.3 – 11.6 mg-COD methane comparing to 9.3 – 10.8 mg-COD methane under N_2 conditions). This observation supports the hypothesis that a GAC enriched microbial consortia can perform butyrate oxidation under hydrogen inhibitory conditions by DIET with the presence of AC. Similar results have been reported when magnetite was supplemented to a potential DIET consortium (Guo et al., 2020a).

Although DIET was enabled for both GAC-enriched consortia, the GMix seed showed enhanced DIET function comparing to the GDS seed, with reduced methane production lag phase (in both propionate and butyrate tests) and remarkably higher methane production rate (for propionate oxidation test). Cultured in proximity with GAC may increase the DIET potential of the microbial consortia, which exhibit high interspecies electron transfer efficiency oxidizing VFAs using fresh AC as electrical conduits.

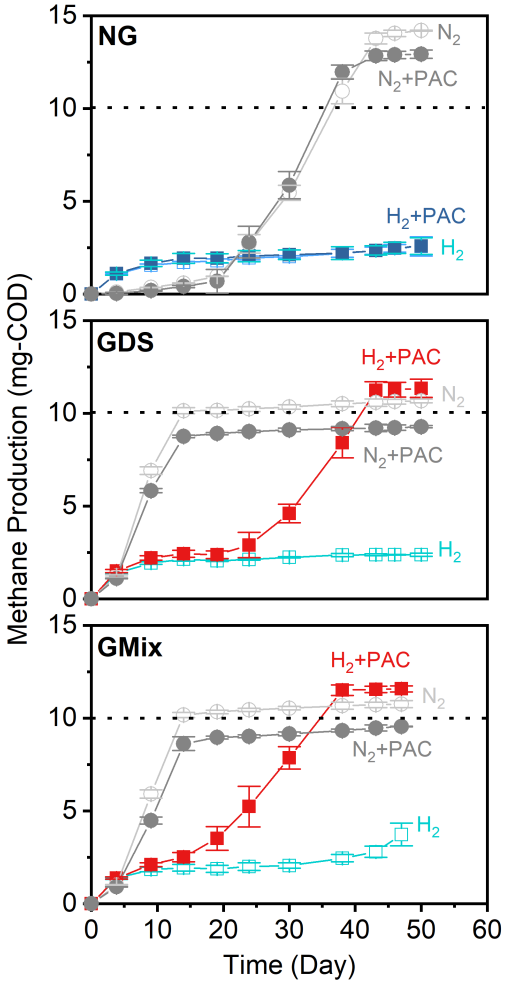

Fig. 6.10. Cumulative methane production from butyrate batch tests in batch reactors seeded with conventional anaerobic digestion sludge (NG), sludge enriched in GAC downstream area (GDS), and sludge mixed with GAC (GMix), under four operation conditions, including N_2 flushed and no PAC (N_2), N_2 flushed and supplemented with PAC (N_2 + PAC), H_2 injected and no PAC (H_2), and H_2 injected and supplemented with PAC (H_2 + PAC). Error bars represented the standard deviation of three replicates.

6.3.4 AHLs distribution

Eleven kinds of AHL were extracted and detected from the sludge and water phase in three UASB reactors as shown in Fig. 6.11. The AHLs were more abundant in the sludge phase than the water phase, indicating the intensive communications between microbes mainly happened in the sludge phase of the reactors and the poor diffusivity and low solubility of AHLs, as also discussed in previous studies (Wang et al., 2019b). The total AHL concentration in the sludge phase of SF-GAC was 61.48 ng/L, higher than that detected in the non-GAC and GAC-only reactors (45.08 ng/L and 44.25 ng/L, respectively). The AHL composition in each reactor was also different. In the non-GAC reactor, the long-chain AHLs (*i.e.*, C10- to C14-HSL) were more abundant than the short and medium chain AHLs (*i.e.*, C4- to C8-HSL) with 3O-C10-HSL (10.52 ng/L) and C14-HSL (10.62 ng/L) as the predominant AHLs in the sludge phase. In the GAC-only reactor, the medium-chain AHLs were abundant, especially 3O-C8-HSL (8.21 ng/L), followed by 3O-C10-HSL (5.92 ng/L), C8-HSL (5.56 ng/L), and 3O-C6-HSL (5.51 ng/L). Interestingly, both medium- and long-chain AHLs increased in the SF-GAC reactor with four types of AHLs including C8-HSL (9.64 ng/L), 3O-C8-HSL (11.44 ng/L), C12-HSL (8.33 ng/L), and C14-HSL (13.83 ng/L). Overall, the plastic media added in the non-GAC and SF-GAC reactors promoted the excretion of long-chain AHLs, especially 3O-C10-HSL (for non-GAC), C12-HSL (for SF-GAC), and C14-HSL (for both non-GAC and SF-GAC), while the medium-chain AHLs, such as 3O-C8-HSL and C8-HSL, were promoted in both GAC-amended reactors (GAC-only and SF-GAC reactors).

The total concentration of short- and medium-chain AHLs showed a positive correlation with the methane production in all three UASB reactors. Processes such as plasmid transfer, swarming, bio-surfactants production, EPS excretion, growth, and motility were reported to be influenced by 3O-C8-HSL and C8-HSL, which were predominantly found in GAC-amended reactors (Calatrava-

Morales et al., 2018; Zhang et al., 2019a; Zhu et al., 2020; Zhu et al., 2019), implying the stimulating effect of conductive material on system performance might be associated with the elevated levels of medium-chain AHLs. C4-HSL, 3O-C6-HSL and 3O-C8-HSL were identified as the specific QS signals of hydrolytic-fermentative bacteria, which might be associated with the enhanced fermentation in SF-GAC reactor comparing to the non-GAC reactor (Zhang et al., 2019d). Further, 3O-C8-HSL and C12-HSL have been reported to positively correlated with hydrogenotrophic methanogens, which were promoted by GAC addition, indicating an interspecific coordination of syntrophic oxidizing bacteria and hydrogenotrophic methanogens mediated by the signal molecules (Li et al., 2019a). Specifically, cellular morphology such as the growth of long filaments of *Methanosaeta harundinacea* 6Ac were reported to be promoted by AHLs and altered carbon metabolic flux that favored the conversion of acetate to methane (Li et al., 2015; Zhang et al., 2012), which might be the case in the GAC-amended reactors since the acetate conversion by filaments had a higher reaction rate comparing to short cells (Zhang et al., 2012). Long-chain AHLs, such as 3O-C10-HSL, C12-HSL, and C14-HSL, were mainly found in the carrier-supplied reactors (non-GAC and SF-GAC reactors), which might be related to the biofilm formation on the carriers (Wang et al., 2018).

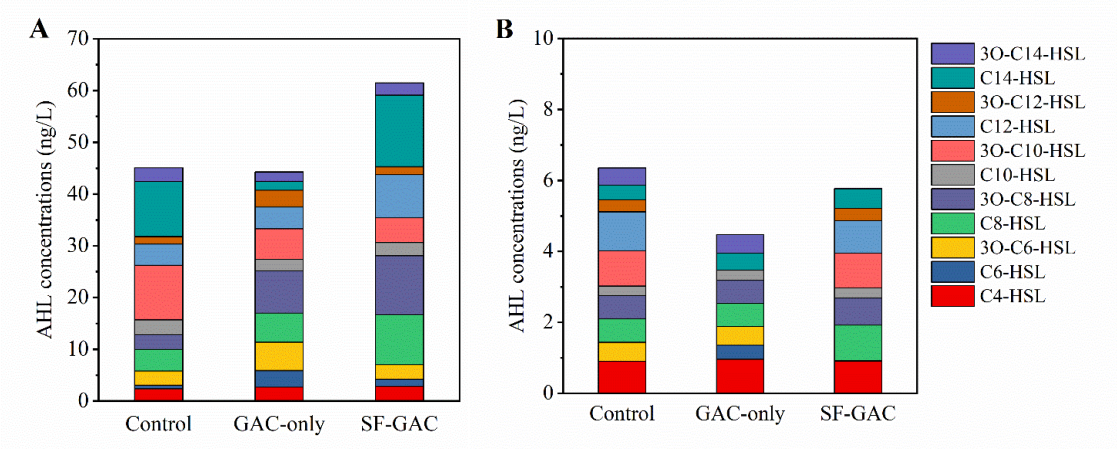

Fig. 6.11. The concentrations of AHLs in (A) sludge phase and (B) water phase of the three UASB reactors.

6.3.5 Microbial community

The most abundant and representative genera in three UASB reactors were shown in Fig. 6.12. At the bottom layers, non-GAC and SF-GAC reactors had the dominant bacteria being an unclassified genus in family *Enterobacteriaceae* (27.0% and 37.1%, respectively). *Enterobacteriaceae* ferment glucose with acid production, which correlated well to the low pH and high VFA concentrations in these zones (Fig. 6.6), indicating that acidogenesis was the main process at the plastic-carriers-amended reactors bottom. In the presence of GAC at the bottom layer of the UASB, the dominant genera for GAC-only reactor were one uncultured genus in *Clostridiales* order (28.6%) and *Clostridium* (24.2%). *Clostridium* are often observed in the presence of sugar to produce organic solvents such as butanol. Further, this fermenter has been reported to acting as an electron sink that consumes extracellular electrons, which may play an important role in controlling the redox balances in a GAC-filled zone (Moscoviz et al., 2017).

In the middle and top layers, one uncultured genus in *Clostridiales* order and *Lactococcus* were predominant in the non-GAC control reactor, which accounted for 18.9% and 18.8% in the top layer, and 45.7% and 10.8% in the middle layer, respectively. However, an unclassified genus in order *Bacteroidales*, *Treponema* and genus *T78* were more abundant in the middle and top layers of both GAC-amended reactors. *Treponema* contains known homoacetogens that produce acetate from hydrogen and carbon dioxide (Graber and Breznak, 2004), which was consistent with the significantly higher SAMA observed in the GAC-amended reactors. The syntrophic fatty acid metabolizers such as *Syntrophus*, *Syntrophomonas* and *Geobacter* only existed with low abundance in control reactor (less than 0.2%), but had much higher abundance at the upper reactor zones with GAC addition (0.3% to 2.3%). It has been reported that *Syntrophus* is likely to produce e-pili and grow via DIET (Walker et al., 2020). Similarly, *Syntrophomonas* was a previously reported putative DIET participant and was greatly enriched on the GAC surface (Zhang et al., 2020a). Further, many *Geobacter* species are exo-electrogens and are considered as DIET indicator microorganisms, the relative abundance of which increased up to 8 times and 44 times in the GAC-only reactor and the SF-GAC reactor comparing to the control reactor, respectively.

At the genus level, 13 archaeal taxa were detected among all samples (Fig. 6.12B). The dominant genera were *Methanosarcina* and *Methanobacterium*, accounting for 36.0% to 47.1% and 27.5% to 42.5% in the control reactor, respectively. With GAC added at the bottom of the reactor (GAC-only UASB), *Methanosarcina* was enriched throughout the GAC-only reactor, and *Methanobacterium* only accounted for 15.5% to 24.4% in the reactor. In comparison, *Methanosarcina* was greatly enriched at the middle and top zones (62.9% to 77.5%) of the SF-GAC reactor, and the hydrogenotrophic *Methanobacterium* dominated the reactor bottom (64.2%). Our results suggested that location of GAC amended played a significant role in controlling the

spatial distribution of microbial community in the UASB reactors. *Methanosarcina*, a potential DIET-active methanogenic archaea that could accept extracellular electrons (Park et al., 2018), was remarkably enriched in the GAC-only reactor and the upper zones in SF-GAC reactor. The coexist of exo-electrogenic bacteria (*e.g.*, *Geobacter*) and *Methanosarcina* indicated that DIET-based syntropy between these microorganisms occurred in GAC amended reactors (throughout the GAC-only reactor and middle to top layers in SF-GAC reactor). Further, *Methanospirillum*, which was not detected in the non-GAC reactor, but has been reported to produce electrically conductive archaellum enabling long-range electron transfer (Walker et al., 2019), was enriched in GAC-amended reactors, with the relative abundance ranging from 2.4% to 5.1% in the GAC-only reactor and from 4.3% to 11.4% in the SF-GAC reactor. These results indicated that GAC supplementation would stimulate the growth of previous reported DIET-active microorganisms and GAC fluidization further enriched well-known DIET partners such as *Geobacter* and *Methanosarcina*, boosting methane production by enhancing DIET.

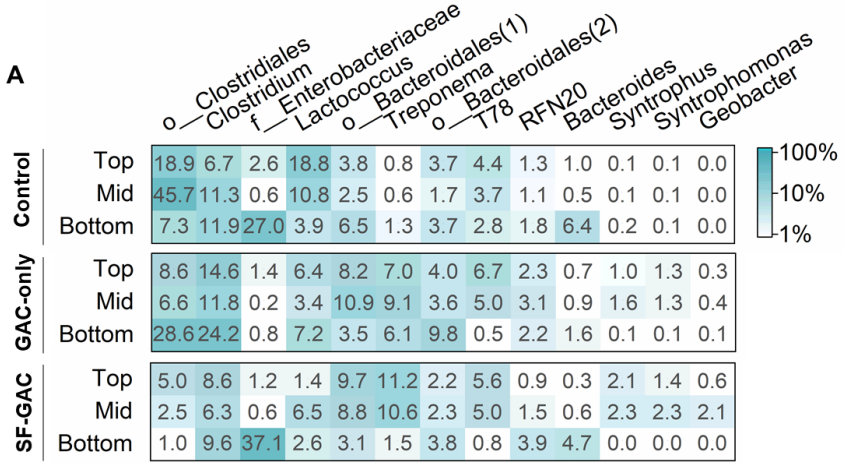

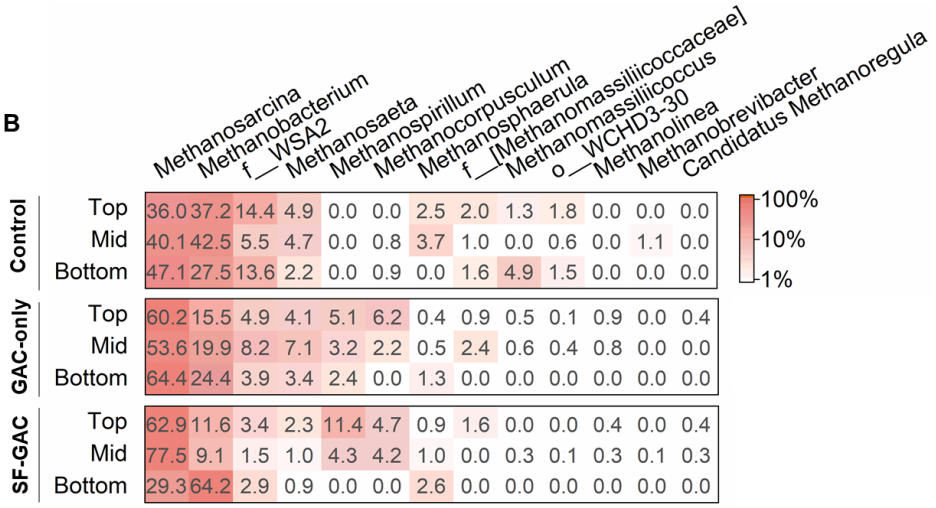

Fig. 6.12. Relative abundance of major (A) bacterial and (B) archaeal communities at genus level. The taxonomic names were shown for genus level or higher level (family: f_; order: o_) if not identified at genus level.

6.3.6 Network analysis

Three microbial co-occurrence networks were constructed for batch reactors with different seeds (*i.e.*, NG, GDS, and GMix sludge) as shown in Fig. 6.13. Each group contains 10 samples, and the data was screened with average relative abundance > 0.1% in each group, which was 133, 89, and 93 genera (nodes) in the NG, GDS, and GMix group, respectively. Pink and blue lines indicate significant positive and negative correlations between genera (Spearman's correlation coefficient $r > 0.6$, $P < 0.01$). The NG network showed remarkably higher number of connections (799 edges) than the GDS (289 edges) and GMix (255 edges) networks. In fact, the NG network was the most complex and compact one among three networks. Connectance and average degree have been recognized as central network properties that suggest the complexity of ecological communities (Guo et al., 2022). The NG network showed the highest connectance (0.09) and average degree (12.02), followed by the GDS network (0.07 and 6.49) and the GMix network (0.06 and 5.48).

Meanwhile, it showed the lowest average path length (3.06) and average normalized betweenness (0.01). Further, although all three networks showed high ratios of positive correlations, the NG network presented the lowest (0.95). These network properties reveal the high level of microbial interaction yet low dependence on connector OTUs of the NG network, indicating its strong responses to hydrogen inhibition and AC addition, but the syntrophic interactions remained low as demonstrated by its low level of inter-module communication. In comparison, the GMix network presented the lowest clustering coefficient (0.51), connectance, average degree and modularity (0.56), illustrating the already well-developed microbial community in the GMix seed, which was barely affected by the inhibitory conditions in the batch tests.

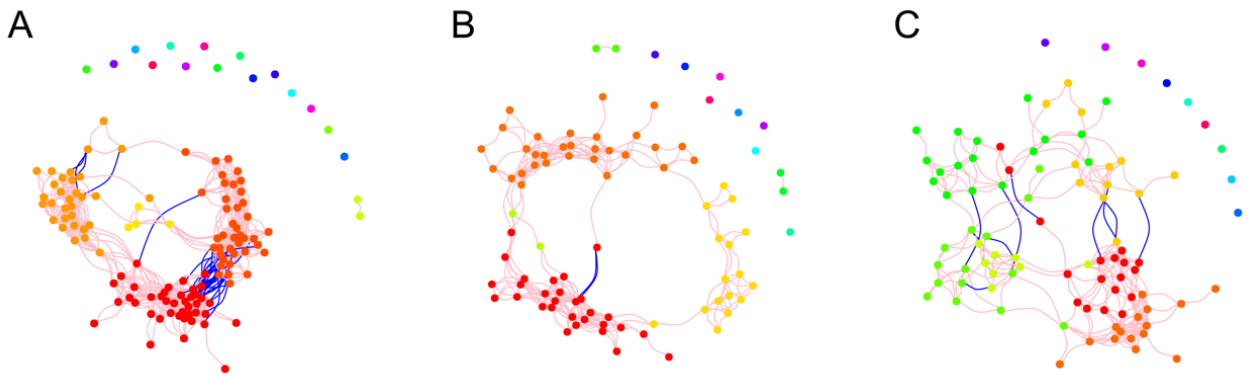

Fig. 6.13. The co-occurrence network of three groups including (A) NG, (B) GDS, and (C) GMix. Color of nodes indicates OTUs in the same module of each network. Color of lines represents positive (pink) and negative (blue) correlation coefficient.

6.3.7 Functionality and key environmental conditions prediction

The functional profiles of the microbial communities in three UASB reactors were predicted using PICRUSt as shown in Fig. 6.14. At the reactors bottom, control and SF-GAC reactors showed similar functional patterns, which were significantly different from those observed in the GAC-

only reactor, indicating that the presence of GAC at the reactor bottom greatly influenced the characteristics of the microbial functional profiles. At the bottom layer of both control and SF-GAC reactors, microbial functions in relation to membrane transport, signal transduction, transcription, and metabolism including carbohydrate metabolism, glycan biosynthesis and metabolism, metabolism of other amino acids, and xenobiotics biodegradation and metabolism were promoted, as compared to the bottom layer of the GAC-only reactor. This observation correlated with the higher substrate concentrations in control and SF-GAC reactors (see Section 6.3.3); suggesting that the nutrient availability plays significant roles in the development of these functional profiles. In comparison, the bottom of GAC-only reactor showed the highest prevalence of translation, replication and repair, folding, sorting and degradation in the genetic information processing group, which may be correlated to the accelerated cellular response to GAC. Further, the cell motility function, which can be used as an indicator of conductive pili growth that facilitates cell-to-cell attachment and electron transfer (Guo et al., 2020a; Lee et al., 2020; Wall and Kaiser, 1999), was greatly increased in the bottom of GAC-only reactor.

For the top layer biomass, both GAC amendment strategies stimulated similar microbial functions, different from those from the control reactor. For instance, as compared to the control reactor, the cell motility was promoted at the top layer of both GAC-amended reactors (*i.e.*, GAC-only and SF-GAC). Higher energy metabolism was also observed in GAC-amended reactors, which correlated well with the enhanced methane metabolism in these reactors, similar to the results reported in the literature (Zhang et al., 2017).

Moreover, compared to the control and GAC-only reactors, SF-GAC showed the highest prevalence of the signal transduction function in both top and bottom zones. This result correlated well with the AHL variations. These findings further demonstrate that SF-GAC configuration

achieved better performance through process segregation (hydrolysis at the bottom and methanogenesis at the top), while the GAC-only reactor indistinctively enhanced the microbial activities throughout the reactor.

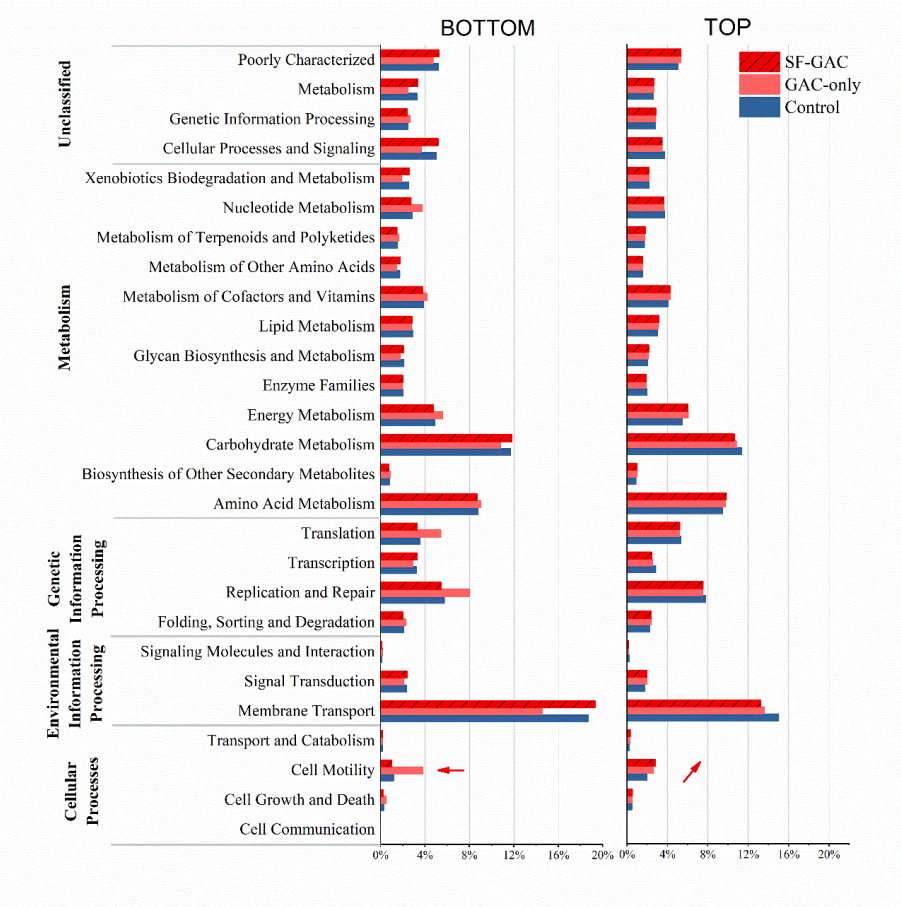

Fig. 6.14. Predicated metagenome functions of the sludge at the top and bottom layers of three UASB reactors.

The predictions of dominant bacterial and archaeal profile are based on the five experimental conditions in propionate/butyrate oxidation tests (Fig. 6.15). The R^2 for the fitting of observed relative abundance (directly from sequencing results) to predicted relative abundance of the bacteria and archaea were 0.623 and 0.948, respectively. Based on the regression, the permutation

importance was calculated. Seed source was the most significant feature for both communities. The MDI was 1.02 and 0.91 for bacterial and archaeal communities, respectively. The headspace gas composition (MDI 0.72) was also crucial in shaping the dominant bacterial communities, while the substrate (MDI 0.68) play a more important role determining the archaeal communities. Adding fresh AC (MDI 0.35) may slightly change the bacterial communities, and the batch cultivation (MDI 0.06) was the least important factor for the bacterial community. On the contrary, the archaeal communities may shift after the batch culture (MDI 0.26), while the AC addition (MDI 0.15) barely affect the archaeal communities. These results demonstrated that the hydrogen inhibitory condition and AC supplementation had bigger impacts on the electron donating bacterial communities than the electron accepting archaeal communities, and the community variation within group (*i.e.*, reactors inoculated with the same seed) was limited.

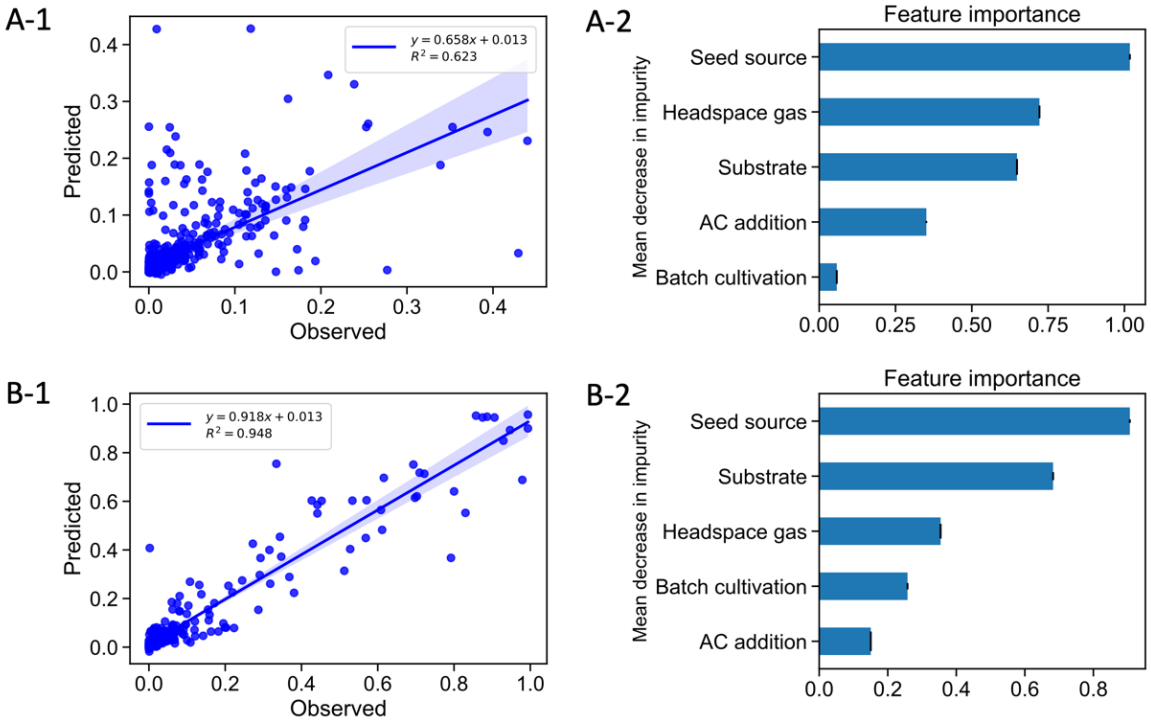

Fig. 6.15. The comparison (panel 1) of the prediction (from XGBoost regression) and observation (from sequencing results) of relative abundance and the ranking of feature importance (panel 2) for the top (A) bacterial and (B) archaeal genera.

6.3.8 Implications

Enhanced methane recovery was achieved through self-fluidizing GAC in a UASB reactor, which enhanced the contact of GAC with the digester sludge without the need for mechanical mixing. Enhanced hydrogenotrophic methanogenic activities were observed throughout the reactor depth. Although previous studies have demonstrated that adding conductive materials to anaerobic digesters can improve methane recovery, no direct evidence of DIET has been reported for continuously operating AD reactors (Zhao et al., 2017). In the present study, hydrogen inhibition experiments provided direct evidence of the enrichment of DIET-active microbiome in both GAC-amended reactors. Further, various GAC-amendment strategies influenced the methanogenic activities differently. Efficient VFA reduction in GAC-only reactor (where GAC accumulated at the bottom of the UASB) and an elevated VFA at the bottom of the reactor, which was then significantly reduced through syntrophic metabolism at the top of the reactor (observed in SF-GAC reactor, where GAC was well distributed throughout the reactor depth) demonstrate the importance of optimizing the reactor design to realize the full benefits of DIET-active reactors.

6.4 Conclusion

This study evaluated the performance of a modified UASB reactor amended with self-fluidized GAC. Enhanced methanation rates and organics removal were achieved in the novel configuration without external heating and mixing requirements as compared to the non-GAC and the GAC-only reactors. The enriched microbial consortium in both GAC-amended reactors can mitigate hydrogen inhibition with the supplement of small-size activated carbon, while the non-GAC

reactor cannot. DIET participants (*e.g.*, *Geobacter* and *Methanosarcina*) were enriched in the GAC-amended reactors especially the SF-GAC reactor. Medium-chain AHLs (3O-C8-HSL and C8-HSL) were identified as key signaling molecules, which might associate with the promotion of DIET between syntrophic partners. The self-fluidized GAC reactor exhibited a clear separation in reaction zones, where fermentation largely existed in the lower zone and enhanced methanogenesis dominated in the upper zone of the reactor. Our study suggests an economical and efficient reactor configuration that increases methanogenic activity by reinforcing the contact between GAC and sludge, providing a novel strategy for future reactor design.

CHAPTER 7 SHAPING DIFFERENTIATED BIOFILM MICROBIOMES BY CHANGING GAC LOCATION IN WASTEWATER ANEROBIC DIGESTION[5]

A version of this chapter has been published in Science of The Total Environment.

7.1 Introduction

The last chapter demonstrated that a novel UASB reactor configuration containing floated GAC can achieve 16.7% higher methane production as compared to a conventional GAC-amended UASB reactor (*i.e.*, GAC settled to the bottom of the reactor) (Yu et al., 2020b). However, the methanogenic activities of the suspended sludge were not significantly different between the two reactors, inferring a strong effect of the GAC biofilm to the methane production. The microbial communities of biofilm that formed on settled or floated GAC in UASB reactors were analyzed in this chapter. DIET-related microbial functions in biofilms and surrounding sludge flocs in the settled GAC and floated GAC reactors were investigated along with the structure, diversity, and correlation of the microbial communities.

7.2 Materials and methods

7.2.1 Reactor operation

Two up-flow anaerobic sludge blanket (UASB) reactors with 2.0 L working volume were fed with synthetic glucose wastewater, supplemented with 50 g pre-washed activated carbon pellets (3 mm diameter, Acurel® Extreme Activated Filter Carbon Pellets (Item #2343), USA), and operated continuously at room temperature (20 ± 0.5 ºC) for 120 days (Fig. 7.1). As shown in Fig. 7.1,

[5] Yu, N., Guo, B. and Liu, Y. 2021a. Shaping biofilm microbiomes by changing GAC location during wastewater anaerobic digestion. Science of The Total Environment 780, 146488.

although the total volume of GAC added to both reactors are the same, the GAC distribution in these reactors was different; with settled GAC stacked at the conical settler of the reactor and only occupied 3% of reactor volume, while the floated GAC packed in plastic media widely distributed in the middle and upper regions of the reactor (~50% of the total volume). Reactors were fed with synthetic glucose wastewater (3000 mg/L) with macro- and micro-nutrients according to a previously described recipe (Yu et al., 2020b). Steady state operational conditions and performances of the UASB reactors are summarized in Table 7.1.

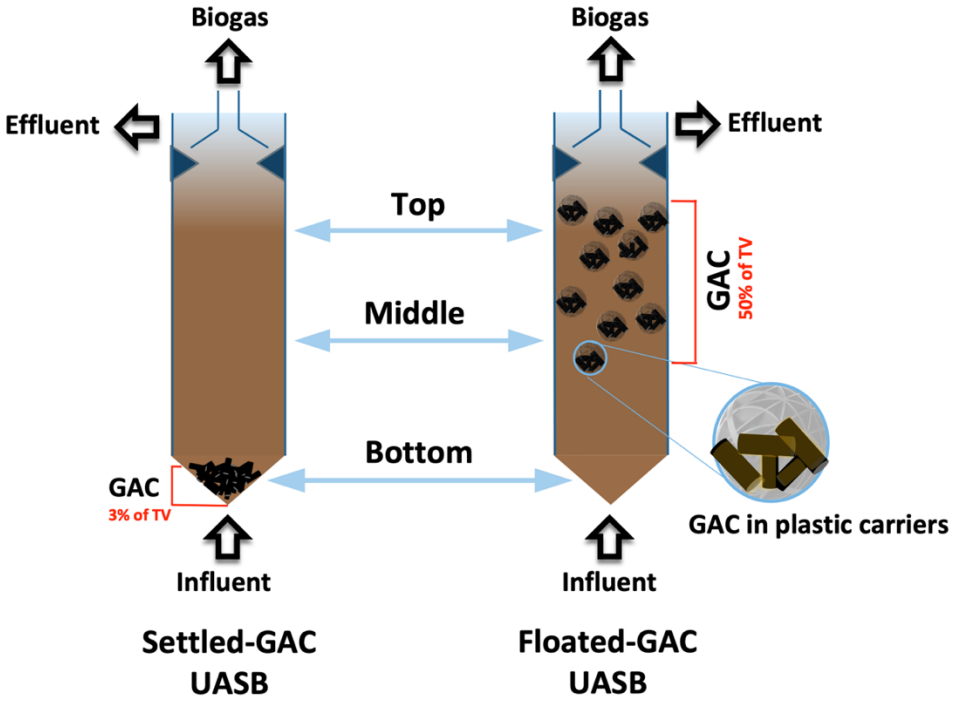

Fig. 7.1. The schematic layout and sampling depth of the UASB reactors.

Table 7.1. Comparison of UASB reactors with different GAC supplement strategies at maximum loading condition.

		Settled GAC UASB	**Floated GAC UASB**
Feed glucose concentration (mg/L)		3000	
Reactor working volume (L)		2	
Operationa6.3.1 l temperature		20 ± 0.5℃	
GAC distribution volume		3%	50%
At steady state operation			
Organic loading rate (mg COD/L/d)		1500	
COD removal efficiency (%)		93 ± 1	95 ± 2
Methanation rate (% CH_4-COD/feed-COD)		66 ± 2	77 ± 2
Volatile fatty acid acetate; propionate; butyrate (mg/L)	Top sludge blanket	178; 169; 1	101; 127; 1
	Middle sludge blanket	173; 157; 1	107; 116; 1
	Bottom sludge blanket	290; 376; 1	985; 657; 45
pH	Top	6.53	6.63
	Middle	6.51	6.69
	Bottom	6.47	5.34
Suspended sludge properties			
Volatile suspended solids	Top	8	10

(VSS) (g/L)	Bottom	10	22
SMA for acetate	Top	30	15
(mg CH_4-COD/g VSS/d)	Bottom	27	25
SMA for H_2/CO_2	Top	37	52
(mg CH_4-COD/g VSS/d)	Bottom	52	34

7.2.2 Sample collection and microbial gene sequencing

At the end of the reactor operation, duplicate GAC samples were taken from the reactor with GAC settled at the bottom and from the reactor with GAC floated with plastic carriers in the middle and top of the reactor. The GAC samples were washed with deionized water to remove loosely attached biomass or suspended sludge from the biofilm formed on the GAC. Suspended sludge floc samples were taken from the bottom, middle, and top of the reactors and centrifuged at 4000 *g* for 10 min to remove the supernatant. Genomic DNA was extracted from the biofilm attached to the GAC particles and the sludge pellets using the DNeasy PowerSoil Kit (QIAGEN, Hilden, Germany) according to the manufacturer's protocol. The DNA extraction was performed twice for each sample and mixed before downstream analysis. The 16S rRNA genes were amplified using the universal primer pair 515F/806R and purified with QIAquick PCR purification kit (Qiagen Inc. Toronto, Canada) and sent for sequencing on the Illumina Miseq platform at the McGill University and Génome Québec Innovation Centre (Montréal, QC, Canada).

7.2.3 Bioinformatics analysis

The raw gene sequences of the samples taken from the reactors were processed using the DADA2 algorithm on the QIIME2 platform to remove low-quality sequences and chimeras (Callahan et al., 2016). Taxonomy was assigned with 99% similarity with reference to the Silva database, version

132. Alpha diversity and canonical correspondence analysis (CCA) were computed using the "vegan" package in RStudio, version 4.0.2. Co-occurrence network analysis was conducted for microbial communities in spatially sampled biomass in the two reactors, including the suspended sludge biomass at different heights in the UASB reactors and the biofilm attached to the GAC or the plastic carriers, using "igraph" and "psych" packages in R. The correlation matrix was obtained by using the "corr.test" function of the "psych" package, and the species were considered statistically significant correlated when $P < 0.05$ and $r > 0.6$. Metagenome predictions and functional gene annotations were performed based on 16S rRNA gene amplicon sequence data using the Phylogenetic Investigation of Communities by Reconstruction of Unobserved States (PICRUSt) on the Kyoto Encyclopedia of Genes and Genomes (KEGG) database (Langille et al., 2013).

7.3 Results and discussion

7.3.1 Reactor performance enhanced by floated GAC

At the steady state, elevating the position and actuating the range of GAC increased the methane transformation efficiency (from 66% in the reactor containing settled GAC to 77% in the reactor containing floated GAC) and slightly improved the COD removal efficiency (from 93% in the reactor with settled GAC to 95% in the reactor with floated GAC). Moreover, the methane content in the biogas produced by the floated GAC reactor (70.0 ± 8.1% at the steady state) was higher than that in the settled GAC reactor (65.8 ± 8.4% at the steady state). The performance results in the present study are comparable to other continuous reactors operated at low temperatures, with methane production rate varies from 16 to 328 mL CH_4/L reactor/d (21.7% to 71% of the fed COD) and COD removal efficiency from 50% to 83% (Guo et al., 2020b; Tian et al., 2017; Zhang et al., 2020d). Settled GAC stimulated volatile fatty acid (VFA) utilization in the bottom sludge layer.

The sludge layer at the bottom of the settled GAC reactor had much lower VFA concentrations (total VFAs concentration 667 mg/L) than the sludge layer at the bottom of the floated GAC reactor (total VFAs concentration 1687 mg/L). The middle and top layers of the sludge blanket showed similar VFA compositions in each reactor (173-178 mg/L acetate, 157-169 mg/L propionate and 1 mg/L butyrate in the settled GAC UASB; 101-107 mg/L acetate, 116-127 mg/L propionate and 1 mg/L butyrate in the floated GAC UASB), indicating homogenous conditions in the reactor columns. Further, with GAC in the upper and middle sludge bed of the floated GAC reactor, VFAs were effectively consumed, and the upper sludge bed had lower VFA concentrations than the reactor containing settled GAC, suggesting that methanogenesis was enhanced in the middle to top zones of the floated GAC reactor.

Suspended sludge characteristics were compared between the two UASB reactors. In both upper and lower layers of the sludge, the UASB containing floated GAC showed a higher concentration of volatile suspended solids (VSS) (22 g/L at the bottom and 10 g/L at the top) than the UASB containing settled GAC (10 g/L at the bottom and 8 g/L at the top). This could be explained by the higher sludge retention capacity of the plastic carriers amended reactor, which was consistent with previous studies (Gijzen and Kansiime, 1996; Tawfik et al., 2012). However, the promotion of methanogenesis by the improved mixing due to carrier addition can be minimal, as also reported in previous studies (Gijzen and Kansiime, 1996; Parawira et al., 2006). The specific methanogenic activity (SMA) of the suspended sludge for hydrogenotrophic methanogens (H_2/CO_2) dominated both reactors (37-52 mg CH_4-COD/g VSS/d in the settled GAC UASB and 34-52 mg CH_4-COD/g VSS/d in the floated GAC UASB), which was higher near to GAC flocs than far from GAC flocs (*i.e.*, higher at the bottom in the reactor with settled GAC and higher at the top in the reactor

containing floated GAC). However, the SMA for acetate was not improved in the floated GAC reactor relative to the settled GAC reactor.

7.3.2 Effects of different GAC supplementation strategies on archaeal community compositions

The taxonomic compositions of archaeal communities at the genus level in settled-GAC biofilm and floated-GAC biofilm and the GAC surrounding flocs are shown in Fig. 7.2. Floated-GAC biofilm (Shannon diversity index 0.99-1.37) had a higher archaeal diversity than settled-GAC biofilm (Shannon diversity index 0.61-0.67). In floated-GAC biofilm, the most abundant genera were *Methanosarcina* (56.3-73.3%), followed by *Methanospirillum* (8.8-19.8%) and *Methanobacterium* (6.5-10.2%). Settled-GAC biofilm was dominated by *Methanobacterium* (84.9-85.1%), with other genera existing at low abundances (< 10%). *Methanosarcina* species are metabolically versatile with a high maximum specific growth rate and a high half-saturation coefficient, which are often observed at high organic loading rates (De Vrieze et al., 2012). *Geobacter* and *Methanosarcina* have been reported to form a DIET partnership via conductive particles in coastal sediments (Rotaru et al., 2018). Here, the enrichment of both genera may indicate the establishment of DIET in the floated-GAC biofilm, a finding that was correlated to the enhanced methane production in the UASB reactor containing floated GAC. However, the strict hydrogenotrophic methanogens, *Methanobacterium*, predominated in the settled-GAC biofilm. This could be explained by the enrichment of hydrogen producing bacteria on the settled-GAC surface. The piling up of GAC at the reactor bottom might hinder hydrogen transfer and create localized high hydrogen partial pressures, which favor the development of hydrogenotrophic methanogens such as *Methanobacterium* (Zhang et al., 2020d; Zhang et al., 2021d). Further, *Methanobacterium* is commonly found in the cathode biofilm in

bioelectrochemical systems, suggesting a potential participation in electron capture (Eerten-Jansen et al., 2013; Perona-Vico et al., 2019; Siegert et al., 2015).

The suspended sludge and the biofilm in the floated GAC reactor showed similar archaeal communities, whereas in the settled GAC reactor *Methanosarcina* were enriched in the sludge flocs but were not enriched in the biofilm; this result might have been due to the high substrate concentrations at the bottom of the settled GAC reactor that benefit the growth of *Methanosarcina*. These results demonstrated that floated GAC provided a more homogeneous condition for archaea growth than settled GAC, and the enrichment of hydrogen utilizing methanogens in the settled-GAC biofilm contributed largely to the methane production in the settled GAC reactor.

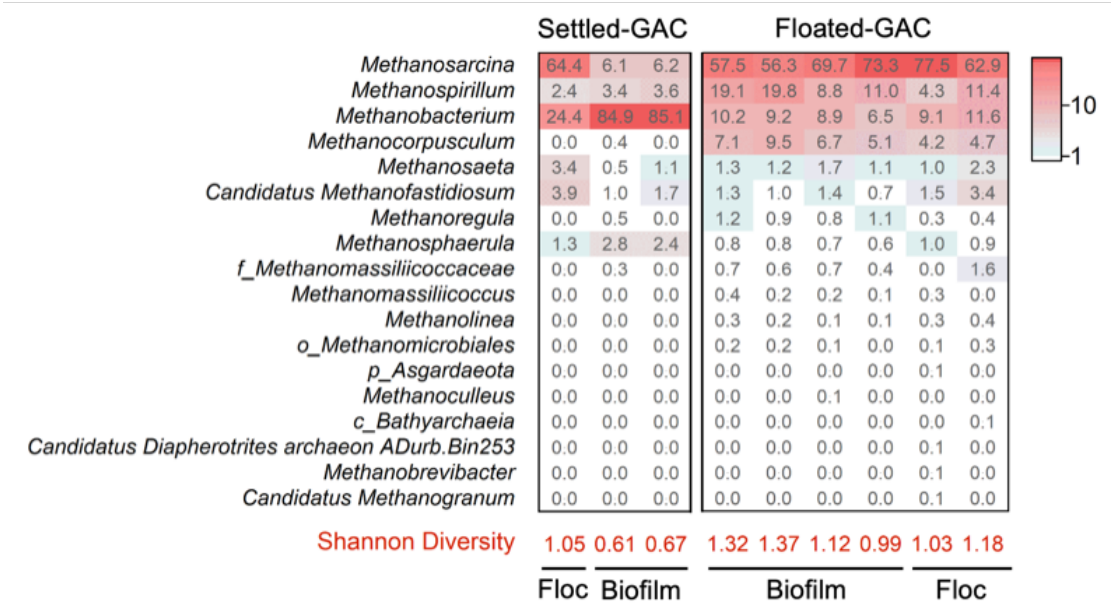

Fig. 7.2. Relative abundances of archaeal genera in settled-GAC biofilm and floated-GAC biofilm, along with the surrounding flocs. The Shannon diversity is reported at the bottom of the heatmap.

7.3.3 Effects of different GAC supplementation strategies on bacterial community compositions

GAC ascent increased the bacterial diversity in both sludge flocs and in biofilm attached to GAC as indicated by the higher Shannon diversity index value in the reactor containing floated GAC (4.12 to 4.24 for sludge floc and 4.08 to 4.36 for biofilm) compared to the reactor containing settled GAC (2.81 for sludge floc and 3.27 to 3.34 for biofilm) (Fig. 7.3).

Different GAC locations contained different bacterial communities in the GAC attached biofilm. Biofilm on floated GAC was dominated by *Geobacter*, *Smithella*, and *Syntrophomonas*, with relative abundances of 5.2-16.5%, 5.5-7.8%, and 5.2-7.7%, respectively, whereas biofilm on settled GAC was enriched with an unidentified species belonging to the family *Veillonellaceae*, the genus *Clostridium sensu stricto 1*, and the genus *Lactococcus*, comprising 12.1-16.4%, 10.4-11.3%, and 7.3-10.5% of the total bacteria, respectively. *Geobacter* biofilms were reported to bridge small non-conductive gaps by performing extracellular electron transfer with electrically conductive PilA (Hussain et al., 2021). The several conditions described below could explain the enrichment of this electrochemically active bacteria in the floated-GAC biofilm. The loosely packed GAC in the plastic wraps might provide more sites for bacteria attachment and thus increased the electron transfer efficiency compared to the settled GAC. The fermentation zone at the bottom of the floated GAC reactor converted large molecules into volatile fatty acids (VFA), which provided more principal electron donors for *Geobacter*. Further, *Smithella* and *Syntrophomonas* are known as syntrophic propionate and butyrate oxidizing bacteria, respectively (Muller et al., 2010), which benefit the establishment of an unimpeded electron flow that eventually enhanced methanogenic performance in the reactor containing floated GAC. In comparison, the settled-GAC biofilm was enriched with *Veillonellaceae*, most members of which

produce propionate and acetate by polysaccharide degradation (Gamage et al., 2017), and *Lactococcus*, which ferments glucose to lactic acids (Teuber, 1995). *Clostridium sensu stricto 1*, an iron-reducing bacterium, was shown to be electrochemically active, and might play an important role in stimulating DIET with methanogens in the settled GAC reactor (Guo et al., 2020c; Gupta and Sar, 2019). *Clostridium sensu stricto 1* also contributed to the high hydrogen yield achieved, by providing substrates for hydrogen utilizers such as hydrogenotrophic methanogens (Yang and Wang, 2018).

For the GAC surrounding flocs, an uncultured genus in the family *Eubacteriaceae* and the genus *Clostridium sensu stricto 1* (both belong to the same order, *Clostridiales*) dominated the settled GAC reactor, with relative abundances of 27.6% and 22.8%, respectively. In the floated GAC reactor, an unidentified genus in the *Spirochaetaceae* family was enriched 10.5-11.0%. Members of the *Spirochaetaceae* family ferment glucose, yielding ethanol, acetate, and formate (Ritalahti et al., 2012). Most fermentative bacteria have a preference to grow in the suspended flocs rather than attach to GAC in both reactors, such as family *Spirochaetaceae*, *Clostridium sensu stricto 1*, family *Eubacteriaceae* and *Candidatus Omnitrophus* (Table 7.2), while syntrophic bacteria such as *Geobacter*, *Syntrophomonas*, and *Desulfuromonas* tend to inhabit in the GAC-biofilm. Further, the floated GAC drew the largest number of bacterial genera to its biofilm (288 in floated-GAC biofilm, 232 in floated-GAC surrounding sludge flocs, 177 in settled-GAC surrounding sludge flocs and 125 in settled-GAC biofilm), indicating that floated GAC hosted a bacterial community with the highest redundancy and resilience in the GAC-biofilm. In comparison, more bacteria stayed in the sludge flocs in settled-GAC amended reactor.

Overall, different fermentative bacteria were enriched in the sludge adjacent to different GAC locations. More syntrophic VFA oxidizing bacteria were found in the floated-GAC biofilm,

whereas the settled-GAC biofilm was observed to enrich for bacteria that ferment larger molecules and produce hydrogen. The different microbiomes observed in the two reactors may be caused by the different organic loading conditions in the different reactor zones.

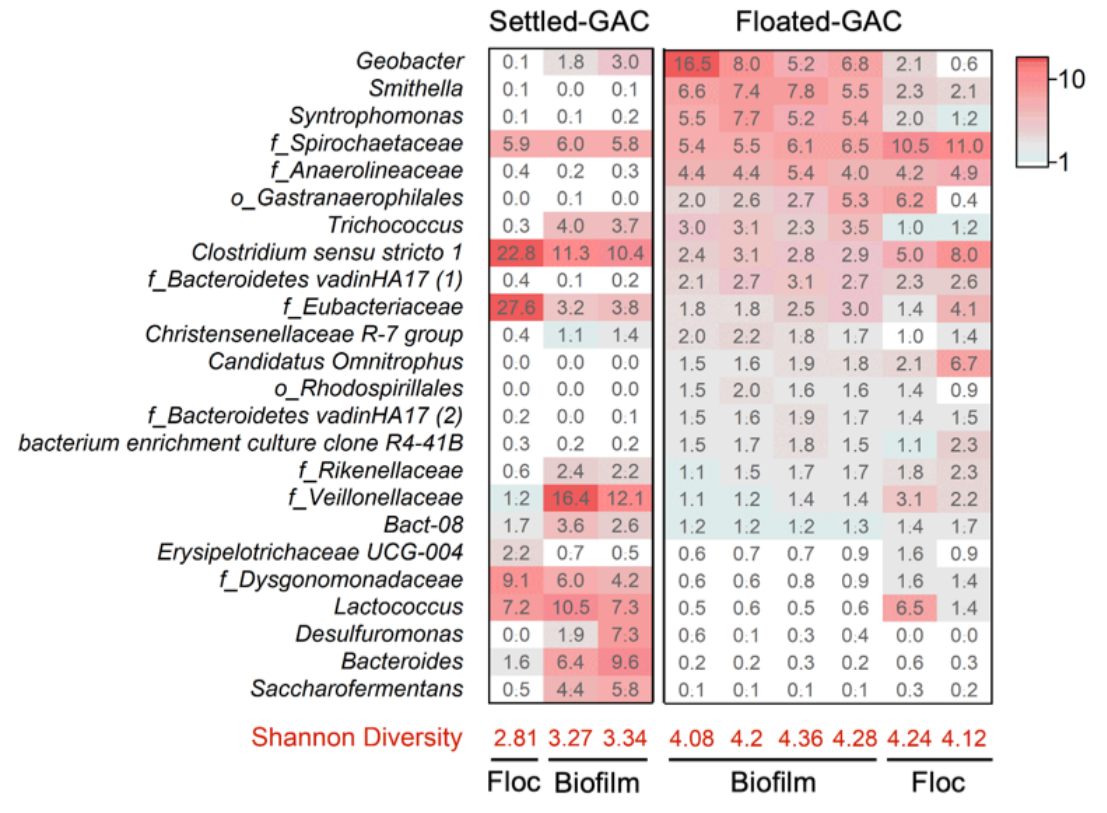

Fig. 7.3. Relative abundances of bacterial genera in the settled-GAC biofilm and the floated-GAC biofilm, along with the surrounding sludge flocs (average relative abundances >1%). The Shannon diversity is reported at the bottom of the heatmap. Unidentified genera were named according to family (f_) or order (o_).

Table 7.2. Comparison of bacterial communities of the GAC-biofilm and the surrounding sludge flocs in settled- and floated-GAC amended UASB reactors (listed in descending order by the discrepancy of average relative abundances in parallel samples).

Higher relative abundances in floc		**Higher relative abundances in biofilm**	
Settled-GAC	**Floated-GAC**	**Settled-GAC**	**Floated-GAC**
f_Eubacteriaceae	*f_Spirochaetaceae*	*f_Veillonellaceae*	*Geobacter*
Clostridium sensu stricto 1	*Clostridium sensu stricto 1*	*Bacteroides*	*Smithella*
f_Dysgonomonadaceae	*Lactococcus*	*Desulfuromonas*	*Syntrophomonas*
Erysipelotrichaceae UCG-004	*Candidatus Omnitrophus*	*Saccharofermentans*	*Trichococcus*
f_Enterobacteriaceae	*f_Chthoniobacteraceae*	*Trichococcus*	*f_Syntrophomonadaceae*
o_Mollicutes RF39	*f_Veillonellaceae*	*Geobacter*	*o_Cloacimonadales*
o_WCHB1-41	*Blvii28 wastewater-sludge group*	*f_Lachnospiraceae*	*f_Syntrophomonadaceae*
f_Chthoniobacteraceae	*f_Dysgonomonadaceae*	*f_Rikenellaceae*	*Christensenellaceae R-7 group*
f_Clostridiales vadinBB60 group	*c_MVP-15*	*Lactococcus*	*Lentimicrobium*
o_Cloacimonadales	*o_WCHB1-41*	*Bact-08*	*o_Rhodospirillales*

Dysgonomonas	*f_Rikenellaceae*	*Christensenellaceae R-7 group*	*f_Synergistaceae*
f_SR-FBR-L83	*f_Eubacteriaceae*	*Macellibacteroides*	*c_Alphaproteobacteria*
Blvii28 wastewater-sludge group	*Erysipelotrichaceae UCG-004*	*Clostridium sensu stricto 12*	*Candidatus Endomicrobium*
f_Bacteroidetes vadinHA17	*Paludibacter*	*Caproiciproducens*	*Desulfuromonas*
o_Saccharimonadales	*f_Paludibacteraceae*	*A7P-90m*	*uncultured Firmicutes bacterium*
f_Puniceicoccaceae	*Bact-08*	*Acetobacterium*	*f_Rhodocyclaceae*
DMER64	*Phaselicystis*	*Clostridium sensu stricto 11*	*f_Ruminococcaceae*
Candidatus Cloacimonas	*f_Clostridiaceae 1*	*f_Eubacteriaceae*	*f_Cloacimonadaceae*
f_Anaerolineaceae	*ADurb.Bin063-1*	*Anaerocolumna*	*f_Bacteroidetes vadinHA17*
bacterium enrichment culture clone R4-41B	*f_Puniceicoccaceae*	*f_Acidaminococcaceae*	*f_Bacteroidetes vadinHA17*
f_Prolixibacteraceae	*Bacteroides*	*Propionispira*	*Anaerovorax*
uncultured Merismopedia sp.	*o_Rhodospirillales*	*uncultured Coriobacteriales bacterium*	*p_Omnitrophicaeota*

o_Sphingobacteriales	*Clostridium sensu stricto 12*	*Desulfovibrio*	*c_LD1-PA32*
f_Syntrophaceae	*Coprobacillus*	*f_Paludibacteraceae*	*uncultured Bacteroidetes bacterium*
f_Bacteroidetes vadinHA17	*f_SR-FBR-L83*	*o_Saccharimonadales*	*f_Izimaplasmataceae*
o_Clostridiales	*uncultured soil bacterium*	*Candidatus Endomicrobium*	*o_OPB41*
o_OPB56	*Dysgonomonas*	*f_Veillonellaceae*	*Aminivibrio*
Ruminococcaceae UCG-014	*Ruminococcaceae UCG-014*	*Lactivibrio*	*c_V2072-189E03*
Niveibacterium	*o_Gastranaerophilales*	*Clostridium sensu stricto 6*	*f_Veillonellaceae*
Aeromonas	*WCHB1-32*	*f_Synergistaceae*	*Lactivibrio*
Pseudomonas	*o_Cloacimonadales*	*c_V2072-189E03*	*f_M2PB4-65 termite group*
f_Syntrophomonadaceae	*Saccharofermentans*	*Ruminiclostridium 1*	*f_GZKB124*
Elusimicrobium	*c_Bacteroidia*	*Treponema 2*	*Romboutsia*
uncultured rumen bacterium	*f_Syntrophaceae*	*Syntrophomonas*	*Thermovirga*
Chryseobacterium	*metagenome*	*Anaerofilum*	*f_Lentimicrobiaceae*

f_Clostridiaceae 1	*A7P-90m*	*f_Ruminococcaceae*	*f_Anaerolineaceae*
Thermovirga	*Niveibacterium*	*Lachnotalea*	*JGI-0000079-D21*
c_MVP-15	*DMER64*	*Clostridium sensu stricto 3*	*o_Rhodospirillales*
Syntrophorhabdus	*Rikenellaceae RC9 gut group*	*Paludibacter*	*f_SHA-4*
f_Tannerellaceae	*f_Pedosphaeraceae*	*f_Ruminococcaceae*	*Sulfurospirillum*
f_Anaerolineaceae	*o_WCHB1-41*	*f_Microbacteriaceae*	*Clostridium sensu stricto 7*
Rikenellaceae RC9 gut group	*iron-reducing bacterium enrichment culture clone HN105*	*metagenome*	*o_OPB41*
W5	*Syntrophorhabdus*	*Anaerocella*	*f_Peptococcaceae*
metagenome	*p_BRC1*	*Acidaminococcus*	*f_Family XIII*
Phaselicystis	*uncultured prokaryote*	*Tolumonas*	*f_Christensenellaceae*
uncultured organism	*Tyzzerella*	*Sporomusa*	*Acetoanaerobium*
f_009E01-B-SD-P15	*Victivallis*	*Anaerovorax*	*[Eubacterium] coprostanoligenes group*
f_Lachnospiraceae	*f_Pedosphaeraceae*	*Tyzzerella*	*Pelospora*

o_WCHB1-41	*metagenome*	*f_Christensenellaceae*	*uncultured Selenomonadales bacterium*
LD29	*bacterium enrichment culture clone R4-41B*	*o_Ignavibacteriales*	*Macromonas*
Pseudoxanthomonas	*Tetrasphaera*	*uncultured prokaryote*	*f_Syntrophomonadaceae*
Tetrasphaera	*c_Parcubacteria*	*Telmatospirillum*	*Flexilinea*
Sporolactobacillus	*Sporomusa*	*metagenome*	*o_Clostridiales*
Coprobacillus	*Caproiciproducens*	*c_LD1-PA32*	*Candidatus Caldatribacterium*
metagenome	*Ruminiclostridium 1*	*Anaerolineaceae UCG-001*	*uncultured prokaryote*
Aquabacterium	*o_SAR324 clade(Marine group B)*	*o_Cloacimonadales*	*Acidovorax*
Candidatus Omnitrophus	*Chryseobacterium*	*Leptolinea*	*Paludibaculum*
ADurb.Bin120	*f_S15A-MN91*	*f_Actinomycetaceae*	*Anaerocolumna*
Desulfomicrobium	*denitrifying bacterium enrichment culture clone NOB_2_E8*	*o_Myxococcales*	*f_Hydrogenedensaceae*

uncultured prokaryote	*uncultured Chlorobi bacterium*	*f_Paludibacteraceae*	*Desulfovibrio*
f_Izimaplasmataceae	*Ruminococcaceae UCG-010*	*k_Bacteria*	*Candidatus Soleaferrea*
Sedimentibacter	*f_Weeksellaceae*	*JGI-0000079-D21*	*Candidatus Cloacimonas*
Devosia	*o_Lineage IV*	*Ruminococcaceae UCG-002*	*o_Babeliales*
Petrimonas	*o_Saccharimonadales*	*GWE2-42-42*	*o_Ignavibacteriales*
p_Armatimonadetes	*W5*	*Oscillibacter*	*f_Ruminococcaceae*
uncultured Chlorobi bacterium	*p_Armatimonadetes*	*Syntrophobotulus*	*Anaerofustis*
Ruminococcaceae UCG-009	*Macellibacteroides*	*bacterium enrichment culture clone M624*	*Arcobacter*
p_Armatimonadetes	*uncultured soil bacterium*	*Ruminiclostridium*	*Advenella*
Thermomonas	*f_Lachnospiraceae*	*Ercella*	*Sediminispirochaeta*
[Eubacterium] coprostanoligenes group	*f_Enterobacteriaceae*	*p_BRC1*	*uncultured Coriobacteriales bacterium*

f_Rhodocyclaceae	*p_BRC1*	*p_BRC1*	*endosymbiont 'TC1' of Trimyema compressum*
Rhodococcus	*o_Gastranaerophilales*	*c_Bacteroidia*	*Ruminococcaceae NK4A214 group*
c_Berkelbacteria	*f_Microbacteriaceae*	*Acetoanaerobium*	*Sulfurovum*
RBG-16-49-21	*metagenome*	*Parabacteroides*	*Proteocatella*
o_SAR324 clade(Marine group B)	*f_Prolixibacteraceae*	*f_Clostridiaceae 1*	*k_Bacteria*
f_Family XIII	*c_Berkelbacteria*	*Clostridium sensu stricto 7*	*Dehalobacter*
o_Rhodospirillales	*o_Sphingobacteriales*	*uncultured Bacteroidetes bacterium*	*p_Firmicutes*
Mycobacterium	*metagenome*	*Lachnoclostridium*	*f_LF045*
Smithella	*Parabacteroides*	*WCHB1-32*	*f_uncultured bacterium mle1-9*
Methylotenera	*f_Lachnospiraceae*	*Sulfurospirillum*	*Treponema*
Fastidiosipila	*Oscillibacter*	*f_Pedosphaeraceae*	*metagenome*
f_Saccharimonadaceae	*f_009E01-B-SD-P15*	*o_Gastranaerophilales*	*Treponema 2*

f_Spirochaetaceae	*uncultured eubacterium WCHB1-25*	*Ruminococcaceae UCG-010*	*f_Intrasporangiaceae*
f_W27	*f_Clostridiales vadinBB60 group*	*p_WS1*	*f_GWF2-44-16*
Brevundimonas	*f_Burkholderiaceae*	*Erysipelothrix*	*Anaeromusa*
o_Gastranaerophilales	*f_FTLpost3*	*Victivallis*	*Erysipelothrix*
Fluviicola	*Clostridium sensu stricto 3*	*Acetanaerobacterium*	*Anaerocella*
uncultured Bacteroidetes bacterium	*Candidatus Berkelbacteria bacterium RIFOXYA2_FULL_43_10*	*Anaerosinus*	*f_GZKB75*
p_Firmicutes	*f_Saprospiraceae*	*f_Devosiaceae*	*Intestinibacter*
Prevotellaceae UCG-004	*o_Aminicenantales*	*o_D8A-2*	*LNR A2-18*
f_GZKB124	*f_Clostridiales vadinBB60 group*	*f_Bacteroidetes BD2-2*	*Syner-01*
Paenibacillus	*Fastidiosipila*	*Candidatus Accumulibacter*	*uncultured organism*
f_Rikenellaceae	*Fodinicola*	*o_Bacteroidales*	*Desulfomicrobium*

denitrifying bacterium enrichment culture clone NOB_2_E8	*Rhodoferax*	*UBA1819*	*f_Pirellulaceae*
Lentimicrobium	*uncultured Fusobacteria bacterium*	*Flexilinea*	*ADurb.Bin120*
p_Armatimonadetes	*f_Acidaminococcaceae*	*Candidatus Falkowbacteria bacterium GW2011_GWF2_43_32*	*Petrimonas*
Lautropia	*o_mle1-8*	*o_OPB41*	*f_Xanthobacteraceae*
Paludibaculum	*LD29*	*metagenome*	*Turicibacter*
ADurb.Bin063-1	*f_Chitinophagaceae*	*Sulfurovum*	*p_WS1*
iron-reducing bacterium enrichment culture clone HN105	*f_Rikenellaceae*	*f_KD1-131*	*uncultured Clostridiaceae bacterium*
Desulfobulbus	*c_V2072-189E03*	*Candidatus Caldatribacterium*	*IheB3-7*
f_Victivallaceae	*Aquabacterium*	*f_GWF2-44-16*	*Candidatus Falkowbacteria bacterium*

			GW2011_GWF2_43_32
Romboutsia	*uncultured actinobacterium*	*o_Lactobacillales*	*Clostridium sensu stricto 11*
uncultured Parcubacteria group bacterium	*f_Erysipelotrichaceae*	*Bifidobacterium*	*GWE2-42-42*
f_Burkholderiaceae	*Methylotenera*	*p_BRC1*	*Rhodobacter*
Fodinicola	*f_Bacteroidetes vadinHA17*	*Anaeroarcus*	*f_KD1-131*
o_mle1-8	*Lautropia*	*uncultured Fusobacteria bacterium*	*Bacteroidetes bacterium GWE2_42_24*
Cellulomonas	*o_Mollicutes RF39*	*f_Rhodanobacteraceae*	*Leptolinea*
o_Babeliales	*metagenome*	*f_Sphingomonadaceae*	*Candidatus Vogelbacteria bacterium RIFOXYB1_FULL_42_16*
f_Pedosphaeraceae	*Candidatus Accumulibacter*	*Arcobacter*	*f_Rhodobacteraceae*
c_Parcubacteria	*Pseudoxanthomonas*	*f_Peptococcaceae*	*uncultured organism*

o_Absconditabacteria les (SR1)	*Acidaminococcus*	*f_Sphingomonadacea e*	*Syntrophobacter*
Acholeplasma	*Novosphingobium*	*o_Candidatus Shapirobacteria*	*Meniscus*
Proteiniphilum	*Plasticicumulans*	*uncultured Selenomonadales bacterium*	*Pelolinea*
o_Lineage IV	*f_vadinBE97*	*AUTHM297*	*Bryobacter*
Novosphingobium	*f_Saccharimonadace ae*	*f_Hydrogenedensace ae*	*f_Fimbriimonadacea e*
Bacteroidetes bacterium ADurb.BinA012	*OLB12*	*Phenylobacterium*	*Anaerolinea*
metagenome	*o_D8A-2*	*Treponema*	*c_Anaerolineae*
f_Leptospiraceae	*f_KCLunmb-38-53*	*Chlorobium*	*Propionivibrio*
Turicibacter	*p_FCPU426*	*f_Vermiphilaceae*	*Chlorobium*
f_Saprospiraceae	*Hyphomicrobium*	*Proteocatella*	*Devosia*
uncultured eubacterium WCHB1-25	*Methylomonas*	*BD1-7 clade*	*c_Mollicutes*
Candidatus Berkelbacteria bacterium	*Verrucomicrobia bacterium ADurb.Bin118*	*p_FCPU426*	*RBG-16-49-21*

RIFOXYA2_FULL_43_10			
metagenome	*Z20*	*Ruminococcaceae NK4A214 group*	*Roseimarinus*
Verrucomicrobia bacterium ADurb.Bin118	*Proteiniphilum*	*Ruminococcaceae UCG-005*	*Candidatus Latescibacter*
Z20	*Reyranella*		*f_Bacteroidetes BD2-2*
f_Bacteroidales UCG-001	*f_Eubacteriaceae*		*Ercella*
Nubsella	*metagenome*		*bacterium enrichment culture clone M624*
o_Bacteroidales	*p_Proteobacteria*		*Ignavibacterium*
f_GZKB75	*f_Rhizobiaceae*		*uncultured Lentisphaerae bacterium*
f_Chitinophagaceae	*Lentisphaerae bacterium GWF2_50_93*		*f_Holophagaceae*
Flavobacterium	*AUTHM297*		*f_MSB-3C8*

c_Alphaproteobacteria	*metagenome*		*Acholeplasma*
o_Micavibrionales	*o_Gaiellales*		*Cryptanaerobacter*
Meniscus	*p_FCPU426*		*Ornithinibacter*
f_Lentimicrobiaceae	*o_Myxococcales*		*Acetobacterium*
o_Gaiellales	*GCA-900066225*		*o_Gaiellales*
f_Saccharimonadaceae	*Thermomonas*		*c_JS1*
Sulfurimonas	*p_Armatimonadetes*		*Pseudomonas*
Sphingobacterium	*Tomitella*		*Stenotrophomonas*
Candidatus Vogelbacteria bacterium GWA1_51_14	*f_Rhodanobacteraceae*		*Coxiella*
Bdellovibrio	*o_Micavibrionales*		*c_Lineage IIb*
uncultured organism	*uncultured Spirochaetales bacterium*		*f_Anaerolineaceae*
uncultured soil bacterium	*p_BRC1*		*o_Absconditabacteriales (SR1)*
metagenome	*metagenome*		*uncultured Verrucomicrobia bacterium*

Ruminococcaceae UCG-013	*Mycobacterium*		*f_Caldilineaceae*
Actinobacteria bacterium RBG_19FT_COMBO _36_27	*f_W27*		*f_Hydrogenedensaceae*
Bosea	*f_possible family 01*		*uncultured Acidobacteria bacterium*
o_Sva0485	*metagenome*		*Jatrophihabitans*
f_Pirellulaceae	*Flavobacterium*		*uncultured eubacterium WCHB1-50*
f_Xanthobacteraceae	*c_Berkelbacteria*		*metagenome*
Alistipes	*c_Alphaproteobacteria*		*Lachnospiraceae UCG-010*
metagenome	*Sulfuritalea*		*Magnetospirillum*
Insolitispirillum	*Sedimentibacter*		*o_MSB-5E12*
uncultured soil bacterium	*o_SAR324 clade(Marine group B)*		*f_Marinilabiliaceae*
Iamia	*Desulfobulbus*		*o_LD1-PB3*

Desulforegula	*uncultured planctomycete*		*Fusibacter*
o_Micavibrionales	*Syntrophus*		*o_Subgroup 7*
Corynebacterium 1	*uncultured candidate division JS1 bacterium*		*p_FBP*
f_Rikenellaceae	*o_Gaiellales*		*f_Beijerinckiaceae*
Candidatus Soleaferrea	*f_Paludibacteraceae*		*[Anaerorhabdus] furcosa group*
Allorhizobium-Neorhizobium-Pararhizobium-Rhizobium	*SC103*		*Sulfuricurvum*
f_M2PB4-65 termite group	*c_vadinHA49*		*Roseomonas*
uncultured organism	*Prosthecomicrobium*		*BSV13*
o_Candidatus Nomurabacteria	*Sarcina*		*metagenome*
c_vadinHA49	*Insolitispirillum*		*o_SJA-15*
f_Micropepsaceae	*f_Verrucomicrobiaceae*		*o_Mollicutes RF39*
f_Desulfovibrionaceae	*Ruminococcaceae UCG-005*		*metagenome*

o_Rhodospirillales	*uncultured organism*		*Peptoclostridium*
Thiobacillus	*MSBL3*		*metagenome*
f_TC1	*p_WS4*		*o_Victivallales*
o_Rhodospirillales	*f_Micropepsaceae*		*f_Acetobacteraceae*
o_Candidatus Falkowbacteria	*f_Fibrobacteraceae*		*Pirellula*
c_JS1	*Ruminiclostridium 9*		*o_Desulfuromonadales*
Anaerofustis	*o_Izimaplasmatales*		*f_053A03-B-DI-P58*
f_FTLpost3	*UBA1819*		*o_Candidatus Shapirobacteria*
Ruminiclostridium 9	*Sulfurimonas*		*Lacunisphaera*
	Terrisporobacter		*Desulfatiferula*
	Spirochaeta 2		*o_OPB56*
	Sphingobium		*f_Pirellulaceae*
	f_BSV40		*Anaerolineaceae UCG-001*
	o_CCM19a		*o_Myxococcales*
	o_SJA-15		*p_Armatimonadetes*
	uncultured Microgenomates group bacterium		*f_Rikenellaceae*

	Acinetobacter		*f_Rhizobiales Incertae Sedis*
	Fervidobacterium		*o_SJA-15*
	p_Armatimonadetes		*uncultured organism*
	f_Acetobacteraceae		*Pir4 lineage*
	f_WCHB1-02		*f_Leptospiraceae*
	f_Propionibacteriaceae		*f_CMW-169*
	Subgroup 10		*p_WPS-2*
	p_Armatimonadetes		*Leucobacter*
	Syntrophobotulus		*f_Family XIII*
	f_Desulfobacteraceae		*Zoogloea*
	Pseudoflavitalea		*Gordonia*
	uncultured cyanobacterium		*Aquimonas*
	c_Subgroup 18		*Aeromonas*
	Haliangium		*Phenylobacterium*
	f_WD2101 soil group		*c_WCHB1-81*
	Solirubrobacterales bacterium 67-14		*o_Sva0485*
	o_Bacteroidales		*Phreatobacter*
	f_Caulobacteraceae		*metagenome*
	f_Syntrophaceae		*o_Gaiellales*

	c_vadinHA49		*uncultured Parcubacteria group bacterium*
	f_Rhizobiaceae		*f_Tannerellaceae*
	p_WS1		*f_JG30-KF-CM45*
	metagenome		*Cellulomonas*
	o_Victivallales		*c_MD2902-B12*
	SH-PL14		*uncultured Bacteroidetes bacterium*
	o_Planctomycetales		*o_SBR1031*
	BD1-7 clade		*metagenome*
	f_Candidatus Raymondbacteria		*Dokdonella*
	Chryseolinea		*Levilinea*
	uncultured Bacteroidetes bacterium		*Bdellovibrio*
	Lentisphaerae bacterium GWF2_44_16		*f_SG8-4*
	Actinomyces		*metagenome*
	c_JS1		*Leptonema*

	o_Xanthomonadales		*o_Saccharimonadales*
	f_Microtrichaceae		*o_Mollicutes RF39*
	terrestrial metagenome		*metagenome*
	c_MVP-15		*Bacteroidetes bacterium ADurb.BinA012*
	p_Omnitrophicaeota		*o_Microtrichales*
	Ruminofilibacter		*IMCC26207*
	f_Desulfovibrionaceae		*p_Armatimonadetes*
	CL500-29 marine group		*o_Campylobacterales*
	o_MSBL9		*Hirschia*
	Brevundimonas		*f_Vermiphilaceae*
	Sphingobacterium		*f_Caulobacteraceae*
	uncultured soil bacterium		*o_Micavibrionales*
	o_Bacteroidales		*f_possible family 01*
	Flavihumibacter		*p_Elusimicrobia*
	f_Lenti-02		*o_Bacillales*
			f_Victivallaceae

			Ruminiclostridium
			o_Chitinophagales
			f_SC-I-84
			p_Armatimonadetes
			f_B18
			uncultured prokaryote
			Marmoricola
			o_SAR324 clade(Marine group B)
			Legionella
			f_Peptostreptococcaceae
			f_Barnesiellaceae
			c_uncultured Verrucomicrobia bacterium
			o_Izimaplasmatales
			Bacteroidetes bacterium GWF2_29_10
			OLB8

			Berkelbacteria
			Subdoligranulum
			Bosea
			f_Dysgonomonadaceae
			uncultured Cytophagales bacterium
			Zavarzinia
			uncultured planctomycete
			c_Gracilibacteria
			o_ADurb.Bin180
			f_Hydrogenedensaceae
			o_NKB15
			Candidatus Microthrix
			o_Pla1 lineage
			Myxococcus
			uncultured soil bacterium

			f_3M1PL1-52 termite group
			Atopobium
			o_DG-20
			Sphingoaurantiacus
			p_RsaHF231
			Alicyclobacillus
			o_Candidatus Roizmanbacteria
			uncultured Bacteroides sp.
			p_BRC1
			Thermincola
			Acetanaerobacterium
			Pedobacter
			UKL13-1
			o_Rhodospirillales
			f_MidBa8
			f_AKAU3564 sediment group
			Inquilinus
			Tissierella
			f_LF045

			toluene-degrading methanogenic consortium bacterium
			Nitrosomonas
			o_Candidatus Vogelbacteria
			o_Rhodospirillales
			o_Micavibrionales
			Family XIII AD3011 group

7.3.4 Canonical correlation analysis

Microbial community (Fig. 7.4A for bacteria, Fig. 7.4B for archaea) is influenced by environmental and operational factors including methanogenesis, VFA concentrations, the proportions of microorganisms capable of syntrophic metabolism (syntrophs ratio), and the proportions of archaea in all sequences (arc.ratio). These variables were subjected to a canonical correlation analysis (CCA) with biplot scaling focused on inter-sample distances, as shown in Figure 3. Generally, the floc and biofilm samples from the settled GAC reactor projected toward the left, whereas the floated GAC samples projected toward the right. The CCA model of bacterial and archaeal communities explained 62.3% and 49%, respectively, of the total community variance. Strong correlations were shown for different GAC locations among methanogenesis, VFA, syntrophs ratio and archaea ratio. The methanogenesis, archaea ratio and syntrophs ratio were in the same direction as floated GAC, whereas volatile fatty acids (VFA) were located on the

contrary coordinate. To be more specific, the proportions of syntrophic bacteria were in the same direction with the flocs in floated GAC reactor, while the biofilm contained higher proportions of archaea and contributed most to the methanogenesis. This was in accordance with the observation that a higher abundance of VFA producing bacteria were present in the bottom of settled GAC reactor, whereas the floated GAC reactor was enriched with syntrophic bacteria in the floc and archaea in the biofilm, and performed high methanogenesis.

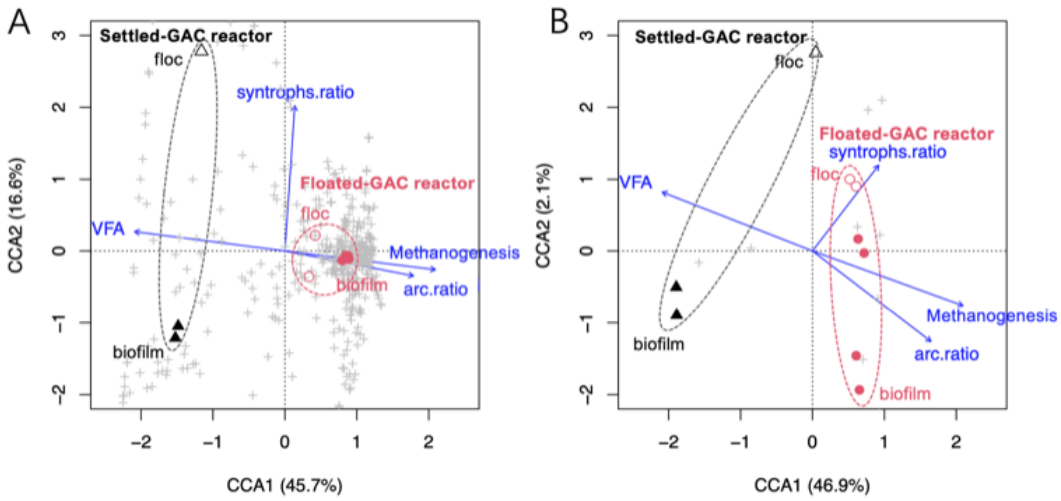

Fig. 7.4. Canonical correlation analysis (CCA) of (A) bacterial and (B) archaeal communities. Grey plus signs indicate individual OTUs.

7.3.5 Syntrophic co-occurrence analysis

The syntrophic partnership between bacteria and methanogens was analyzed through the co-occurrence network. Microorganisms capable of syntrophic metabolism were indicated with blue labels and methanogens were indicated with red labels, as shown in Fig. 7.5. Strong correlations ($P < 0.05$, Spearman's correlation coefficient $r > 0.6$) were shown for 48 bacteria and 9 methanogens. Among these interactions, 20 positive correlations belonged to syntrophic bacteria and methanogens Fig. 7.6, indicating their established syntrophic methanogenesis partnerships.

The dominant methanogens *Methanosarcina* and *Methanobacterium* were shown to be positively correlated with an unidentified genus in the family *Syntrophomonadaceae* and with the genus *Clostridium sensu stricto 12*, respectively. Syntrophic bacteria, including *Geobacter, Smithella*, *Syntrophomonas*, and two unidentified genera in family *Syntrophomonadaceae*, were correlated with hydrogenotrophic methanogens, including *Methanospirillum* and *Methanoregula*, indicating that GAC addition induced potential DIET functions between these microorganisms, consistent with previous studies (Lin et al., 2017; Mei et al., 2018; Walker et al., 2019).

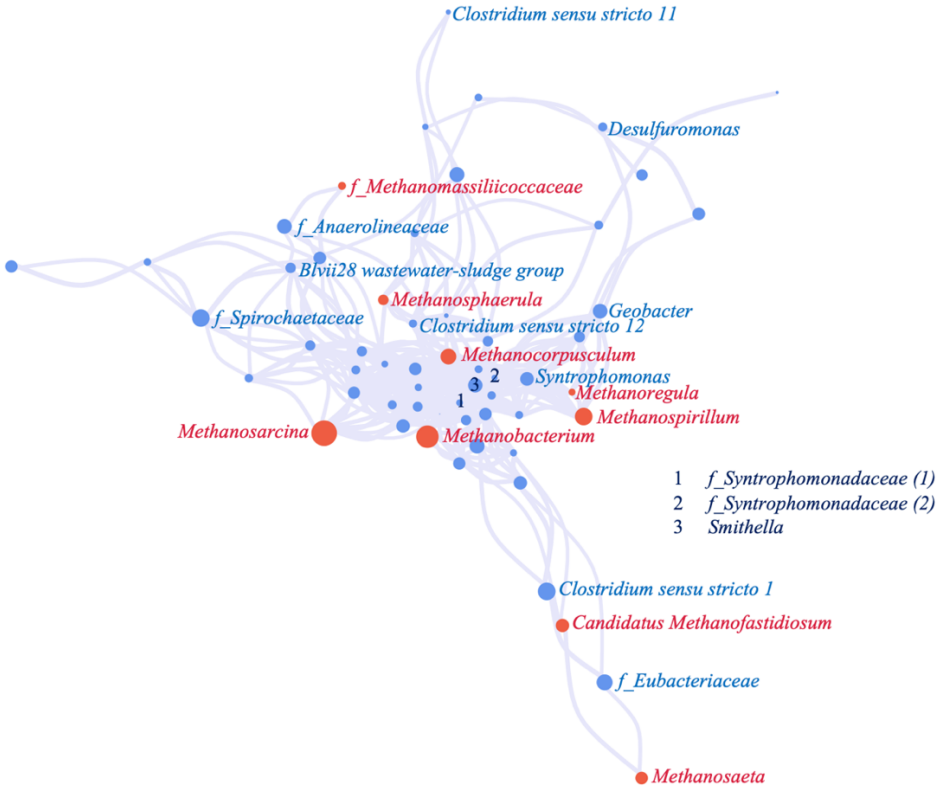

Fig. 7.5. Co-occurrence networks between microbial communities (up to 0.1% of the relative abundance), observed in two UASB reactors. Connections between dots represent strong positive correlations.

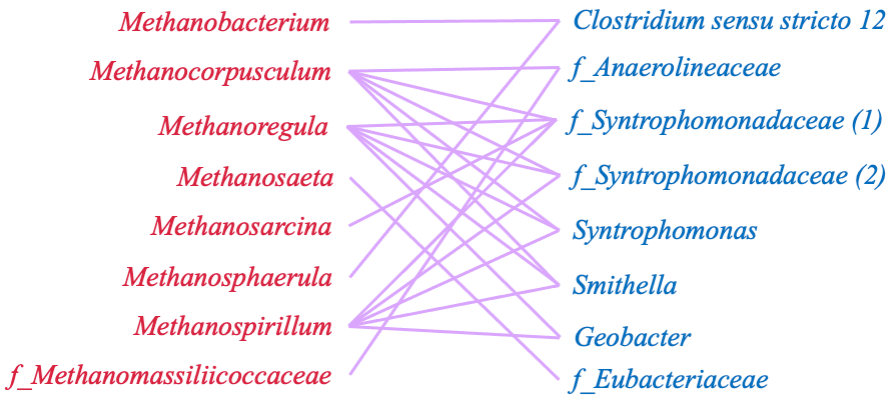

Fig. 7.6. Strong positive correlations (lavender lines) between syntrophic bacteria (blue text in the right) and archaea (red text in the left).

7.3.6 DIET-related functional gene prediction

Cellular appendices, such as electrically conductive pilus-like structures, play an important role in direct interspecies electron transfer (DIET) between syntrophic partners at centimeter scales (Walker et al., 2020; Xu et al., 2019; Yin et al., 2020b). To reveal the potential DIET within methanogenic processes in different layers of the two GAC-amended reactors, pili-related genes were predicted based on 16S rRNA information by Phylogenetic Investigation of Communities by Reconstruction of Unobserved States. As shown in Fig. 7.7, *pilA* (encoding the type IV pilus assembly protein) showed the highest relative abundance at the bottom floc in the settled GAC reactor, implying that GAC stimulated pili growth in the surrounding sludge. In comparison, at the floated GAC reactor bottom, where there was no GAC, the sludge floc was pili deficient. PilA genes increased in the middle and top layers of the floated GAC reactor, especially in the GAC biofilm, suggesting that GAC ascent increased the pili growth in the upper reactor zones. However, even without close contact, the settled GAC promoted pili growth in the entire settled GAC reactor.

Interestingly, as the only bacteria demonstrated to be DIET-active, *Geobacter* species were not predominant in the settled GAC reactor, suggesting that the *pilA* sequences may be assigned to other syntrophic bacteria, such as *Smithella*, *Syntrophomonas* and *Clostridium*. This observation agrees with previous studies in which bacteria other than *Geobacter*, such as *Desulfotomaculum hydrothermale* and *Syntrophobacter fumaroxidans*, were responsible for growing e-pili in many potential DIET-active systems (Walker et al., 2020; Yin et al., 2020b); this might be the case in the settled GAC reactor.

Floated GAC formed stratified microbial communities in the UASB reactor and stimulated DIET in upper reactor zones (sludge well mixed with GAC), whereas settled GAC may promote DIET throughout the reactor as indicated by the high abundances of pilA gene in the entire reactor. Similar observation has been reported in previous studies that adding GAC at the UASB reactor bottom can impact microbial dynamics throughout the reactor (Guo et al., 2020b; Zhang et al., 2021d). The underlying mechanisms can be associated with the changes in quorum sensing systems and oxidation-reduction potential (Wu et al., 2020; Yin et al., 2020b). Therefore, the conventional GAC amended configuration (unpackaged, or settled GAC) should still be considered for simple substrate (*e.g.*, VFAs) treatments that do not require a pre-fermentation zone, which takes full advantage of GAC throughout the reactor and might perform better than the floated-GAC amended reactors. On the other hand, settled GAC stacked at the wastewater inlet, impeding the influent flow especially for the solids-rich wastewater and may block the reaction site and reduce the GAC functionality. Overall, the GAC amended reactor configuration should be designed basing on specific wastewater treatment context.

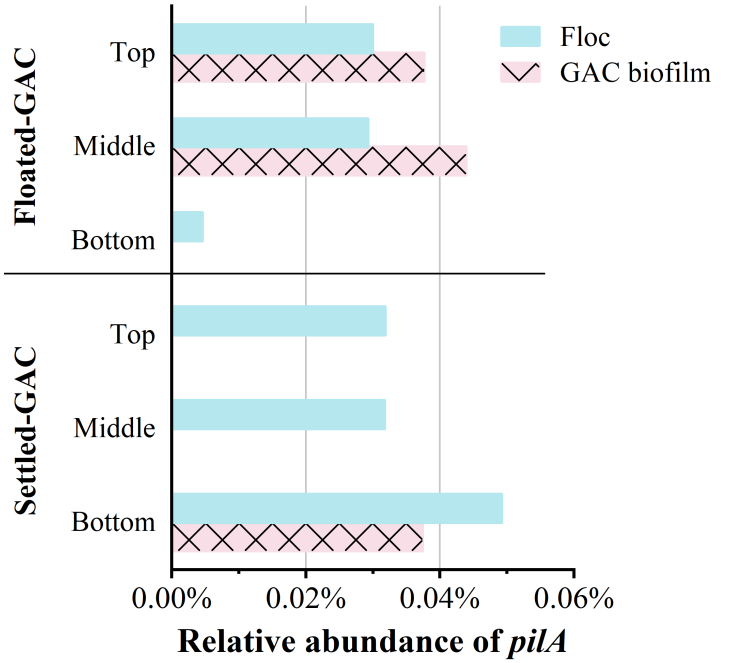

Fig. 7.7. Relative abundance of putative conductive PilA genes predicted by PICRUSt.

7.4 Conclusion

Microorganisms attached to GAC (biofilm) and the surrounding sludge floc were compared between a settled GAC reactor and a floated GAC reactor. Different spatial locations of GAC resulted in different dominant archaea, with *Methanosarcina* associated with high-rate methanogenesis in the floated-GAC biofilm and hydrogenotrophic *Methanobacterium* in the settled-GAC biofilm. Pili-related gene predictions revealed that GAC promoted conductive pili growth in niches flowing through the GAC. Floated GAC achieved enhanced methane production (with 16.7% higher methane yield as compared to the settled GAC UASB), slightly improved effluent quality, as well as enriched syntrophic microorganisms; while settled GAC promoted DIET throughout the UASB reactor. The novel floated GAC configuration allows for pre-hydrolysis/fermentation of complex organic wastes at the reactor inlet, which mitigates the solids

loading pressure and the potential clogging problems found in settled GAC reactors. This study provided detailed information on microbiome development under different GAC amendment strategies, critical for future application of GAC in anaerobic digestion processes. Further investigations on the feasibility of applying floated GAC for the treatment of complex and solid-rich wastewaters are recommended.

CHAPTER 8 CONCLUSIONS AND RECOMMENDATIONS

8.1 Thesis overview

High strength wastewaters with high solid contents are generated in large amounts in both urban and rural areas adapting centralized and decentralized wastewater collection systems, while the current treatment system is not compatible with the sustainable development goals. Anaerobic treatment of organic wastes allows for pollutants removal and recovering value-added products such as biogas and volatile fatty acids, which has been applied for treating various wastes. However, AD is susceptible to several factors such as low temperatures, accumulation of intermediate compounds, pH decrease, and toxicants, leading to unsatisfactory performances. Various pretreatment technologies and energy-intensive reactors design have been evaluated in previous studies to improve the treatment efficiencies, but high operational costs and intensive energy input are often required. Energy and cost-efficient technologies are still in demand to facilitate AD performance when treating ubiquitous wastes including blackwater and WAS.

Aiming at enhancing bioenergy recovery from high-strength wastes with different solid contents, this research developed three low cost/energy input strategies targeting three types of wastes, *i.e.*, WAS, blackwater, and synthetic glucose wastewater. The treatment strategies were selected according to the properties of the waste and the limitations of the anaerobic treatment process. Hydrolysis is considered as the rate-limiting step in WAS and blackwater treatment processes due to high biomass contents (10 – 24% of volatile solids in WAS and 25 – 54 wt% of total solids in blackwater). The decomposition of these solids can be challenging, especially when operating temperature is below 25 ^{o}C, and can result in longer HRT and a larger physical footprint. $Ca(ClO)_2$ and micro-aeration pretreatments were applied to the treatment of WAS and blackwater, respectively. Different $Ca(ClO)_2$ or oxygen dosages were tested in ASBRs with step-wise reduced

HRT to demonstrate the system stability and evaluate the long-term effects of the pretreatment strategies. Then, a modified UASB reactor was developed to achieve phase separation in a single reactor, with enhanced fermentation near the wastewater inlet and boosted methanogenesis in the reactor column. Synthetic glucose wastewater was used as substrate to reduce the complexity. The microbial community dynamics and functional profiles were analyzed to elucidate the biodegradation mechanisms.

8.2 Conclusions

This doctoral thesis focused on exploring novel, effective and low investment technologies for energy recovery from high-strength organic wastes. The results provide insights into the significance of developing functional microbiome and the syntrophic relationships between them. The major conclusions are summarized as the following:

Oxidation pretreatments to enhance WAS and blackwater hydrolysis

- The feasibility of applying calcium hypochlorite as a WAS pretreatment strategy to improve AD treatment efficiency using laboratory batch and continuous reactors was described in Chapter 3 and 4, respectively. The results in Chapter 3 showed that pretreatment with 5 – 20% $Ca(ClO)_2$ (total suspended solids basis) significantly enhanced WAS anaerobic digestibility, and led to significantly enhanced methane production rate and biomethane yield comparing to the AD of raw WAS ($P<0.05$). Low $Ca(ClO)_2$ pretreatment (5 – 10%) significantly enhanced digestion efficiency, which can be attributed to the development of fermentative and syntrophic bacteria. However, high $Ca(ClO)_2$ doses (>20%) reduced microbial activities, leading to slow release of dissolved organic compounds and prolonged methane production lag phase. In addition, high $Ca(ClO)_2$ removed 82.7% of the initial phosphate by calcium-phosphate binding, reducing the phosphorus in liquid digestate.

- For thickened WAS treatment in ASBRs at mesophilic conditions (35 °C), three loading shocks were introduced to each reactor to compare the performance stability and resilience between the digestion of $Ca(ClO)_2$ pretreated TWAS and untreated TWAS as described in Chapter 4. Microbial community shifts were quantified to reveal the microbiome responses to disturbances. The results suggested that 1% $Ca(ClO)_2$ enhanced the digestion of TWAS by inactivating and transforming the biomass to more easily digested substrates. Co-occurrence network analysis revealed that the strongest interactions in the microbial community occurred in the steady state of TWAS anaerobic digestion.

- The effects of micro-aeration on the performance of anaerobic sequencing batch reactors (ASBR) for blackwater treatment were demonstrated in Chapter 5. Source-diverted blackwater (toilet water) contains high organic contents which can be recovered as biogas. Previous studies have found that anaerobic digestion of blackwater without micro-aeration can only recover upwards of less than 40% of chemical oxygen demand (COD) to methane at room temperature due to the low hydrolysis rate of biomass content in blackwater. This study achieved increases in blackwater hydrolysis (from 34.7 % to 48.7 %) and methane production (from 39.6 % to 50.7 %) with controlled micro-aeration (5 mg O_2/L-reactor/cycle). The microbial analysis results showed that hydrolytic/fermentative bacteria and acetoclastic methanogens (*e.g. Methanosaeta*) were in higher abundances in low-dose micro-aeration reactors (5 and 10 mg O_2/L-reactor/cycle), which facilitated syntrophic interactions between microorganisms. The relative abundance of oxygen-tolerant methanogen such as *Methanosarcina* greatly increased (from 1.5 % to 11.4 %) after oxygen injection. High oxygen dosages (50 and 150 mg O_2/L-reactor/cycle) led to reduced methane production and higher accumulation of volatile fatty acids, largely due to the oxygen inhibition on methanogens and degradation of organic matters by aerobic growth and respiration,

as indicated by the predicted metagenome functions. By combining reactor performance results and microbial community analyses, this study demonstrated that low-dose micro-aeration improves blackwater biomethane recovery by enhancing hydrolysis efficiency and promoting the development of a functional microbial population, while medium to high-dose micro-aeration reduced the activities of certain anaerobes. It was also observed that medium-dose micro-aeration maximizes VFA accumulation, which may be used in two-stage anaerobic digesters.

Modified UASB reactor with fluidized GAC to realize phase separation and enhance methane production

- Chapter 6 and 7 demonstrated the performance and microbiome of a modified UASB reactor that fluidizes GAC by encaging GAC in plastic carriers. The results described in Chapter 6 showed enhanced performance with respect to methane production and COD removal at an organic loading rate of 1500 g COD/m^3/d under the temperature of 20 ^oC using the self-fluidized GAC configuration; with the methanation rate increased from 0.33 ± 0.08 g CH_4-COD/g influent COD in the non-GAC reactor, to 0.66 ± 0.02 g CH_4-COD/g influent COD in the GAC-only reactor, and further increased to 0.77 ± 0.02 g CH_4-COD/g influent COD in the self-fluidized GAC reactor. The concentrations of medium-chain acyl-homoserine lactones increased in the GAC-amended reactors, potentially associated with the promotion of syntrophic interactions between bacteria and archaea. Batch tests were performed for syntrophic propionate degradation under hydrogen-inhibition conditions, and showed that microbial consortium enriched in both GAC amended reactors can overcome hydrogen inhibition. Further microbial community analysis unveiled a variation in spatial distribution in the GAC enriched microbial consortium (including DIET indicator microorganisms such as *Geobacter* and *Methanosarcina*) based on the location of GAC in the reactors.

- The methanogenic activities of the suspended sludge were not significantly different between two GAC-amended reactors as described in Chapter 6, inferring a strong effect of the GAC biofilm to the methane production. Microbial communities in the biofilms developed on settled or floated GAC were compared in Chapter 7. *Methanosarcina* (56.3-73.3%) dominated the floated-GAC biofilm whereas *Methanobacterium* (84.9-85.1%) was greatly enriched in the settled-GAC biofilm. *Methanospirillum* and *Methanocorpusculum* were enriched in the floated-GAC biofilm (8.8-19.8% and 5.1-9.5%, respectively), but only existed in low abundances in the settled-GAC biofilm (3.4-3.6% and 0-0.4%, respectively). The floated GAC developed bacterial communities with higher diversity and more syntrophic bacteria enrichments on its surface, including *Geobacter*, *Smithella*, and *Syntrophomonas*, than the settled-GAC biofilm. Common hydrogen-donating syntrophs and hydrogenotrophic archaea, *Methanospirillum* and *Methanoregula*, were identified as potential electro-active microorganisms related to DIET.

8.3 Recommendations

The results of this study indicated oxidation pretreatments (micro-aeration and hypochlorite addition) can facilitate solids hydrolysis at lower doses, while deteriorated the activity of obligate anaerobes and biomethane recovery with higher doses. This opens the opportunity of applying these pretreatments in fermentation processes for VFAs production. Two-phase anaerobic digestion should also be considered to provide optimum conditions for fermentative bacteria and the methanogenic archaea separately and achieve high-efficient methane production. Further, the current study only tested the pretreatments in ASBRs, other reactor configurations (*e.g.*, UASB) and operational conditions (*e.g.*, thermophilic temperatures) can be explored in the future.

In addition to WAS generated in the biological treatment units, primary sludge (PS) that consists of settled organic matter of raw wastewater is also a by-product that requires safe disposal in

wastewater treatment plants. The anaerobic biodegradability of primary sludge is higher than WAS. In this context, the co-digestion of PS and the hypochlorite pretreated WAS may be an effective and economical choice to stabilize both sewage sludge types. Further studies should be developed to determine the optimum dosage, pretreatment time, mixing ratios and the treatment capacity of PS and pretreated WAS co-digestion.

The current work demonstrated an innovative design of UASB reactors with GAC amendment that achieved increased methanogenic activity in lab-scale reactors, yet questions remain in transferring the configuration into the engineering practice of operating full-scale bioreactors. In addition, the current work used synthetic glucose wastewater as the substrate, which only contains soluble organic matters and eliminated the hydrolysis process of particulate substances. Future research is warranted for the treatment of more complex substrates with different solid contents. Further, the settled GAC and the floated GAC may benefit the AD process in different mechanisms: settled GAC may influence the downstream biological activities by secreting quorum sensing molecules, while floated GAC leaves more space for condensed biomass to hydrolyze particulates near the wastewater inlet and creates better mixing between GAC and sludge at upper reaction zones. Future investigations using metagenomics and metaproteomic analysis are recommended. In addition, the minimum amount of GAC that can facilitate methane production should be identified in various reactor configurations to further reduce the cost for easy application.

BIBLIOGRAPHY

Abbassi, B. and Baz, I.A. 2008. Integrated wastewater management: A review. Efficient Management of Wastewater, 29-40.

Adeleke, O.A., Saphira, M.R., Daud, Z., Ismail, N., Ahsan, A., Ab Aziz, N.A., Al-Gheethi, A., Kumar, V., Fadilat, A. and Apandi, N. (2019) Nanotechnology in Water and Wastewater Treatment, pp. 1-33, Elsevier.

Anglada, A., Urtiaga, A. and Ortiz, I. 2009. Contributions of electrochemical oxidation to waste-water treatment: fundamentals and review of applications. Journal of Chemical Technology & Biotechnology 84(12), 1747-1755.

Angle, J.C., Morin, T.H., Solden, L.M., Narrowe, A.B., Smith, G.J., Borton, M.A., Rey-Sanchez, C., Daly, R.A., Mirfenderesgi, G., Hoyt, D.W., Riley, W.J., Miller, C.S., Bohrer, G. and Wrighton, K.C. 2017. Methanogenesis in oxygenated soils is a substantial fraction of wetland methane emissions. Nature Communications 8(1), 1567.

APHA (1985) Standard methods for the examination of water and wastewater, Apha.

Appels, L., Baeyens, J., Degrève, J. and Dewil, R. 2008. Principles and potential of the anaerobic digestion of waste-activated sludge. Progress in energy and combustion science 34(6), 755-781.

Ariesyady, H.D., Ito, T. and Okabe, S. 2007. Functional bacterial and archaeal community structures of major trophic groups in a full-scale anaerobic sludge digester. Water Research 41(7), 1554-1568.

Azman, S., Khadem, A.F., Plugge, C.M., Stams, A.J., Bec, S. and Zeeman, G. 2017a. Effect of humic acid on anaerobic digestion of cellulose and xylan in completely stirred tank reactors:

inhibitory effect, mitigation of the inhibition and the dynamics of the microbial communities. Applied Microbiology and Biotechnology 101(2), 889-901.

Azman, S., Khadem, A.F., Plugge, C.M., Stams, A.J.M., Bec, S. and Zeeman, G. 2017b. Effect of humic acid on anaerobic digestion of cellulose and xylan in completely stirred tank reactors: inhibitory effect, mitigation of the inhibition and the dynamics of the microbial communities. Applied Microbiology and Biotechnology 101(2), 889-901.

Baek, G., Kim, J., Kim, J. and Lee, C. 2018. Role and Potential of Direct Interspecies Electron Transfer in Anaerobic Digestion. Energies 11(1).

Baloch, M., Akunna, J.C. and Collier, P.J. 2007. The performance of a phase separated granular bed bioreactor treating brewery wastewater. Bioresource Technology 98(9), 1849-1855.

Barua, S. and Dhar, B.R. 2017. Advances towards understanding and engineering direct interspecies electron transfer in anaerobic digestion. Bioresource Technology 244(Pt 1), 698-707.

Bi, D., Guo, X. and Chen, D. 2013. Phosphorus release mechanisms during digestion of EBPR sludge under anaerobic, anoxic and aerobic conditions. Water Science and Technology 67(9), 1953-1959.

Bi, W., Li, Y. and Hu, Y. 2014. Recovery of phosphorus and nitrogen from alkaline hydrolysis supernatant of excess sludge by magnesium ammonium phosphate. Bioresource Technology 166, 1-8.

Bigda, R.J. 1995. Consider Fentons chemistry for wastewater treatment. Chemical Engineering Progress 91(12).

Bordeleau, E., Purcell, E.B., Lafontaine, D.A., Fortier, L.C., Tamayo, R. and Burrus, V. 2015. Cyclic di-GMP riboswitch-regulated type IV pili contribute to aggregation of Clostridium difficile. Journal of Bacteriology 197(5), 819-832.

Botheju, D. and Bakke, R. 2011. Oxygen effects in anaerobic digestion-a review.

Braguglia, C., Mininni, G., Tomei, M. and Rolle, E. 2006. Effect of feed/inoculum ratio on anaerobic digestion of sonicated sludge. Water Science and Technology 54(5), 77-84.

Braz, G.H.R., Fernandez-Gonzalez, N., Lema, J.M. and Carballa, M. 2019. Organic overloading affects the microbial interactions during anaerobic digestion in sewage sludge reactors. Chemosphere 222, 323-332.

Brioukhanov, A.L. and Netrusov, A.I. 2007. Aerotolerance of strictly anaerobic microorganisms and factors of defense against oxidative stress: A review. Applied Biochemistry and Microbiology 43(6), 567-582.

Brioukhanov, A.L., Netrusov, A.I. and Eggen, R.I. 2006. The catalase and superoxide dismutase genes are transcriptionally up-regulated upon oxidative stress in the strictly anaerobic archaeon Methanosarcina barkeri. Microbiology 152(6), 1671-1677.

Bunce, J.T., Ndam, E., Ofiteru, I.D., Moore, A. and Graham, D.W. 2018. A review of phosphorus removal technologies and their applicability to small-scale domestic wastewater treatment systems. Frontiers in Environmental Science 6, 8.

Butkovskyi, A., Leal, L.H., Rijnaarts, H. and Zeeman, G. 2015. Fate of pharmaceuticals in full-scale source separated sanitation system. Water Research 85, 384-392.

Calatrava-Morales, N., McIntosh, M. and Soto, M.J. 2018. Regulation mediated by N-Acyl Homoserine Lactone quorum sensing signals in the Rhizobium-Legume symbiosis. Genes 9(5), 263.

Calderon, A.G., Duan, H., Meng, J., Zhao, J., Song, Y., Yu, W., Hu, Z., Xu, K., Cheng, X. and Hu, S. 2021. An integrated strategy to enhance performance of anaerobic digestion of waste activated sludge. Water Research 195, 116977.

Callahan, B.J., McMurdie, P.J., Rosen, M.J., Han, A.W., Johnson, A.J.A. and Holmes, S.P. 2016. DADA2: high-resolution sample inference from Illumina amplicon data. Nature Methods 13(7), 581-583.

Campo, G., Cerutti, A., Zanetti, M., Scibilia, G., Lorenzi, E. and Ruffino, B. 2018. Enhancement of waste activated sludge (WAS) anaerobic digestion by means of pre-and intermediate treatments. Technical and economic analysis at a full-scale WWTP. Journal of Environmental Management 216, 372-382.

Cao, B., Zhang, T., Zhang, W. and Wang, D. 2021. Enhanced technology based for sewage sludge deep dewatering: A critical review. Water Research 189, 116650.

Capodaglio, A., Callegari, A., Cecconet, D. and Molognoni, D. 2017. Sustainability of decentralized wastewater treatment technologies. Water Practice and Technology 12(2), 463-477.

Caporaso, J.G., Kuczynski, J., Stombaugh, J., Bittinger, K., Bushman, F.D., Costello, E.K., Fierer, N., Pena, A.G., Goodrich, J.K., Gordon, J.I., Huttley, G.A., Kelley, S.T., Knights, D., Koenig, J.E., Ley, R.E., Lozupone, C.A., McDonald, D., Muegge, B.D., Pirrung, M., Reeder, J., Sevinsky, J.R., Turnbaugh, P.J., Walters, W.A., Widmann, J., Yatsunenko, T., Zaneveld, J. and Knight, R. 2010. QIIME allows analysis of high-throughput community sequencing data. Nature Methods 7(5), 335-336.

Charles, W., Walker, L. and Cord-Ruwisch, R. 2009. Effect of pre-aeration and inoculum on the start-up of batch thermophilic anaerobic digestion of municipal solid waste. Bioresource Technology 100(8), 2329-2335.

Chen, L., Chen, H., Lu, D., Xu, X. and Zhu, L. 2020. Response of methanogens in calcified anaerobic granular sludge: Effect of different calcium levels. Journal of Hazardous Materials 389, 122131.

Chen, Z., Zhang, W., Wang, D., Ma, T., Bai, R. and Yu, D. 2016. Enhancement of waste activated sludge dewaterability using calcium peroxide pre-oxidation and chemical re-flocculation. Water Research 103, 170-181.

Cichy, B., Kużdżał, E. and Krztoń, H. 2019. Phosphorus recovery from acidic wastewater by hydroxyapatite precipitation. Journal of Environmental Management 232, 421-427.

Cohen, A., Breure, A., Van Andel, J. and Van Deursen, A. 1982. Influence of phase separation on the anaerobic digestion of glucose—II: stability, and kinetic responses to shock loadings. Water Research 16(4), 449-455.

Coral, T., Descostes, M., De Boissezon, H., Bernier-Latmani, R., De Alencastro, L.F. and Rossi, P. 2018. Microbial communities associated with uranium in-situ recovery mining process are related to acid mine drainage assemblages. Science of The Total Environment 628, 26-35.

Cosgun, S. and Semerci, N. 2019. Combined and individual applications of ozonation and microwave treatment for waste activated sludge solubilization and nutrient release. Journal of Environmental Economics and Management 241, 76-83.

Cremonez, P.A., Teleken, J.G., Weiser Meier, T.R. and Alves, H.J. 2021. Two-Stage anaerobic digestion in agroindustrial waste treatment: A review. Journal of Environmental Economics and Management 281, 111854.

Cunha, J.R., Tervahauta, T., van der Weijden, R.D., Temmink, H., Hernández Leal, L.a., Zeeman, G. and Buisman, C.J. 2018. The effect of bioinduced increased pH on the enrichment of calcium phosphate in granules during anaerobic treatment of black water. Environmental Science & Technology 52(22), 13144-13154.

Czatzkowska, M., Harnisz, M., Korzeniewska, E. and Koniuszewska, I. 2020. Inhibitors of the methane fermentation process with particular emphasis on the microbiological aspect: A review. Energy Science & Engineering 8(5), 1880-1897.

Dai, X., Hu, C., Zhang, D. and Chen, Y. 2017. A new method for the simultaneous enhancement of methane yield and reduction of hydrogen sulfide production in the anaerobic digestion of waste activated sludge. Bioresource Technology 243, 914-921.

Dang, Y., Holmes, D.E., Zhao, Z., Woodard, T.L., Zhang, Y., Sun, D., Wang, L.Y., Nevin, K.P. and Lovley, D.R. 2016. Enhancing anaerobic digestion of complex organic waste with carbon-based conductive materials. Bioresource Technology 220, 516-522.

De Kreuk, M.K. and van Loosdrecht, M.C. 2006. Formation of aerobic granules with domestic sewage. Journal of Environmental Engineering 132(6), 694-697.

De Vrieze, J., Hennebel, T., Boon, N. and Verstraete, W. 2012. Methanosarcina: the rediscovered methanogen for heavy duty biomethanation. Bioresource Technology 112, 1-9.

del Castillo, A.F., Garibay, M.V., Senés-Guerrero, C., Orozco-Nunnelly, D.A., de Anda, J. and Gradilla-Hernández, M.S. 2022. A review of the sustainability of anaerobic reactors

combined with constructed wetlands for decentralized wastewater treatment. Journal of Cleaner Production, 133428.

Demirbas, A., Edris, G. and Alalayah, W.M. 2017. Sludge production from municipal wastewater treatment in sewage treatment plant. Energy Sources, Part A: Recovery, Utilization, and Environmental Effects 39(10), 999-1006.

Deng, L., Chen, H., Chen, Z., Liu, Y., Pu, X. and Song, L. 2009. Process of simultaneous hydrogen sulfide removal from biogas and nitrogen removal from swine wastewater. Bioresource Technology 100(23), 5600-5608.

Diak, J., Ormeci, B. and Kennedy, K.J. 2013. Effect of micro-aeration on anaerobic digestion of primary sludge under septic tank conditions. Bioprocess and Biosystems Engineering 36(4), 417-424.

Ding, L., Chen, Y., Xu, Y. and Hu, B. 2021. Improving treatment capacity and process stability via a two-stage anaerobic digestion of food waste combining solid-state acidogenesis and leachate methanogenesis/recirculation. Journal of Cleaner Production 279.

Ding, Y., Feng, H., Huang, W., Li, N., Zhou, Y., Wang, M., Zhang, X. and Shen, D. 2015. The effect of quorum sensing on anaerobic granular sludge in different pH conditions. Biochemical Engineering Journal 103, 270-276.

Dodane, P.-H., Mbéguéré, M., Sow, O. and Strande, L. 2012. Capital and operating costs of full-scale fecal sludge management and wastewater treatment systems in Dakar, Senegal. Environmental Science & Technology 46(7), 3705-3711.

Duan, Z., Cruz Bournazou, M.N. and Kravaris, C. 2017. Dynamic model reduction for two-stage anaerobic digestion processes. Chemical Engineering Journal 327, 1102-1116.

Duarte, M.S., Silva, S.A., Salvador, A.F., Cavaleiro, A.J., Stams, A.J.M., Alves, M.M. and Pereira, M.A. 2018. Insight into the Role of Facultative Bacteria Stimulated by Microaeration in Continuous Bioreactors Converting LCFA to Methane. Environmental Science & Technology 52(11), 6497-6507.

Eerten-Jansen, V., Mieke, C., Veldhoen, A.B., Plugge, C.M., Stams, A.J., Buisman, C.J. and Ter Heijne, A. 2013. Microbial community analysis of a methane-producing biocathode in a bioelectrochemical system. Archaea 2013.

Feng, J., Jiang, M., Li, K., Lu, Q., Xu, S., Wang, X., Chen, K. and Ouyang, P. 2020. Direct electron uptake from a cathode using the inward Mtr pathway in Escherichia coli. Bioelectrochemistry 134, 107498.

Florentino, A.P., Xu, R., Zhang, L. and Liu, Y. 2019. Anaerobic digestion of blackwater assisted by granular activated carbon: From digestion inhibition to methanogenesis enhancement. Chemosphere 233, 462-471.

Fry, L.M., Mihelcic, J.R. and Watkins, D.W. 2008. Water and nonwater-related challenges of achieving global sanitation coverage. Environmental Science & Technology 42(12), 4298-4304.

Fu, S.-F., Wang, F., Shi, X.-S. and Guo, R.-B. 2016. Impacts of microaeration on the anaerobic digestion of corn straw and the microbial community structure. Chemical Engineering Journal 287, 523-528.

Fu, S.F., Shi, X.S., Xu, X.H., Wang, C.S., Wang, L., Dai, M. and Guo, R.B. 2015. Secondary thermophilic microaerobic treatment in the anaerobic digestion of corn straw. Bioresource Technology 186, 321-324.

Gamage, H.K., Tetu, S.G., Chong, R.W., Ashton, J., Packer, N.H. and Paulsen, I.T. 2017. Cereal products derived from wheat, sorghum, rice and oats alter the infant gut microbiota in vitro. Scientific Reports 7(1), 1-12.

Gao, M. 2020. Anaerobic treatment of source-diverted blackwater-maximizing biomethane recovery.

Gao, M., Guo, B., Li, L. and Liu, Y. 2020a. Role of syntrophic acetate oxidation and hydrogenotrophic methanogenesis in co-digestion of blackwater with food waste. Journal of Cleaner Production, 125393.

Gao, M., Guo, B., Zhang, L., Zhang, Y. and Liu, Y. 2019a. Microbial community dynamics in anaerobic digesters treating conventional and vacuum toilet flushed blackwater. Water Research 160, 249-258.

Gao, M., Guo, B., Zhang, L., Zhang, Y., Yu, N. and Liu, Y. 2020b. Biomethane recovery from source-diverted household blackwater: Impacts from feed sulfate. Process Safety and Environmental Protection 136, 28-38.

Gao, M., Zhang, L., Florentino, A.P. and Liu, Y. 2019b. Performance of anaerobic treatment of blackwater collected from different toilet flushing systems: Can we achieve both energy recovery and water conservation? Journal of Hazardous Materials 365, 44-52.

Gao, M., Zhang, L., Guo, B., Zhang, Y. and Liu, Y. 2019c. Enhancing biomethane recovery from source-diverted blackwater through hydrogenotrophic methanogenesis dominant pathway. Chemical Engineering Journal 378, 122258.

Gao, M., Zhang, L. and Liu, Y. 2020c. High-loading food waste and blackwater anaerobic co-digestion: Maximizing bioenergy recovery. Chemical Engineering Journal, 124911.

Gautam, P., Kumar, S. and Lokhandwala, S. 2019. Advanced oxidation processes for treatment of leachate from hazardous waste landfill: A critical review. Journal of Cleaner Production 237.

Ghimire, U., Sarpong, G. and Gude, V.G. 2021. Transitioning wastewater treatment plants toward circular economy and energy sustainability. ACS omega 6(18), 11794-11803.

Gijzen, H.J. and Kansiime, F. 1996. Comparison of start-up of an upflow anaerobic sludge blanket reactor and a polyurethane carrier reactor. Water Science and Technology 34(5-6), 509-515.

Gonzalez, A., Hendriks, A., Van Lier, J. and De Kreuk, M. 2018. Pre-treatments to enhance the biodegradability of waste activated sludge: Elucidating the rate limiting step. Biotechnology Advances 36(5), 1434-1469.

Goux, X., Calusinska, M., Lemaigre, S., Marynowska, M., Klocke, M., Udelhoven, T., Benizri, E. and Delfosse, P. 2015. Microbial community dynamics in replicate anaerobic digesters exposed sequentially to increasing organic loading rate, acidosis, and process recovery. Biotechnology for Biofuels 8, 122.

Graber, J.R. and Breznak, J.A. 2004. Physiology and nutrition of Treponema primitia, an H2/CO2-acetogenic spirochete from termite hindguts. Applied and Environmental Microbiology 70(3), 1307-1314.

Groh, S., Van der Straeten, J., Lasch, B.E., Gershenson, D., Leal Filho, W. and Kammen, D.M. (2015) Decentralized Solutions for Developing Economies, Springer.

Gu, M., Yin, Q., Liu, Y., Du, J. and Wu, G. 2019. New insights into the effect of direct interspecies electron transfer on syntrophic methanogenesis through thermodynamic analysis. Bioresource Technology Reports 7, 100225.

Guerra-Rodríguez, S., Oulego, P., Rodríguez, E., Singh, D.N. and Rodríguez-Chueca, J. 2020. Towards the implementation of circular economy in the wastewater sector: Challenges and opportunities. Water 12(5), 1431.

Guo, B., Zhang, L., Sun, H., Gao, M., Yu, N., Zhang, Q., Mou, A. and Liu, Y. 2022. Microbial co-occurrence network topological properties link with reactor parameters and reveal importance of low-abundance genera. npj Biofilms and Microbiomes 8(1), 1-13.

Guo, B., Zhang, Y., Yu, N. and Liu, Y. 2020a. Impacts of Conductive Materials on Microbial Community during Syntrophic Propionate Oxidization for Biomethane Recovery. Water Environment Research 93(1), 84-93.

Guo, B., Zhang, Y., Zhang, L., Zhou, Y. and Liu, Y. 2020b. RNA-based spatial community analysis revealed intra-reactor variation and expanded collection of direct interspecies electron transfer microorganisms in anaerobic digestion. Bioresource Technology 298, 122534.

Guo, L., Lu, M., Li, Q., Zhang, J., Zong, Y. and She, Z. 2014. Three-dimensional fluorescence excitation–emission matrix (EEM) spectroscopy with regional integration analysis for assessing waste sludge hydrolysis treated with multi-enzyme and thermophilic bacteria. Bioresource Technology 171, 22-28.

Guo, X., Sun, C., Lin, R., Xia, A., Huang, Y., Zhu, X., Show, P.-L. and Murphy, J.D. 2020c. Effects of foam nickel supplementation on anaerobic digestion: direct interspecies electron transfer. Journal of Hazardous Materials, 122830.

Gupta, A. and Sar, P. 2019. Role of cost-effective organic carbon substrates in bioremediation of acid mine drainage–impacted soil of Malanjkhand Copper Project, India: a biostimulant

for autochthonous microbial populations. Environmental Science and Pollution Research, 1-15.

Holm-Nielsen, J.B., Al Seadi, T. and Oleskowicz-Popiel, P. 2009. The future of anaerobic digestion and biogas utilization. Bioresource Technology 100(22), 5478-5484.

Hophmayer-Tokich, S. 2006. Wastewater Management Strategy: centralized v. decentralized technologies for small communities. Center for Clean Technology and Environmental Policy: Enschede, The Netherlands 27.

Hou, H., Li, Z., Liu, B., Liang, S., Xiao, K., Zhu, Q., Hu, S., Yang, J. and Hu, J. 2020. Biogas and phosphorus recovery from waste activated sludge with protocatechuic acid enhanced Fenton pretreatment, anaerobic digestion and microbial electrolysis cell. Science of The Total Environment 704, 135274.

Hu, J., Zhang, J., Li, Z. and Tao, W. 2022. Enhanced methane yield through sludge two-phase anaerobic digestion process with the addition of calcium hypochlorite. Bioresource Technology, 126693.

Hu, S., Zhao, W., Hu, J., Liu, B., Wang, D., Zhu, Q., Yang, J. and Hou, H. 2021. Integration of electrochemical and calcium hypochlorite oxidation for simultaneous sludge deep dewatering, stabilization and phosphorus fixation. Science of The Total Environment 750, 141408.

Huang, B.-C., Li, W.-W., Wang, X., Lu, Y. and Yu, H.-Q. 2019. Customizing anaerobic digestion-coupled processes for energy-positive and sustainable treatment of municipal wastewater. Renewable and Sustainable Energy Reviews 110, 132-142.

Huang, Q., Liu, Y. and Dhar, B.R. 2022. A multifaceted screening of applied voltages for electro-assisted anaerobic digestion of blackwater: Significance of temperature,

hydrolysis/acidogenesis, electrode corrosion, and energy efficiencies. Bioresource Technology 360, 127533.

Hussain, A., Lee, J., Ren, H. and Lee, H.-S. 2021. Spatial distribution of biofilm conductivity in a Geobacter enriched anodic biofilm. Chemical Engineering Journal 404.

Igarashi, K., Miyako, E. and Kato, S. 2020. Direct interspecies electron transfer mediated by graphene oxide-based materials. Frontiers in microbiology 10, 3068.

Ikumi, D.S., Harding, T.H. and Ekama, G.A. 2014. Biodegradability of wastewater and activated sludge organics in anaerobic digestion. Water Research 56, 267-279.

Islam, M.S., Dong, T., McPhedran, K.N., Sheng, Z., Zhang, Y., Liu, Y. and Gamal El-Din, M. 2014. Impact of ozonation pre-treatment of oil sands process-affected water on the operational performance of a GAC-fluidized bed biofilm reactor. Biodegradation 25(6), 811-823.

Jang, J.-H. and Ahn, J.-H. 2013. Effect of microwave pretreatment in presence of NaOH on mesophilic anaerobic digestion of thickened waste activated sludge. Bioresource Technology 131, 437-442.

Jari Oksanen, F.G.B., Michael Friendly, Roeland Kindt,, Pierre Legendre, D.M., Peter R. Minchin, R. B. O'Hara, Gavin L., Simpson, P.S., M. Henry H. Stevens, Eduard Szoecs and Helene and Wagner 2017 vegan: Community Ecology Package.

Jenal, U., Reinders, A. and Lori, C. 2017. Cyclic di-GMP: second messenger extraordinaire. Nature Reviews Microbiology 15(5), 271.

Jensen, P.D., Astals, S., Bai, X., Nieradzik, L., Wardrop, P., Batstone, D.J. and Clarke, W.P. 2022. Established full-scale applications for energy recovery from water: anaerobic digestion.

Jimenez, J., Gonidec, E., Rivero, J.A.C., Latrille, E., Vedrenne, F. and Steyer, J.-P. 2014. Prediction of anaerobic biodegradability and bioaccessibility of municipal sludge by coupling sequential extractions with fluorescence spectroscopy: towards ADM1 variables characterization. Water Research 50, 359-372.

Kainthola, J., Kalamdhad, A.S. and Goud, V.V. 2019. A review on enhanced biogas production from anaerobic digestion of lignocellulosic biomass by different enhancement techniques. Process Biochemistry 84, 81-90.

Kamali, M., Gameiro, T., Costa, M.E.V. and Capela, I. 2016. Anaerobic digestion of pulp and paper mill wastes–An overview of the developments and improvement opportunities. Chemical Engineering Journal 298, 162-182.

Kanazawa, S., Matsuura, N., Honda, R. and Yamamoto-Ikemoto, R. 2020. Enhancement of methane production and phosphorus recovery with a novel pre-treatment of excess sludge using waste plaster board. Journal of Environmental Management 255, 109844.

Khandaker, N.R., Afreen, I., Huq, F.B. and Akter, T. 2020. Treatment of textile wastewater using calcium hypochlorite oxidation followed by waste iron rust aided rapid filtration for color and COD removal for application in resources challenged Bangladesh. Groundwater for Sustainable Development 10, 100342.

Kim, J., Park, C., Kim, T.-H., Lee, M., Kim, S., Kim, S.-W. and Lee, J. 2003. Effects of various pretreatments for enhanced anaerobic digestion with waste activated sludge. Journal of Bioscience and Bioengineering 95(3), 271-275.

Kim, M.-J. and Kim, S.-H. 2020. Conditions of lag-phase reduction during anaerobic digestion of protein for high-efficiency biogas production. Biomass and Bioenergy 143, 105813.

Kleerebezem, R., Joosse, B., Rozendal, R. and Van Loosdrecht, M. 2015. Anaerobic digestion without biogas? Reviews in Environmental Science and Bio/Technology 14(4), 787-801.

Klimeski, A. 2007. Phosphorus recovery from black water by chemical precipitation.

Kor-Bicakci, G. and Eskicioglu, C. 2019. Recent developments on thermal municipal sludge pretreatment technologies for enhanced anaerobic digestion. Renewable and Sustainable Energy Reviews 110, 423-443.

Kristensen, J.M., Singleton, C., Clegg, L.-A., Petriglieri, F. and Nielsen, P.H. 2021. High diversity and functional potential of undescribed "Acidobacteriota" in Danish wastewater treatment plants. Frontiers in microbiology 12, 906.

Kümmerer, K., Dionysiou, D.D., Olsson, O. and Fatta-Kassinos, D. 2018. A path to clean water. Science 361(6399), 222-224.

Kuramae, E.E., Dimitrov, M.R., da Silva, G.H., Lucheta, A.R., Mendes, L.W., Luz, R.L., Vet, L.E. and Fernandes, T.V. 2020. On-site blackwater treatment fosters microbial groups and functions to efficiently and robustly recover carbon and nutrients. Microorganisms 9(1), 75.

Langille, M.G., Zaneveld, J., Caporaso, J.G., McDonald, D., Knights, D., Reyes, J.A., Clemente, J.C., Burkepile, D.E., Vega Thurber, R.L., Knight, R., Beiko, R.G. and Huttenhower, C. 2013. Predictive functional profiling of microbial communities using 16S rRNA marker gene sequences. Nature Biotechnology 31(9), 814-821.

Ledezma, P., Kuntke, P., Buisman, C.J., Keller, J. and Freguia, S. 2015. Source-separated urine opens golden opportunities for microbial electrochemical technologies. Trends in Biotechnology 33(4), 214-220.

Lee, J.W. and Jeffries, T.W. 2011. Efficiencies of acid catalysts in the hydrolysis of lignocellulosic biomass over a range of combined severity factors. Bioresource Technology 102(10), 5884-5890.

Lee, J.Y., Lee, S.H. and Park, H.D. 2016. Enrichment of specific electro-active microorganisms and enhancement of methane production by adding granular activated carbon in anaerobic reactors. Bioresource Technology 205, 205-212.

Lee, S.H., Kang, H.J., Lim, T.G. and Park, H.D. 2020. Magnetite and granular activated carbon improve methanogenesis via different metabolic routes. Fuel 281, 118768.

Li, J., Liu, F., Li, J. and Zhang, Y. 2019a. Regulation of endogenous acyl homoserine lactones by microbial density to enhance syntrophism of acetogens and methanogens in anaerobic digestion. Chemical Engineering Journal 378.

Li, L., Kong, X., Yang, F., Li, D., Yuan, Z. and Sun, Y. 2012. Biogas production potential and kinetics of microwave and conventional thermal pretreatment of grass. Appl Biochem Biotechnol 166(5), 1183-1191.

Li, L., Zheng, M., Ma, H., Gong, S., Ai, G., Liu, X., Li, J., Wang, K. and Dong, X. 2015. Significant performance enhancement of a UASB reactor by using acyl homoserine lactones to facilitate the long filaments of Methanosaeta harundinacea 6Ac. Applied Microbiology and Biotechnology 99(15), 6471-6480.

Li, X., Liu, Y., Xu, Q., Liu, X., Huang, X., Yang, J., Wang, D., Wang, Q., Liu, Y. and Yang, Q. 2019b. Enhanced methane production from waste activated sludge by combining calcium peroxide with ultrasonic: performance, mechanism, and implication. Bioresource Technology 279, 108-116.

Liang, J., Huang, J., Zhang, S., Yang, X., Huang, S., Zheng, L., Ye, M. and Sun, S. 2019. A highly efficient conditioning process to improve sludge dewaterability by combining calcium hypochlorite oxidation, ferric coagulant re-flocculation, and walnut shell skeleton construction. Chemical Engineering Journal 361, 1462-1478.

Liang, J. and Zhou, Y. 2022. Iron-based advanced oxidation processes for enhancing sludge dewaterability: state of the art, challenges, and sludge reuse. Water Research, 118499.

Lim, J.W., Chiam, J.A. and Wang, J.Y. 2014. Microbial community structure reveals how microaeration improves fermentation during anaerobic co-digestion of brown water and food waste. Bioresource Technology 171, 132-138.

Lim, J.W. and Wang, J.Y. 2013. Enhanced hydrolysis and methane yield by applying microaeration pretreatment to the anaerobic co-digestion of brown water and food waste. Waste Management 33(4), 813-819.

Lin, R., Cheng, J., Zhang, J., Zhou, J., Cen, K. and Murphy, J.D. 2017. Boosting biomethane yield and production rate with graphene: The potential of direct interspecies electron transfer in anaerobic digestion. Bioresource Technology 239, 345-352.

Lins, P., Reitschuler, C. and Illmer, P. 2014. Methanosarcina spp., the key to relieve the start-up of a thermophilic anaerobic digestion suffering from high acetic acid loads. Bioresource Technology 152, 347-354.

Liu, C.G., Xue, C., Lin, Y.H. and Bai, F.W. 2013. Redox potential control and applications in microaerobic and anaerobic fermentations. Biotechnology Advances 31(2), 257-265.

Liu, J., Liu, T., Chen, S., Yu, H., Zhang, Y. and Quan, X. 2020. Enhancing anaerobic digestion in anaerobic integrated floating fixed-film activated sludge (An-IFFAS) system using novel electron mediator suspended biofilm carriers. Water Research 175, 115697.

Liu, X., Shi, L. and Gu, J.D. 2018. Microbial electrocatalysis: Redox mediators responsible for extracellular electron transfer. Biotechnology Advances 36(7), 1815-1827.

Liu, Y. 2003. Chemically reduced excess sludge production in the activated sludge process. Chemosphere 50(1), 1-7.

Luo, J., Huang, W., Zhang, Q., Guo, W., Wu, Y., Feng, Q., Fang, F., Cao, J. and Su, Y. 2020. Effects of different hypochlorite types on the waste activated sludge fermentation from the perspectives of volatile fatty acids production, microbial community and activity, and characteristics of fermented sludge. Bioresource Technology 307, 123227.

Lv, L., Li, W., Zheng, Z., Li, D. and Zhang, N. 2018. Exogenous acyl-homoserine lactones adjust community structures of bacteria and methanogens to ameliorate the performance of anaerobic granular sludge. Journal of Hazardous Materials 354, 72-80.

Ma, J., Frear, C., Wang, Z.-w., Yu, L., Zhao, Q., Li, X. and Chen, S. 2013. A simple methodology for rate-limiting step determination for anaerobic digestion of complex substrates and effect of microbial community ratio. Bioresource Technology 134, 391-395.

Ma, S., Wang, H., Li, L., Gu, X. and Zhu, W. 2021. Enhanced biomethane production from corn straw by a novel anaerobic digestion strategy with mechanochemical pretreatment. Renewable and Sustainable Energy Reviews 146, 111099.

Ma, X., Ye, J., Jiang, L., Sheng, L., Liu, J., Li, Y.Y. and Xu, Z.P. 2019. Alkaline fermentation of waste activated sludge with calcium hydroxide to improve short-chain fatty acids production and extraction efficiency via layered double hydroxides. Bioresource Technology 279, 117-123.

Mahmod, S.S., Azahar, A.M., Luthfi, A.A.I., Abdul, P.M., Mastar, M.S., Anuar, N., Takriff, M.S. and Jahim, J. 2020. Potential utilisation of dark-fermented palm oil mill effluent in

continuous production of biomethane by self-granulated mixed culture. Scientific Reports 10(1), 1-12.

Mara, D. (2013) Domestic wastewater treatment in developing countries, Routledge.

Marsili, E., Rollefson, J.B., Baron, D.B., Hozalski, R.M. and Bond, D.R. 2008. Microbial biofilm voltammetry: direct electrochemical characterization of catalytic electrode-attached biofilms. Applied and Environmental Microbiology 74(23), 7329-7337.

Martins, G., Salvador, A.F., Pereira, L. and Alves, M.M. 2018. Methane Production and Conductive Materials: A Critical Review. Environmental Science & Technology 52(18), 10241-10253.

Mata-Alvarez, J., Macé, S. and Llabres, P. 2000. Anaerobic digestion of organic solid wastes. An overview of research achievements and perspectives. Bioresource Technology 74(1), 3-16.

Maurer, M., Pronk, W. and Larsen, T. 2006. Treatment processes for source-separated urine. Water Research 40(17), 3151-3166.

McCarty, P.L., Bae, J. and Kim, J. 2011 Domestic wastewater treatment as a net energy producer–can this be achieved?, ACS Publications.

McDonald, D., Price, M.N., Goodrich, J., Nawrocki, E.P., DeSantis, T.Z., Probst, A., Andersen, G.L., Knight, R. and Hugenholtz, P. 2012. An improved Greengenes taxonomy with explicit ranks for ecological and evolutionary analyses of bacteria and archaea. The ISME journal 6(3), 610-618.

Mehta, C.M., Khunjar, W.O., Nguyen, V., Tait, S. and Batstone, D.J. 2015. Technologies to recover nutrients from waste streams: a critical review. Critical Reviews in Environmental Science and Technology 45(4), 385-427.

Mei, R., Nobu, M.K., Narihiro, T., Yu, J., Sathyagal, A., Willman, E. and Liu, W.-T. 2018. Novel Geobacter species and diverse methanogens contribute to enhanced methane production in media-added methanogenic reactors. Water Research 147, 403-412.

Mo, W. and Zhang, Q. 2013. Energy-nutrients-water nexus: integrated resource recovery in municipal wastewater treatment plants. Journal of Environmental Economics and Management 127, 255-267.

Moscoviz, R., De Fouchécour, F., Santa-Catalina, G., Bernet, N. and Trably, E. 2017. Cooperative growth of Geobacter sulfurreducens and Clostridium pasteurianum with subsequent metabolic shift in glycerol fermentation. Scientific Reports 7(1), 1-9.

Muller, N., Worm, P., Schink, B., Stams, A.J. and Plugge, C.M. 2010. Syntrophic butyrate and propionate oxidation processes: from genomes to reaction mechanisms. Environmental Microbiology Reports 2(4), 489-499.

Nag, R., Auer, A., Markey, B.K., Whyte, P., Nolan, S., O'Flaherty, V., Russell, L., Bolton, D., Fenton, O. and Richards, K. 2019. Anaerobic digestion of agricultural manure and biomass–critical indicators of risk and knowledge gaps. Science of The Total Environment 690, 460-479.

Nguyen, D. and Khanal, S.K. 2018. A little breath of fresh air into an anaerobic system: How microaeration facilitates anaerobic digestion process. Biotechnology Advances 36(7), 1971-1983.

Nguyen, D., Wu, Z., Shrestha, S., Lee, P.H., Raskin, L. and Khanal, S.K. 2019. Intermittent micro-aeration: New strategy to control volatile fatty acid accumulation in high organic loading anaerobic digestion. Water Research 166, 115080.

Nobu, M.K., Narihiro, T., Kuroda, K., Mei, R. and Liu, W.-T. 2016. Chasing the elusive Euryarchaeota class WSA2: genomes reveal a uniquely fastidious methyl-reducing methanogen. The ISME journal 10(10), 2478-2487.

Ntaikou, I., Kourmentza, C., Koutrouli, E., Stamatelatou, K., Zampraka, A., Kornaros, M. and Lyberatos, G. 2009. Exploitation of olive oil mill wastewater for combined biohydrogen and biopolymers production. Bioresource Technology 100(15), 3724-3730.

Oarga Mulec, A., Mihelič, R., Walochnik, J. and Griessler Bulc, T. 2016. Composting of the solid fraction of blackwater from a separation system with vacuum toilets – Effects on the process and quality. Journal of Cleaner Production 112, 4683-4690.

Oladoja, N.A. 2017. Appropriate technology for domestic wastewater management in under-resourced regions of the world. Applied Water Science 7(7), 3391-3406.

Otterpohl, R., Wendland, C. and Al-Baz, I. (2008) Efficient Management of Wastewater: Its Treatment and Reuse in Water-scarce Countries, Springer.

Palatsi, J., Ripoll, F., Benzal, A., Pijuan, M. and Romero-Güiza, M.S. 2021. Enhancement of biological nutrient removal process with advanced process control tools in full-scale wastewater treatment plant. Water Research 200, 117212.

Panswad, T., Tongkhammak, N. and Anotai, J. 2007. Estimation of intracellular phosphorus content of phosphorus-accumulating organisms at different P: COD feeding ratios. Journal of Environmental Management 84(2), 141-145.

Parawira, W., Murto, M., Zvauya, R. and Mattiasson, B. 2006. Comparative performance of a UASB reactor and an anaerobic packed-bed reactor when treating potato waste leachate. Renewable energy 31(6), 893-903.

Park, J.H., Park, J.H., Lee, S.H., Jung, S.P. and Kim, S.H. 2020. Enhancing anaerobic digestion for rural wastewater treatment with granular activated carbon (GAC) supplementation. Bioresource Technology 315, 123890.

Park, J.H., Kang, H.J., Park, K.H. and Park, H.D. 2018. Direct interspecies electron transfer via conductive materials: A perspective for anaerobic digestion applications. Bioresource Technology 254, 300-311.

Paulo, P.L., Azevedo, C., Begosso, L., Galbiati, A.F. and Boncz, M.A. 2013. Natural systems treating greywater and blackwater on-site: Integrating treatment, reuse and landscaping. Ecological Engineering 50, 95-100.

Pedrouso, A., Tocco, G., Val del Río, A., Carucci, A., Morales, N., Campos, J.L., Milia, S. and Mosquera-Corral, A. 2019. Digested blackwater treatment in a partial nitritation-anammox reactor under repeated starvation and reactivation periods. Journal of Cleaner Production.

Perona-Vico, E., Blasco-Gómez, R., Colprim, J., Puig, S. and Bañeras, L. 2019. [NiFe]-hydrogenases are constitutively expressed in an enriched Methanobacterium sp. population during electromethanogenesis. PloS one 14(4), e0215029.

Pritchard, D., Penney, N., McLaughlin, M., Rigby, H. and Schwarz, K. 2010. Land application of sewage sludge (biosolids) in Australia: risks to the environment and food crops. Water Science and Technology 62(1), 48-57.

Puyol, D., Batstone, D.J., Hülsen, T., Astals, S., Peces, M. and Krömer, J.O. 2017. Resource recovery from wastewater by biological technologies: opportunities, challenges, and prospects. Frontiers in microbiology 7, 2106.

Puyol, D., Monsalvo, V.M., Sanchis, S., Sanz, J.L., Mohedano, A.F. and Rodriguez, J.J. 2015. Comparison of bioaugmented EGSB and GAC–FBB reactors and their combination with aerobic SBR for the abatement of chlorophenols. Chemical Engineering Journal 259, 277-285.

Rajendran, K., Mahapatra, D., Venkatraman, A.V., Muthuswamy, S. and Pugazhendhi, A. 2020. Advancing anaerobic digestion through two-stage processes: Current developments and future trends. Renewable and Sustainable Energy Reviews 123.

Ramos, I. and Fdz-Polanco, M. 2013. The potential of oxygen to improve the stability of anaerobic reactors during unbalanced conditions: results from a pilot-scale digester treating sewage sludge. Bioresource Technology 140, 80-85.

Ramos, I., Perez, R. and Fdz-Polanco, M. 2014. The headspace of microaerobic reactors: sulphide-oxidising population and the impact of cleaning on the efficiency of biogas desulphurisation. Bioresource Technology 158, 63-73.

Rand, M., Greenberg, A.E. and Taras, M.J. (1976) Standard methods for the examination of water and wastewater, Prepared and published jointly by American Public Health Association.

Rice, E.W., Bridgewater, L., Association, A.P.H., Association, A.W.W. and Federation, W.E. (2012) Standard Methods for the Examination of Water and Wastewater, American Public Health Association.

Richter, H., Nevin, K.P., Jia, H., Lowy, D.A., Lovley, D.R. and Tender, L.M. 2009. Cyclic voltammetry of biofilms of wild type and mutant Geobacter sulfurreducens on fuel cell anodes indicates possible roles of OmcB, OmcZ, type IV pili, and protons in extracellular electron transfer. Energy & Environmental Science 2(5).

Ridley, C.M., Jamieson, R.C., Truelstrup Hansen, L., Yost, C.K. and Bezanson, G.S. 2014. Baseline and storm event monitoring of Bacteroidales marker concentrations and enteric pathogen presence in a rural Canadian watershed. Water Research 60, 278-288.

Ritalahti, K.M., Justicia-Leon, S.D., Cusick, K.D., Ramos-Hernandez, N., Rubin, M., Dornbush, J. and Löffler, F.E. 2012. Sphaerochaeta globosa gen. nov., sp. nov. and Sphaerochaeta pleomorpha sp. nov., free-living, spherical spirochaetes. International journal of systematic and evolutionary microbiology 62(1), 210-216.

Roehrdanz, P.R., Feraud, M., Ervin, J., Anumol, T., Jia, A., Park, M., Tamez, C., Morelius, E.W., Gardea-Torresdey, J.L. and Izbicki, J. 2015. Wastewater compounds in urban shallow groundwater wells correspond to exfiltration probabilities of nearby sewers. Water Research 85, 467-475.

Rose, C., Parker, A., Jefferson, B. and Cartmell, E. 2015. The Characterization of Feces and Urine: A Review of the Literature to Inform Advanced Treatment Technology. Crit Rev Environmental Science & Technology 45(17), 1827-1879.

Rosenkranz, F., Cabrol, L., Carballa, M., Donoso-Bravo, A., Cruz, L., Ruiz-Filippi, G., Chamy, R. and Lema, J.M. 2013. Relationship between phenol degradation efficiency and microbial community structure in an anaerobic SBR. Water Research 47(17), 6739-6749.

Rotaru, A.E., Calabrese, F., Stryhanyuk, H., Musat, F., Shrestha, P.M., Weber, H.S., Snoeyenbos-West, O.L., Hall, P.O., Richnow, H.H. and Musat, N. 2018. Conductive particles enable syntrophic acetate oxidation between Geobacter and Methanosarcina from coastal sediments. MBio 9(3).

Rotaru, A.E., Shrestha, P.M., Liu, F., Shrestha, M., Shrestha, D., Embree, M., Zengler, K., Wardman, C., Nevin, K.P. and Lovley, D.R. 2014. A new model for electron flow during

anaerobic digestion: direct interspecies electron transfer to Methanosaeta for the reduction of carbon dioxide to methane. Energy & Environmental Science 7(1), 408-415.

Ruan, D., Zhou, Z., Pang, H., Yao, J., Chen, G. and Qiu, Z. 2019. Enhancing methane production of anaerobic sludge digestion by microaeration: Enzyme activity stimulation, semi-continuous reactor validation and microbial community analysis. Bioresource Technology 289, 121643.

Ryue, J., Lin, L., Liu, Y., Lu, W., McCartney, D. and Dhar, B.R. 2019. Comparative effects of GAC addition on methane productivity and microbial community in mesophilic and thermophilic anaerobic digestion of food waste. Biochemical Engineering Journal 146, 79-87.

Salvador, A.F., Martins, G., Melle-Franco, M., Serpa, R., Stams, A.J., Cavaleiro, A.J., Pereira, M.A. and Alves, M.M. 2017. Carbon nanotubes accelerate methane production in pure cultures of methanogens and in a syntrophic coculture. Environmental Microbiology 19(7), 2727-2739.

Sari Erkan, H. and Onkal Engin, G. 2020. A comparative study of waste activated sludge disintegration by electrochemical pretreatment process combined with hydroxyl and sulfate radical based oxidants. Journal of Environmental Chemical Engineering 8(4).

Sheng, Z., Van Nostrand, J.D., Zhou, J. and Liu, Y. 2018. Contradictory effects of silver nanoparticles on activated sludge wastewater treatment. Journal of Hazardous Materials 341, 448-456.

Siegert, M., Yates, M.D., Spormann, A.M. and Logan, B.E. 2015. Methanobacterium dominates biocathodic archaeal communities in methanogenic microbial electrolysis cells. ACS Sustainable Chemistry & Engineering 3(7), 1668-1676.

Singh, N.K., Kazmi, A.A. and Starkl, M. 2015. A review on full-scale decentralized wastewater treatment systems: techno-economical approach. Water Science and Technology 71(4), 468-478.

Slompo, N.D.M., Quartaroli, L., Zeeman, G., da Silva, G.H.R. and Daniel, L.A. 2019. Black water treatment by an upflow anaerobic sludge blanket (UASB) reactor: a pilot study. Water Science and Technology 80(8), 1505-1511.

Song, Z., Yang, G., Liu, X., Yan, Z., Yuan, Y. and Liao, Y. 2014. Comparison of seven chemical pretreatments of corn straw for improving methane yield by anaerobic digestion. PLoS ONE 9(4).

Sonune, A. and Ghate, R. 2004. Developments in wastewater treatment methods. Desalination 167, 55-63.

Spellman, F.R. (2008) Handbook of water and wastewater treatment plant operations, CRC press.

Sun, H., Mohammed, A.N. and Liu, Y. 2020. Phosphorus recovery from source-diverted blackwater through struvite precipitation. Science of The Total Environment 743, 140747.

Sun, H., Zhang, L., Zhang, Y., Guo, B. and Liu, Y. 2021. A new non-steady-state mass balance model for quantifying microbiome responses to disturbances in wastewater bioreactors. Journal of Environmental Management 296, 113370.

Talekar, G.V. and Mutnuri, S. 2021. Electrochemical removal and recovery of ammonia and phosphates from blackwater and wetland passed blackwater. Sustainable Energy Technologies and Assessments 47, 101374.

Tang, Y., Shigematsu, T., Morimura, S. and Kida, K. 2004. The effects of micro-aeration on the phylogenetic diversity of microorganisms in a thermophilic anaerobic municipal solid-waste digester. Water Research 38(10), 2537-2550.

Tao, Z., Wang, D., Yao, F., Huang, X., Wu, Y., Wu, Y., Chen, Z., Wei, J., Li, X. and Yang, Q. 2020. Influence of low voltage electric field stimulation on hydrogen generation from anaerobic digestion of waste activated sludge. Science of The Total Environment 704, 135849.

Tawfik, A., Badr, N., Taleb, E. and El-Senousy, W. 2012. Sewage treatment in an up-flow anaerobic sponge reactor followed by moving bed biofilm reactor based on polyurethane carrier material. Desalination and Water Treatment 37(1-3), 350-358.

Teuber, M. (1995) The genera of lactic acid bacteria, pp. 173-234, Springer.

Tian, T., Qiao, S., Li, X., Zhang, M. and Zhou, J. 2017. Nano-graphene induced positive effects on methanogenesis in anaerobic digestion. Bioresource Technology 224, 41-47.

Tian, T., Qiao, S., Yu, C. and Zhou, J. 2018. Bio-electrochemically assisting low-temperature anaerobic digestion of low-organic strength wastewater. Chemical Engineering Journal 335, 657-664.

Toutian, V., Barjenbruch, M., Unger, T., Loderer, C. and Remy, C. 2020. Effect of temperature on biogas yield increase and formation of refractory COD during thermal hydrolysis of waste activated sludge. Water Research 171, 115383.

Tsapekos, P., Kougias, P.G., Vasileiou, S.A., Treu, L., Campanaro, S., Lyberatos, G. and Angelidaki, I. 2017. Bioaugmentation with hydrolytic microbes to improve the anaerobic biodegradability of lignocellulosic agricultural residues. Bioresource Technology 234, 350-359.

Tsigkou, K., Zagklis, D., Parasoglou, M., Zafiri, C. and Kornaros, M. 2022. Proposed protocol for rate-limiting step determination during anaerobic digestion of complex substrates. Bioresource Technology 361, 127660.

Turovskiy, I.S. and Mathai, P. (2006) Wastewater sludge processing, John Wiley & Sons.

Tyagi, V.K. and Lo, S.-L. 2011. Application of physico-chemical pretreatment methods to enhance the sludge disintegration and subsequent anaerobic digestion: an up to date review. Reviews in Environmental Science and Bio/Technology 10(3), 215.

van Voorthuizen, E., Zwijnenburg, A., van der Meer, W. and Temmink, H. 2008. Biological black water treatment combined with membrane separation. Water Research 42(16), 4334-4340.

Vavilin, V., Fernandez, B., Palatsi, J. and Flotats, X. 2008. Hydrolysis kinetics in anaerobic degradation of particulate organic material: an overview. Waste Managementement 28(6), 939-951.

Villamil, J., Mohedano, A., San Martín, J., Rodriguez, J. and De la Rubia, M. 2020. Anaerobic co-digestion of the process water from waste activated sludge hydrothermally treated with primary sewage sludge. A new approach for sewage sludge management. Renewable Energy 146, 435-443.

Walker, D.J., Martz, E., Holmes, D.E., Zhou, Z., Nonnenmann, S.S. and Lovley, D.R. 2019. The archaellum of Methanospirillum hungatei is electrically conductive. Mbio 10(2).

Walker, D.J., Nevin, K.P., Holmes, D.E., Rotaru, A.-E., Ward, J.E., Woodard, T.L., Zhu, J., Ueki, T., Nonnenmann, S.S. and McInerney, M.J. 2020. Syntrophus conductive pili demonstrate that common hydrogen-donating syntrophs can have a direct electron transfer option. The ISME Journal 14(3), 837-846.

Wall, D. and Kaiser, D. 1999. Type IV pili and cell motility. Molecular microbiology 32(1), 01-10.

Wang, C., Wang, C., Jin, L., Lu, D., Chen, H., Zhu, W., Xu, X. and Zhu, L. 2019a. Response of syntrophic aggregates to the magnetite loss in continuous anaerobic bioreactor. Water Research 164, 114925.

Wang, J., Ding, L., Li, K., Huang, H., Hu, H., Geng, J., Xu, K. and Ren, H. 2018. Estimation of spatial distribution of quorum sensing signaling in sequencing batch biofilm reactor (SBBR) biofilms. Science of The Total Environment 612, 405-414.

Wang, J., Ding, L., Li, K., Schmieder, W., Geng, J., Xu, K., Zhang, Y. and Ren, H. 2017. Development of an extraction method and LC-MS analysis for N-acylated-l-homoserine lactones (AHLs) in wastewater treatment biofilms. Journal of Chromatography B: Analytical Technologies in the Biomedical and Life Sciences 1041-1042, 37-44.

Wang, J., Liu, Q., Hu, H., Wu, B., Zhang, X.X. and Ren, H. 2019b. Insight into mature biofilm quorum sensing in full-scale wastewater treatment plants. Chemosphere 234, 310-317.

Ware, A. and Power, N. 2017. Modelling methane production kinetics of complex poultry slaughterhouse wastes using sigmoidal growth functions. Renewable Energy 104, 50-59.

Wei, T. and Simko, V. 2017 R package "corrplot": Visualization of a Correlation Matrix.

Wendland, C., Deegener, S., Behrendt, J., Toshev, P. and Otterpohl, R. 2007. Anaerobic digestion of blackwater from vacuum toilets and kitchen refuse in a continuous stirred tank reactor (CSTR). Water Science and Technology 55(7), 187-194.

Werner, J.J., Koren, O., Hugenholtz, P., DeSantis, T.Z., Walters, W.A., Caporaso, J.G., Angenent, L.T., Knight, R. and Ley, R.E. 2012. Impact of training sets on classification of high-throughput bacterial 16s rRNA gene surveys. The ISME journal 6(1), 94-103.

Wilderer, P.A. and Schreff, D. 2000. Decentralized and centralized wastewater management: a challenge for technology developers. Water Science and Technology 41(1), 1-8.

Wong, H.L., Visscher, P.T., White III, R.A., Smith, D.-L., Patterson, M.M. and Burns, B.P. 2017. Dynamics of archaea at fine spatial scales in Shark Bay mat microbiomes. Scientific Reports 7, 46160.

Wu, S.-L., Wei, W. and Ni, B.-J. 2021. Enhanced methane production from anaerobic digestion of waste activated sludge through preliminary pretreatment using calcium hypochlorite. Journal of Environmental Management 295, 113346.

Wu, X. and Conrad, R. 2001. Functional and structural response of a cellulose - degrading methanogenic microbial community to multiple aeration stress at two different temperatures. Environmental Microbiology 3(6), 355-362.

Wu, Y., Wang, S., Liang, D. and Li, N. 2020. Conductive materials in anaerobic digestion: From mechanism to application. Bioresource Technology 298, 122403.

Xu, H., Chang, J., Wang, H., Liu, Y., Zhang, X., Liang, P. and Huang, X. 2019. Enhancing direct interspecies electron transfer in syntrophic-methanogenic associations with (semi)conductive iron oxides: Effects and mechanisms. Science of The Total Environment 695, 133876.

Xu, H., Wang, C., Yan, K., Wu, J., Zuo, J. and Wang, K. 2016. Anaerobic granule-based biofilms formation reduces propionate accumulation under high H2 partial pressure using conductive carbon felt particles. Bioresource Technology 216, 677-683.

Xu, R.-z., Fang, S., Zhang, L., Huang, W., Shao, Q., Fang, F., Feng, Q., Cao, J. and Luo, J. 2021. Distribution patterns of functional microbial community in anaerobic digesters under different operational circumstances: A review. Bioresource Technology 341, 125823.

Xu, S., Han, R., Zhang, Y., He, C. and Liu, H. 2018. Differentiated stimulating effects of activated carbon on methanogenic degradation of acetate, propionate and butyrate. Waste Management 76, 394-403.

Xu, S., Selvam, A. and Wong, J.W. 2014. Optimization of micro-aeration intensity in acidogenic reactor of a two-phase anaerobic digester treating food waste. Waste Management 34(2), 363-369.

Yang, G. and Wang, J. 2018. Pretreatment of grass waste using combined ionizing radiation-acid treatment for enhancing fermentative hydrogen production. Bioresource Technology 255, 7-15.

Yang, Y., Zhang, Y., Li, Z., Zhao, Z., Quan, X. and Zhao, Z. 2017. Adding granular activated carbon into anaerobic sludge digestion to promote methane production and sludge decomposition. Journal of Cleaner Production 149, 1101-1108.

Yi, J., Dong, B., Jin, J. and Dai, X. 2014. Effect of Increasing Total Solids Contents on Anaerobic Digestion of Food Waste under Mesophilic Conditions: Performance and Microbial Characteristics Analysis. PLOS ONE 9(7), e102548.

Yin, C., Shen, Y., Dai, X., Zhu, N., Yuan, H., Lou, Z. and Yuan, R. 2020a. Integrated anaerobic digestion and CO2 sequestration for energy recovery from waste activated sludge by calcium addition: Timing matters. Energy 199.

Yin, J., Yu, X., Zhang, Y., Shen, D., Wang, M., Long, Y. and Chen, T. 2016. Enhancement of acidogenic fermentation for volatile fatty acid production from food waste: Effect of redox potential and inoculum. Bioresource Technology 216, 996-1003.

Yin, Q., Gu, M., Hermanowicz, S.W., Hu, H. and Wu, G. 2020b. Potential interactions between syntrophic bacteria and methanogens via type IV pili and quorum-sensing systems. Environment International 138, 105650.

Yin, Q., He, K., Liu, A. and Wu, G. 2017. Enhanced system performance by dosing ferroferric oxide during the anaerobic treatment of tryptone-based high-strength wastewater. Applied Microbiology and Biotechnology 101(9), 3929-3939.

Yin, Q. and Wu, G. 2019. Advances in direct interspecies electron transfer and conductive materials: Electron flux, organic degradation and microbial interaction. Biotechnology Advances 37(8), 107443.

You, Z., Pan, S.Y., Sun, N., Kim, H. and Chiang, P.C. 2019. Enhanced corn-stover fermentation for biogas production by NaOH pretreatment with CaO additive and ultrasound. Journal of Cleaner Production 238, 117813.

Yu, N., Guo, B. and Liu, Y. 2021a. Shaping biofilm microbiomes by changing GAC location during wastewater anaerobic digestion. Science of The Total Environment 780, 146488.

Yu, N., Guo, B., Zhang, Y., Zhang, L., Zhou, Y. and Liu, Y. 2020a. Different micro-aeration rates facilitate production of different end-products from source-diverted blackwater. Water Research, 115783.

Yu, N., Guo, B., Zhang, Y., Zhang, L., Zhou, Y. and Liu, Y. 2020b. Self-fluidized GAC-amended UASB reactor for enhanced methane production. Chemical Engineering Journal, 127652.

Yu, N., Sun, H., Mou, A. and Liu, Y. 2021b. Calcium hypochlorite enhances the digestibility of and the phosphorus recovery from waste activated sludge. Bioresource Technology 340, 125658.

Yu, W., Wen, Q., Yang, J., Xiao, K., Zhu, Y., Tao, S., Lv, Y., Liang, S., Fan, W. and Zhu, S. 2019. Unraveling oxidation behaviors for intracellular and extracellular from different oxidants (HOCl vs. H2O2) catalyzed by ferrous iron in waste activated sludge dewatering. Water Research 148, 60-69.

Yuan, H. and Zhu, N. 2016. Progress in inhibition mechanisms and process control of intermediates and by-products in sewage sludge anaerobic digestion. Renewable and Sustainable Energy Reviews 58, 429-438.

Yuan, Y., Hu, X., Chen, H., Zhou, Y., Zhou, Y. and Wang, D. 2019. Advances in enhanced volatile fatty acid production from anaerobic fermentation of waste activated sludge. Science of The Total Environment 694, 133741.

Zamalloa, C., Arends, J.B., Boon, N. and Verstraete, W. 2013. Performance of a lab-scale bio-electrochemical assisted septic tank for the anaerobic treatment of black water. New biotechnology 30(5), 573-580.

Zamri, M., Hasmady, S., Akhiar, A., Ideris, F., Shamsuddin, A., Mofijur, M., Fattah, I.R. and Mahlia, T. 2021. A comprehensive review on anaerobic digestion of organic fraction of municipal solid waste. Renewable and Sustainable Energy Reviews 137, 110637.

Zeeman, G., Kujawa, K., De Mes, T., Hernandez, L., De Graaff, M., Abu-Ghunmi, L., Mels, A., Meulman, B., Temmink, H. and Buisman, C. 2008. Anaerobic treatment as a core technology for energy, nutrients and water recovery from source-separated domestic waste (water). Water Science and Technology 57(8), 1207-1212.

Zhang, G., Zhang, F., Ding, G., Li, J., Guo, X., Zhu, J., Zhou, L., Cai, S., Liu, X., Luo, Y., Zhang, G., Shi, W. and Dong, X. 2012. Acyl homoserine lactone-based quorum sensing in a methanogenic archaeon. ISME J 6(7), 1336-1344.

Zhang, J., Mao, L., Zhang, L., Loh, K.-C., Dai, Y. and Tong, Y.W. 2017. Metagenomic insight into the microbial networks and metabolic mechanism in anaerobic digesters for food waste by incorporating activated carbon. Scientific Reports 7(1), 1-10.

Zhang, J., Zhang, R., Wang, H. and Yang, K. 2020a. Direct interspecies electron transfer stimulated by granular activated carbon enhances anaerobic methanation efficiency from typical kitchen waste lipid-rapeseed oil. Science of The Total Environment 704, 135282.

Zhang, J., Zhang, Y.-c., Wang, X.-j., Li, J., Zhou, R.-x., Wei, J., Liang, D.-b. and Zhang, K. 2019a. Effects of substrate shock on release of AHL signals in ANAMMOX granules and properties of granules. Environmental Science: Water Research & Technology 5(4), 756-768.

Zhang, L., Guo, B., Zhang, Q., Florentino, A., Xu, R., Zhang, Y. and Liu, Y. 2019b. Co-digestion of blackwater with kitchen organic waste: Effects of mixing ratios and insights into microbial community. Journal of Cleaner Production 236, 117703.

Zhang, L., Hendrickx, T.L., Kampman, C., Temmink, H. and Zeeman, G. 2013. Co-digestion to support low temperature anaerobic pretreatment of municipal sewage in a UASB-digester. Bioresource Technology 148, 560-566.

Zhang, L., Mou, A., Guo, B., Sun, H., Anwar, M.N. and Liu, Y. 2021a. Simultaneous Phosphorus Recovery in Energy Generation Reactor (SPRING): High Rate Thermophilic Blackwater Treatment. Resources, Conservation and Recycling 164, 105163.

Zhang, L., Mou, A., Sun, H., Zhang, Y., Zhou, Y. and Liu, Y. 2021b. Calcium phosphate granules formation: Key to high rate of mesophilic UASB treatment of toilet wastewater. Science of The Total Environment 773, 144972.

Zhang, Q., Li, R., Guo, B., Zhang, L. and Liu, Y. 2021c. Thermophilic co-digestion of blackwater and organic kitchen waste: Impacts of granular activated carbon and different mixing ratios. Waste Managementement 131, 453-461.

Zhang, Q., Wu, Y., Luo, J., Cao, J., Kang, C., Wang, S., Li, K., Zhao, J., Aleem, M. and Wang, D. 2020b. Enhanced volatile fatty acids production from waste activated sludge with synchronous phosphorus fixation and pathogens inactivation by calcium hypochlorite stimulation. Science of The Total Environment 712, 136500.

Zhang, Q., Zhang, L., Guo, B. and Liu, Y. 2020c. Mesophiles outperform thermophiles in the anaerobic digestion of blackwater with kitchen residuals: Insights into process limitations. Waste Managementement 105, 279-288.

Zhang, X., Zhou, X., Xie, Y., Rong, X., Liu, Z., Xiao, X., Liang, Z., Jiang, S., Wei, J. and Wu, Z. 2019c. A sustainable bio-carrier medium for wastewater treatment: Modified basalt fiber. Journal of Cleaner Production 225, 472-480.

Zhang, Y., Guo, B., Zhang, L. and Liu, Y. 2020d. Key Syntrophic Partnerships Identified in a Granular Activated Carbon Amended UASB Treating Municipal Sewage under Low Temperature Conditions. Bioresource Technology, 123556.

Zhang, Y., Guo, B., Zhang, L., Zhang, H. and Liu, Y. 2021d. Microbial community dynamics in granular activated carbon enhanced up-flow anaerobic sludge blanket (UASB) treating municipal sewage under sulfate reducing and psychrophilic conditions. Chemical Engineering Journal 405.

Zhang, Y., Li, J., Liu, F., Yan, H., Li, J., Zhang, X. and Jha, A.K. 2019d. Specific quorum sensing signal molecules inducing the social behaviors of microbial populations in anaerobic digestion. Bioresource Technology 273, 185-195.

Zhang, Z., Gao, P., Cheng, J., Liu, G., Zhang, X. and Feng, Y. 2018. Enhancing anaerobic digestion and methane production of tetracycline wastewater in EGSB reactor with GAC/NZVI mediator. Water Research 136, 54-63.

Zhao, Z., Li, Y., Quan, X. and Zhang, Y. 2017. Towards engineering application: Potential mechanism for enhancing anaerobic digestion of complex organic waste with different types of conductive materials. Water Research 115, 266-277.

Zheng, W., Li, M., Li, Z., Xu, Y. and Ya, G. 2013. Enhancing the hydrolysis of excess sludge using thermophilic Bacillus sp. Hnu under different oxygen supply conditions. Journal of the Serbian Chemical Society 78(8), 1135-1147.

Zhou, A., Liu, Z., Wang, S., Chen, E., Wei, Y., Liu, W., Wang, A. and Yue, X. 2019a. Bio-electrolysis contribute to simultaneous bio-hydrogen recovery and phosphorus release from waste activated sludge assisted with prefermentation. Energy 185, 787-794.

Zhou, Y., Guo, B., Zhang, L., Zou, X., Yang, S., Zhang, H., Xia, S. and Liu, Y. 2019b. Anaerobically digested blackwater treatment by simultaneous denitrification and anammox processes: Feeding loading affects reactor performance and microbial community succession. Chemosphere 241, 125101.

Zhu, L., Chen, T., Xu, L., Zhou, Z., Feng, W., Liu, Y. and Chen, H. 2020. Effect and mechanism of quorum sensing on horizontal transfer of multidrug plasmid RP4 in BAC biofilm. Science of The Total Environment 698, 134236.

Zhu, M., Lu, F., Hao, L.P., He, P.J. and Shao, L.M. 2009. Regulating the hydrolysis of organic wastes by micro-aeration and effluent recirculation. Waste Management 29(7), 2042-2050.

Zhu, X., Yang, Q., Li, X., Zhong, Y., Wu, Y., Hou, L., Wei, J., Zhang, W., Liu, Y. and Chen, C. 2018a. Enhanced dewaterability of waste activated sludge with Fe (II)-activated

hypochlorite treatment. Environmental Science and Pollution Research 25(27), 27628-27638.

Zhu, X., Yang, Q., Li, X., Zhong, Y., Wu, Y., Hou, L., Wei, J., Zhang, W., Liu, Y., Chen, C. and Wang, D. 2018b. Enhanced dewaterability of waste activated sludge with Fe(II)-activated hypochlorite treatment. Environmental Science and Pollution Research International 25(27), 27628-27638.

Zhu, Y.L., Hou, H.M., Zhang, G.L., Wang, Y.F. and Hao, H.S. 2019. AHLs Regulate Biofilm Formation and Swimming Motility of Hafnia alvei H4. Frontiers in Microbiology 10, 1330.